1977

The crystal and molecular structure of organophosphorus insecticides

Russell George Baughman
Iowa State University

INFORMATION TO USERS

This material was produced from a microfilm copy of the original document. While the most advanced technological means to photograph and reproduce this document have been used, the quality is heavily dependent upon the quality of the original submitted.

The following explanation of techniques is provided to help you understand markings or patterns which may appear on this reproduction.

1. The sign or "target" for pages apparently lacking from the document photographed is "Missing Page(s)". If it was possible to obtain the missing page(s) or section, they are spliced into the film along with adjacent pages. This may have necessitated cutting thru an image and duplicating adjacent pages to insure you complete continuity.

2. When an image on the film is obliterated with a large round black mark, it is an indication that the photographer suspected that the copy may have moved during exposure and thus cause a blurred image. You will find a good image of the page in the adjacent frame.

3. When a map, drawing or chart, etc., was part of the material being photographed the photographer followed a definite method in "sectioning" the material. It is customary to begin photoing at the upper left hand corner of a large sheet and to continue photoing from left to right in equal sections with a small overlap. If necessary, sectioning is continued again — beginning below the first row and continuing on until complete.

4. The majority of users indicate that the textual content is of greatest value, however, a somewhat higher quality reproduction could be made from "photographs" if essential to the understanding of the dissertation. Silver prints of "photographs" may be ordered at additional charge by writing the Order Department, giving the catalog number, title, author and specific pages you wish reproduced.

5. PLEASE NOTE: Some pages may have indistinct print. Filmed as received.

University Microfilms Internationa
300 North Zeeb Road
Ann Arbor, Michigan 48106 USA
St. John's Road, Tyler's Green
High Wycombe, Bucks, England HP10 8HR

The crystal and molecular structure of organophosphorus insecticides

by

Russell George Baughman

A Dissertation Submitted to the
Graduate Faculty in Partial Fulfillment of
The Requirements for the Degree of
DOCTOR OF PHILOSOPHY

Department: Chemistry
Major: Physical Chemistry

Approved:

Signature was redacted for privacy.

In Charge of Major Work

Signature was redacted for privacy.

For the Major Department

Signature was redacted for privacy.

For the Graduate College

Iowa State University
Ames, Iowa

1977

TABLE OF CONTENTS

INTRODUCTION TO ORGANOPHOSPHORUS INSECTICIDES

Accurate three-dimensional structural information is a necessity if one is to better understand the mechanisms, steric effects, *etc.*, involved in the biochemistry of insecticides. Structural investigations involving a variety of insecticides have been performed[1-11] to obtain such structural information *via* X-ray diffraction techniques. However not all studies have resulted in yielding actual atomic positions. Since organophosphorus insecticides are becomming increasingly important, crystal structure studies of this class of insecticides are quite appropriate. The purpose of such a program is to better understand the relationship between structure and mechanism(s) relative to an insecticide's toxicity/activity.

Inactivation of the enzyme acetylcholinesterase (AChE) is generally believed to be the toxic mode of the organophosphorus (OP) insecticides and is a result of the phosphorylation of an enzyme site. O'Brien *et al.*[12] have shown that this site is likely not the same one that is utilized by acetylcholine (ACh). The inhibition reaction may be represented most simply by:

$$(RO)_2POX + EH \rightarrow (RO)_2POE + HX,$$

where EH = the uninhibited AChE[13]. Unlike acetylcholine, the OP insecticides, or their metabolic OP derivatives/analogs, "permanently" react with (*i.e.* phosphorylate) the AChE[13]. Hence, with a sufficiently high insecticide titer (10^{-6} to 10^{-9} M), the enzyme concentration is eventually unable to destroy, *via* hydrolysis, the acetylcholine constantly being produced. Auto-

toxicosis *via* nervous system disruption is the result. In mammals the nervous system disruption leads to respiratory failure and asphyxiation; the ultimate cause of the insect's expiration though is unknown[13]. However, an increase in oxygen consumption for some caterpillars has been noted[14] and NAD (nicotinamide adenine dinucleotide) levels are lowered in chicken embryos[15] after exposure to OP's.

The phosphorylation of AChE was originally thought to be due, in part, to the similarities in charge distribution, size, and shape of the many OP insecticides to acetylcholine (ACh) at the corresponding chemically active portions of each molecule. That is, the OP would mimic ACh. The phosphate ester would correspond to the acetyl group; a portion of the "X" group to the quaternary nitrogen of ACh[16]. Using the active site environment of AChE proposed by Krupka[17] as a model, one noted that the hydroxyl group from a serine unit would be utilized in the phosphorylation process; this unit corresponds to the esteratic site of Wilson's and Bergmann's papers[18-20]. Concurrently an X group would interact with the anionic site on the AChE model. In addition to the recent work of O'Brien[12] regarding the OP active site it has also been observed that "total" AChE is in fact made up of several isozymes[21], each reacting differently with the OP Insecticides[12]. It is this total AChE which will be referred to in any subsequent discussion.

Inhibition of AChE by substituted phenyl diethyl phosphates has already been shown to be a function of the Hammett σ

constant[22]. However, as noted by Fukuto[16], Hansch and Deutsch[23], O'Brien[13], Fukuto and Metcalf[22] and Canepa *et al.*[24], steric effects including van der Waals interactions of the OP insecticide molecule's substituents should also be considered as playing a significant role in the degree of inhibition attained. Consequently, a three-dimensional visualization is a key to understanding the overall process, which is as yet not fully understood.

In the case of AChE inhibition one would ideally like to know the three-dimensional structure of the OP active site(s), or that of a small range of possible low energy conformations. The complexity of this enzyme system virtually prohibits direct elucidation of its structure(s). However, accurate structural determinations of smaller molecules such as the OP's and/or carbamate insecticides, which strongly interact with the "OP" active site(s) of AChE, would allow not only inferences to be made with regards to the topography of AChE (or any of the isozymes) but also yield valuable molecular insight into the insecticides themselves. Structural investigations of the carbamates are also being performed[25-27]. Such information could lead to the construction of insecticides which would better conform structurally as well as chemically to the most favorable (*i.e.* minimum energy) orientation of AChE.

In order to minimize the number of variables and hence to arrive at more valid conclusions, all of the OP's investigated

contain a substituted six-membered ring (phenyl or pyridyl) bonded to a phosphate or thiophosphate group.

THE CRYSTAL AND MOLECULAR STRUCTURE OF RONNEL

Introduction

Ronnel (O,O-dimethyl O-2,4,5-trichlorophenyl phosphorothioate), $(H_3CO)_2P(S)OC_6H_2C\ell_3$, is a general purpose and animal systemic insecticide and has a mammalian LD_{50} of 1740 $mg \cdot kg^{-1}$ [28].

Experimental

Preparation.-- A sample of 99% pure ronnel was kindly supplied by P. A. Dahm and J. G. Laveglia. The compound was recrystallized from reagent grade carbon tetrachloride. This solution had to be evaporated to dryness to obtain the solid colorless species.

Crystal Data.-- A rectangular prismatic crystal with approximate dimensions 0.4 mm x 0.2 mm x 0.1 mm was selected and housed in a 0.2 mm (i.d.) thin-walled Lindemann glass capillary with the long axis of the crystal coincident with the axis of the capillary. Preliminary oscillation photographs indicated a single crystal with 2/m (monoclinic) symmetry. The crystal was then mounted on a four-circle diffractometer and three ω-oscillation photographs were taken at various χ and ϕ settings.

From these photographs eleven independent reflections were selected and their coordinates were input into an automatic

indexing program[29]. The reduced cell and reduced cell scalars which resulted from this program indicated monoclinic symmetry, which was confirmed by inspection of ω-oscillation photographs taken about each of the three axes in turn. Only the *b* axis showed a mirror plane. Observed layer line spacings agreed, within experimental error, to those predicted for this cell.

The lattice constants were obtained from a least-squares refinement using the Nelson-Riley extrapolation function[30] based on the precise ±2θ ($|2\theta|>20^\circ$) measurements of eleven strong independent reflections. At 30°C using Mo Kα radiation (λ = 0.70954 Å) they are a = 12.162(9), b = 9.990(8), c = 11.98(1) Å and β = 113.61(4)°. The observed density of 1.62 ± 0.02 $g \cdot cm^{-3}$ determined by the flotation method is in good agreement with the calculated value of 1.60 $g \cdot cm^{-3}$ for four molecules with a molecular weight of 321.5 $g \cdot mol^{-1}$ per unit cell.

Collection and Reduction of X-ray Intensity Data.-- The data were collected at room temperature (24°C) with graphite monochromated Mo Kα radiation on an automated four-circle diffractometer designed and built in the Ames Laboratory and previously described by Rohrbaugh and Jacobson[31]. All data within a 2θ sphere of 45° ($(\sin\theta)/\lambda$ = 0.538 $Å^{-1}$) in the hkℓ and hk$\bar{\ell}$ octants were measured, using the step-scan technique.

As a general check on electronic and crystal stability, the intensities of three standard reflections were remeasured

every twenty-five reflections. These standard reflections were not observed to vary significantly throughout the entire period of data collection (~2½ days). Hence, a decomposition correction was unnecessary. A total of 3641 reflections were recorded in this manner for the hkℓ and hk$\bar{\ell}$ octants. Examination of the data revealed the following systematic absences: h0ℓ when ℓ = 2n + 1 and 0k0 when k = 2n + 1. These absences uniquely determine the space group as $P2_1/c$.

The intensity data were corrected for Lorentz and polarization effects and, since $\mu = 9.26\ cm^{-1}$, absorption corrections were made. The estimated error in each intensity was calculated by

$$\sigma_I^2 = C_T + 2C_B + (0.03\ C_T)^2 + (0.03\ C_B)^2,$$

where C_T and C_B represent the total and background counts, respectively, and the factor 0.03 represents an estimate of non-statistical errors. The estimated deviations in the structure factors were calculated by the finite difference method of Lawton and Jacobson[32]. Equivalent data were averaged and only those reflections where $|F_o| > 2.5\sigma(F_o)$ were retained for use in subsequent calculations. This yielded 1905 reflections. These data are on file with J. Agric. Food Chem. in the 1975 supplementary material and may be obtained by observing the information given on any current masthead page of that journal.

Solution and Refinement

The program MULTAN[33] was employed to obtain the phases for the 499 strongest reflections. The resultant E-map[34] using the best figure of merit unambiguously showed all 16 non-hydrogen positions.

These atoms were subsequently refined by a full-matrix least-squares procedure[35] minimizing the function $\Sigma\omega(|F_o| - |F_c|)^2$, where $\omega = 1/\sigma_F^2$, to a conventional discrepancy factor of $R = \Sigma||F_o| - |F_c||/|F_o| = 0.057$. At this point all 16 non-hydrogens had anisotropic temperature factors. The scattering factors used were those of Hanson *et al.* [36], modified for the real and imaginary parts of anomalous dispersion[37].

An independent refinement of the ring hydrogen parameters was followed by analysis of an electron density difference map which revealed the methyl hydrogen positions. These positions were then fitted, *via* a least-squares technique, to a tetrahedral model using the corresponding precise oxygen and carbon positions. The C-H distances were set equal to 1.0 Å with isotropic hydrogen temperature factors set equal to 4.5 Å^2.

Subsequent least-squares refinement without varying the methyl hydrogen parameters converged to a final $R = 0.051$. Since this procedure yielded slightly different methoxy carbon and oxygen positions, the methyl hydrogen positions were recalculated. Further refinements did not significantly alter

any atom parameters; the R factor did not change.

The final positional and thermal parameters are listed in Table I. Standard deviations were calculated from the inverse matrix of the final least-squares cycle. Bond lengths and angles are listed in Table II and Table III, respectively[38]. Dihedral angles and least-square planes are listed in Table IV.

Description of Structure and Discussion

The phenoxy group in ronnel shown in Figures 1 and 2[40] is, as expected, essentially planar (*cf.* Table IV). The thiophosphate group is tilted towards the H(1) side of the phenoxy group while the sulfur atom is twisted away from the C(1)-O(1)-P plane towards the Cl(3) side of the ring (*cf.* Table IV and Figure 2).

The molecules stack through the centers of inversion "causing" the phenoxy groups' planes to be parallel within the limits given in Table IV. Crystalline stability in the *y* direction can be seen to be partly a result of the hydrogen bond from the acidic H(2) to the sulfur *via* the two-fold screw operation (*cf.* Tables II and Figure 2).

The unusually elongated methoxy oxygen ellipsoids (*cf.* Figure 1) suggest some disordering of these atoms. Therefore an attempt was made to account for such disorder *via* a refinement substituting two half-oxygens for each methoxy oxygen approximately displaced by 0.9 Å along the major axis of the

Table I. Final atomic positional[a] and thermal[b] parameters for ronnel

	Fractional Coordinates			Atomic Temperature Factors					
Atom	x	y	z	β_{11}	β_{22}	β_{33}	β_{12}	β_{13}	β_{23}
Cl1	-1075(1)[c]	3787(1)	5349(1)	119(1)	164(2)	145(2)	2(1)	63(1)	-51(2)
Cl2	-2530(1)	1779(2)	3210(1)	73(1)	188(2)	131(2)	-12(1)	32(1)	-33(1)
Cl3	1618(1)	-290(2)	3372(1)	120(2)	166(2)	147(2)	42(1)	52(1)	-20(2)
S	2978(1)	3828(2)	3867(1)	107(1)	186(2)	122(2)	44(2)	43(1)	70(2)
P	3625(1)	2748(1)	5294(1)	69(1)	136(2)	97(1)	8(1)	22(1)	32(1)
O1	2780(3)	1610(3)	5441(3)	75(3)	124(5)	137(4)	4(3)	18(3)	31(4)
O2	4012(6)	3442(5)	6530(4)	463(13)	171(7)	310(5)	-140(8)	12(6)	1(5)
O3	4729(4)	1873(6)	5478(5)	134(5)	407(11)	345(9)	-150(7)	152(6)	266(9)
C1	1525(4)	1678(5)	4912(4)	73(5)	104(6)	92(5)	0(4)	20(4)	22(5)
C2	916(5)	2564(5)	5353(5)	91(6)	114(7)	87(5)	-15(5)	27(5)	-12(5)
C3	-331(4)	2600(5)	4830(4)	89(5)	110(6)	89(5)	-16(5)	40(5)	-15(5)
C4	-973(4)	1747(5)	3889(4)	75(4)	112(6)	80(5)	-8(4)	35(4)	-1(5)
C5	-361(5)	833(5)	3467(4)	95(6)	116(7)	75(5)	-13(5)	26(4)	-8(5)
C6	880(4)	824(5)	3966(4)	83(5)	105(6)	93(5)	11(4)	39(5)	11(5)
C7	4180(6)	4741(8)	6864(7)	154(8)	266(13)	166(9)	45(9)	55(7)	-31(9)
C8	5518(6)	1971(7)	4925(7)	138(7)	221(11)	181(9)	69(7)	59(7)	25(8)
H1	136(5)	303(5)	607(5)	220(73)[b]					
H2	-78(4)	29(4)	283(4)	121(63)					
C7H1	342	524	642	450					
C7H2	440	480	776	450					
C7H3	484	511	666	450					
C8H1	610	271	532	450					
C8H2	596	111	502	450					
C8H3	5507	217	404	450					

[a]The positional and thermal parameters for all non-hydrogen atoms are presented in fractional unit cell coordinates (x 10^4). All hydrogen positional parameters are (x 10^3); thermal, (x 10^2).

[b]The β_{ij} are defined by: $T = \exp(-(h^2\beta_{11} + k^2\beta_{22} + \ell^2\beta_{33} + 2hk\beta_{12} + 2h\ell\beta_{13} + 2k\ell\beta_{23}))$.
All methyl hydrogen isotropic B's have been set equal to 4.5. If only the β_{11} column is listed, this corresponds to an isotropic (B) value.

[c]In this and succeeding tables estimated standard deviations are given in parentheses for the least significant figures and include the error in the lattice constants. Since the methyl hydrogens were not refined, no standard deviations are given.

Table II. Selected interatomic distances (Å) for ronnel

Bonding Distances		Non-Bonding Distances			
			Via	Observed Distance	Total van der Waals Distances (Pauling[39])
Cl-C2	1.388(7)				
C2-C3	1.389(7)				
C3-C4	1.382(6)	S···H2	2_1	2.98(5)	3.05
C4-C5	1.393(7)	P=S···H2	"	4.66(5)	4.95[a]
C5-C6	1.379(7)	Cℓ 1···H2	c-glide	2.99(4)	3.0
C6-C1	1.384(7)	C5-H2···Cℓ 1	c-glide	3.495(6)	3.91[a]
		Cℓ 2···C8H1	c-glide	3.217(3)	3.0
C1-O1	1.400(6)	C8-C8H1···Cl 2	c-glide	3.886(8)	3.8[a]
C2-H1	0.95(5)	O2···C8H3	c-glide	2.822(5)	2.6
C3-Cℓ 1	1.750(5)	O3···C7H2	c-glide	3.543(7)	2.6
C4-Cℓ 2	1.736(5)				
C5-H2	0.93(5)	C7H2···C8H2	c-glide	2.76	2.4
C6-Cℓ 3	1.745(5)	C7H2···C8H3	c-glide	2.45	2.4
		C7-H_3···H_3-C8	c-glide	3.77(1)	4.0
O1-P	1.592(4)				
P=S	1.903(2)	Cℓ 2···C8H2	(1 cell in x)	3.430(1)	3.0
P-O2	1.535(5)	Cℓ 2...H_3-C8	(1 cell in x)	3.722(7)	3.8[a]
P-O3	1.545(4)				
O2-C7	1.347(8)	S···C7H1	Intramolecular	3.221(2)	3.05
O3-C8	1.369(7)	S...C7H3	Intramolecular	3.442(2)	3.05
		S···C8H3	Intramolecular	2.978(2)	3.05
		O2···C7H2	Intramolecular	1.927(5)	2.6
		O2···C7H3	Intramolecular	1.928(5)	2.6
		O3···C8H1	Intramolecular	1.945(5)	2.6
		O3···C8H2	Intramolecular	1.946(5)	2.6
		O3···C8H3	Intramolecular	1.946(5)	2.6

[a] Includes distance(s) from this table and assumes linear addition of radii.

Table III. Bond angles (degrees) for ronnel

Angle	Degrees
C1-C2-C3	119.9(5)
C2-C3-C4	120.0(4)
C3-C4-C5	120.0(4)
C4-C5-C6	119.9(5)
C5-C6-C1	120.3(4)
C6-C1-C2	119.9(4)
Cℓ 3-C6-C1	120.8(4)
Cℓ 3-C6-C5	118.9(4)
H2-C5-C6	118(3)
H2-C5-C4	122(3)
Cℓ 2-C4-C5	118.9(4)
Cℓ 2-C4-C3	121.1(4)
Cℓ 1-C3-C4	120.7(4)
Cℓ 1-C3-C2	119.2(4)
H1-C2-C3	119(3)
H1-C2-C1	120(3)
C6-C1-O1	119.6(4)
C2-C1-O1	120.5(4)
C1-O1-P	123.5(3)
S-P-O1	117.0(2)
S-P-O2	117.4(2)
S-P-O3	118.0(2)
O2-P-O3	103.0(4)
O2-P-O1	100.2(3)
O1-P-O3	98.0(3)
P-O2-C7	132.7(5)
P-O3-C8	139.1(4)

Table IV. Dihedral angles (degrees) and least-squares planes

Planes Defined by:	Dihedral Angle of Planes[a]
C1-C3-C5; C1-O1-P	69.4(4) (Towards H1)
C2-C4-C6; C1-O1-P	70.3(3) " "
C1-O1-P; O1-P-S	26.6(4) (Towards Cℓ 3)
C1-C3-C5; O1-O2-O3	23.5(2)

Plane[b] defined by Carbons 1-6:
(0.31008)X + (0.68053)Y - (0.66388)Z - (-2.59893) = 0

Atom	Distance from Plane (Å)
C1	0.0013
C2	-0.0094
C3	0.0059
C4	0.0056
C5	-0.0137
C6	0.0102

Plane[b] defined by all 12 phenoxy group members:
(0.32061)X + (-0.68689)Y + (0.65222)Z - (-2.55113) = 0

Atom	Distance from Plane (Å)	Atom	Distance from Plane (Å)
C1	0.0217	Cℓ 1	0.0803
C2	0.0123	Cℓ 2	-0.0085
C3	0.0078	Cℓ 3	0.0507
C4	-0.0134	H1	-0.0994
C5	-0.0340	H2	-0.0330
C6	0.0096	O1	0.0059

Plane[b] defined by C1,O1,P and S:
(0.40141)X + (0.68891)Y + (0.60355)Z - (4.53683) = 0

Atom	Distance from Plane (Å)
C1	0.0713
O1	-0.1355
P	0.1120
S	-0.0478

[a]Angles correspond to proper orientation shown in Figures 1 and 2, so that the phosphorus is tilted towards the H1 side of the ring and the sulfur is directed away from H1. This was also verified on the basis of intramolecular distances.

[b]Planes are defined as $c_1X + c_2Y + c_3Z - d = 0$, where X, Y, and Z are Cartesian coordinates which are related to the triclinic cell coordinates (x, y, z) by the transformations:

$X = xa \sin\gamma + zc((\cos\beta - \cos\alpha\cos\gamma)/\sin\gamma) = xa + zc\cos\beta$,

$Y = xa\cos\gamma + yb + zc\cos\alpha = yb$, and

$Z = zc\{(1-\cos^2\alpha - \cos^2\beta - \cos^2\gamma + 2\cos\alpha\cos\beta\cos\gamma)^{\frac{1}{2}}/\sin\gamma\} = zc\sin\beta$.

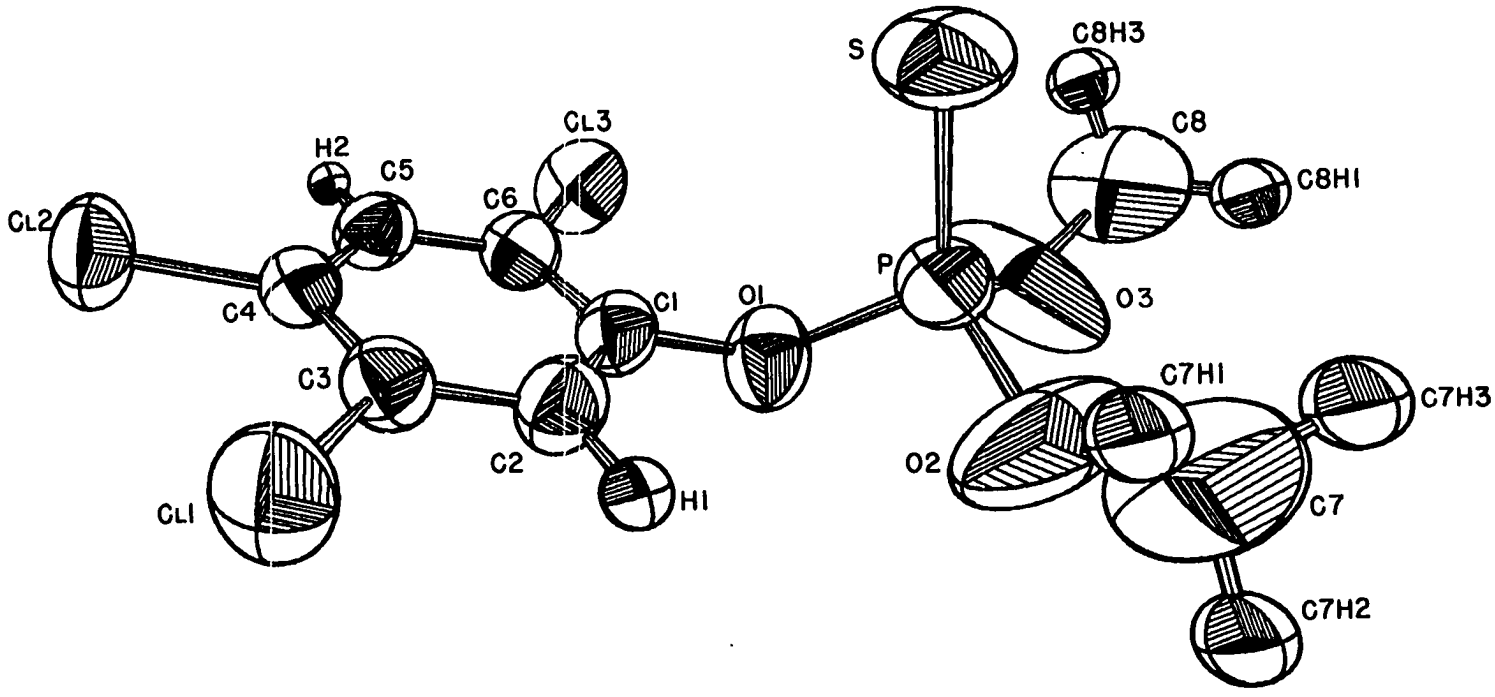

Figure 1. The ronnel molecule showing 50% probability ellipsoids.

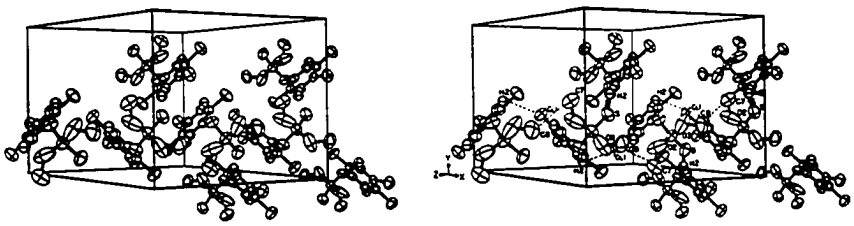

Figure 2. Stereographic view of two adjacent unit cells of ronnel illustrating intermolecular interactions.

ellipsoid. No splitting of methyl carbons was attempted though due to the much smaller elongation of these ellipsoids. This refinement reduced R by only 0.01 and did not produce a physically meaningful result. More importantly, distances and angles in the remaining and chemically significant part of the molecule remained essentially unchanged throughout either refinement. Therefore only the time-averaged model will be reported here.

Dilation of the P-O(2)-C(7) and P-O(3)-C(8) angles (*cf.* Table III) can easily be explained as a result of intramolecular van der Waals repulsions of the sulfur and methyl hydrogens. In fact, many of the hydrogens are less than the calculated van der Waals distance from the sulfur (*cf.* Table II).

The S-P-O set of angles ranges from 117° to 118°; the O-P-O set, from 98° to 103° (*cf.* Table III). Thus the phosphate group of ronnel displays a distorted tetrahedral geometry similar to that reported by Furberg[41] for H_3PO_4 and Coroxon[42]. The distorted geometry effectively corresponds to a tetrahedron which has been elongated along the three-fold axis, forming a trigonal pyramid.

In the present example there is rotational hindrance of the ester about the C(1)-O(1) bond arising from S···H(1) and S···Cl(3) interactions (*cf.* Figure 1). Each methyl group's rotation about a P-O(2 or 3) bond is restricted due to methyl hydrogen-sulfur interactions *vs.* lone pair-lone pair repulsions. In addition, the relatively long packing distances imply no

appreciable change in the solid state *vs. in vivo* structures.

The nitrogen to carboxyl carbon distance in the bromide salt of acetylcholine is 4.10 Å[24]. Since this is a direct measurement, as opposed to a deduced measurement, it provides a starting value for comparative analysis, as it is frequently possible to make solid state and significant *in vivo* comparisons. However, the value of 4.10 Å may not represent the true OP site-separation distance, as it is presently unknown[12].

On the other hand, using Krupka's[17] model of AChE and the distance of ~4.10 Å as starting guidelines, the following distances become quite interesting: P to H(2), 5.51; P to H(1), 2.83; S to H(1), 3.95; S to H(2), 5.49 Å. These distances initially seem to rule out the utilization of the acid ring hydrogens as an electrophilic "anchor" to any anionic site of AChE. However, the distance from the phosphorus to the center of the δ(+) ring is 4.05 Å. If only a weak bond is required for the anchoring of the non-esteratic portion of the molecule, the ring-anionic site interaction may be quite plausible. This would imply that the plane of the ring would almost have to arrive parallel to the enzyme surface.

The phosphorus ester displays a "scorpion-like" configuration (*cf.* Figure 1) with the C(1)-O(1)-P plane being only 20° away from the normal to the plane of the phenoxy group while the O(1)-P-S plane is only 27° from the C(1)-O(1)-P plane (*cf.* Table IV). This nearly perpendicular alignment of planes, then,

would facilitate phosphorylation, as would the exposed phosphorus. The exposed, scorpion-like configuration has also been observed in Coroxon[42] and some others to be presented, regardless of whether the insecticide, or its toxic metabolic derivative, is a phosphate or a thiophosphate ester. In frequent instances the study of only the parent insecticide may be all that is necessary to correlate structure with toxicity. But in other cases concurrent structural studies of the metabolic derivative(s) would also be desirable.

Work on acetylcholine bromide[24], choline chloride[43] and muscarine iodide[44] show, as pointed out by Canepa[24], that the structurally similar portions of the three molecules have very nearly identical three-dimensional structures. Their pharmacological effects are quite different even though the molecules are presumably unchanged *in vivo vs.* the solid state[24]. This would seem to imply that the portions which are not chemically and structurally in common are causing the observed variations in the inhibition of AChE. Similarly, there is a strong case for steric involvement in the mechanism of many, if not all, OP insecticides. Consequently, the precise distances afforded by X-ray crystallographic techniques will prove indispensable in the overall study of these processes.

THE CRYSTAL AND MOLECULAR STRUCTURE OF RONNEL OXON

Introduction

Ronnel oxon (O,O-dimethyl O-2,4,5- trichlorophenyl phosphate), $(H_3CO)_2P(O)C_6H_2Cl_3$, is the oxon form of ronnel. That is, P=S is replaced by P=O. This structure is quite important to know since *in vivo* many thiophosphates are converted to phosphates with one or both substances being toxic.

Experimental

Crystal Data.-- From a 99+% pure sample of the title compound, supplied by D. W. Osborne, a rectangular prismatic crystal with approximate dimensions 0.22 x 0.16 x 0.18 mm was selected and mounted on the end of a glass fiber using Elmer's Glue-All. Other glues with an organic solvent base tend to dissolve the OP insecticides. The crystal was then mounted on a four-circle diffractometer and three ω-oscillation photographs were taken at various χ and ϕ settings, and verified that the crystal was indeed single.

From these photographs fifteen independent reflections were selected and their coordinates were input into an automatic indexing program[29]. The reduced cell scalars which resulted indicated monoclinic symmetry, which was confirmed by inspection of ω-oscillation photographs taken about each of the three axes in turn. Only the *b* axis showed a mirror plane.

Observed layer-line spacings agreed, within experimental error, with those predicted for this cell by the indexing program.

The lattice constants were obtained from a least-squares refinement based on the precise $\pm 2\theta$ ($45^{\circ} > |2\theta| > 20^{\circ}$) measurements of fourteen strong independent reflections. At 27°C using Mo Kα (λ = 0.70954 Å) they are a = 9.659(5), b = 11.388(2), c = 14.465(9) Å and β = 130.09(4)°. The observed density of 1.63(3) $g \cdot cm^{-3}$ determined by the flotation method is in good agreement with the calculated value of 1.668 $g \cdot cm^{-3}$ for four molecules having a molecular weight of 305.5 $g \cdot mol^{-1}$ in a unit cell having a volume of 1217.25 $Å^3$.

Collection and Reduction of X-ray Intensity Data.-- The data were collected at 27°C with graphite monochromated Mo Kα radiation on an automated four-circle diffractometer designed and built in the Ames Laboratory and previously described by Rohrbaugh and Jacobson[31]. All data within a 2θ sphere of 50° ($(\sin\theta)/\lambda$ = 0.596 $Å^{-1}$) in the hkℓ and $\bar{h}k\ell$ octants were measured using an ω-stepscan technique.

As a general check on electronic and crystal stability, the intensities of three standard reflections were remeasured every seventy-five reflections. These standard reflections were not observed to vary significantly throughout the entire period of data collection (∿ 2 days). Hence a decomposition correction was unnecessary. A total of 2420 reflections were recorded in this manner. Examination of the data revealed the following systematic absences: h0ℓ when ℓ = 2n + 1 and 0k0 when

$k = 2n + 1$. These absences uniquely determine the space group as $P2_1/c$.

The intensity data were corrected for Lorentz and polarization effects and, since $\mu = 9.21\ cm^{-1}$, absorption corrections were not made; maximum and minimum transmission factors were 0.863 and 0.817, respectively. The estimated variance in each intensity was calculated by:

$$\sigma_I^2 = C_T + 2C_B + (0.03C_T)^2 + (0.03C_B)^2,$$

where C_T and C_B represent the total and background counts, respectively, and the factor 0.03 represents an estimate of non-statistical errors. The estimated deviations in the structure factors were calculated by the finite difference method[32]. Equivalent data were averaged and 1848 reflections with $|F_o| > 2.5\sigma(F_o)$ were retained for use in subsequent calculations. During later work it was discovered that six large reflections showed appreciable secondary extinction effects. The data were corrected *via* the approximation $I_o^{corr} = I_o(1+2gI_c)$, where an average value for $g = 4.68 \times 10^{-5}$ was determined using the fifteen largest I_o's. The data will be found in the 1978 supplementary material section of J. Agric. Food Chem. See any current masthead page for ordering the information.

Solution and Refinement

The program MULTAN[33] was employed to obtain the phases for the 499 strongest reflections. The resultant E-map[34] using the best figure of merit unambiguously showed the positions of

thirteen of the sixteen total non-hydrogen atoms. All remaining atoms were found by successive structure factor[35] and electron density map calculations[34]. These atomic positions were subsequently refined by a full-matrix least-squares procedure[35] minimizing the function $\Sigma\omega(|F_o| - |F_c|)^2$, where $\omega = 1/\sigma_F^2$. This refinement yielded a conventional discrepancy factor of $R = \Sigma||F_o|-|F_c||/\Sigma|F_o| = 0.153$. At this stage of the refinement all non-hydrogen atoms had been refined using isotropic thermal parameters. The scattering factors used were those of Hanson, *et al.*[36], modified for the real and imaginary parts of anomalous dispersion[37]. The scattering factors for hydrogen were those of Stewart, *et al.*[45].

Analysis of an electron density difference map did not reveal either the ring or the methyl hydrogens. Consequently, the ring hydrogen atom positions were fixed at 0.95 Å from the corresponding carbons (C(3) and C(6)). Methyl hydrogens were approximated by two sets of half-hydrogens inserted at tetrahedral positions using the precise positions of the corresponding methyl carbon and the methoxy oxygen and rotated by 60° relative to one another. This created a "doughnut of hydrogens". The methyl C-H distances were set equal to 1.0 Å; all isotropic hydrogen temperature factors were set equal to 4.5 Å^2.

Subsequent anisotropic least-squares refinement without varying the hydrogen parameters converged to R = 0.060. Since this procedure yielded slightly different non-hydrogen atom positions, all of the hydrogen positions were recalculated.

The final positional and thermal parameters are listed in Table V. Standard deviations were calculated from the inverse matrix of the final least-squares cycle. Bond lengths and angles are listed in Table VI and Table VII, respectively[38]. Dihedral angles and least-square planes are listed in Table VIII.

Description of Structure and Discussion

The phenoxy group in ronnel oxon, shown in Figures 3 and 4[40], is essentially planar (*cf.* Table VIII, Plane III). For the most part, packing in the ronnel oxon crystal can be regarded as either weakly coulombic or van der Waals in nature. The former is a manifestation of the charge density distribution within each individual molecule and hence corroborates one's "chemical intuition" of atoms with $\delta(+)$ and $\delta(-)$ charges. The H(1)···O(2) interaction related *via* the c-glide operation serves as such an example (*cf.* Figure 4 and Tables VI and VII), while on the other hand, the O(2)···C(7)H_3 and C(8)H_3···Cℓ(3) interactions appear to be van der Waals in character (*cf.* Table VI).

The C(1)-O(1) bond in ronnel oxon is significantly (>10σ) shorter than the two methoxy C-O bonds (*cf.* Table VI), while the P-O(1) bond is the longest of the three P-O bonds, being at least 10σ longer than the other two. These observations, which are in agreement with CNDO II molecular orbital calculations of the Pople and Beveridge[47] type, are consistent with a bonding formulation in which there is a weak π overlap of the

Table V. Final atomic positional[a] and thermal[b] parameters for ronnel oxon

	Fractional Coordinates			Atomic Temperature Factors					
Atom	x	y	z	β_{11}	β_{22}	β_{33}	β_{12}	β_{13}	β_{23}
Cℓ(1)	0.0754(1)[c]	0.7603(1)	0.5886(1)	21.6(2)	9.5(1)	11.0(1)	-0.4(1)	10.7(1)	1.4(1)
Cℓ(2)	-0.1213(2)	0.9231(1)	0.1870(1)	25.0(3)	12.6(1)	6.6(1)	2.2(1)	7.3(1)	-0.5(1)
Cℓ(3)	0.2408(2)	1.0730(1)	0.3475(1)	29.7(3)	12.6(1)	11.0(1)	-1.0(1)	13.7(2)	1.4(1)
P	0.5180(1)	0.8459(1)	0.8083(1)	15.2(2)	7.7(1)	7.0(1)	1.0(1)	5.6(1)	0.8(1)
O(1)	0.3394(3)	0.9222(2)	0.7150(2)	17.3(5)	9.0(2)	6.8(2)	2.3(3)	6.4(3)	0.7(2)
O(2)	0.5843(4)	0.7909(3)	0.7530(3)	23.2(7)	14.4(4)	10.7(3)	6.0(4)	9.4(4)	1.0(3)
O(3)	0.6439(4)	0.9343(3)	0.9129(3)	22.4(6)	11.4(3)	8.1(3)	-2.6(3)	6.7(3)	0.2(2)
O(4)	0.4716(4)	0.7570(3)	0.8646(3)	25.6(7)	10.0(3)	11.7(3)	0.9(4)	10.1(4)	2.6(2)
C(1)	0.2384(5)	0.9169(3)	0.5912(3)	14.0(6)	7.0(3)	6.7(3)	2.0(3)	5.6(4)	0.5(2)
C(2)	0.0840(5)	0.8476(3)	0.5209(3)	15.7(7)	7.2(3)	8.2(3)	1.3(4)	7.4(4)	0.9(3)
C(3)	-0.0265(5)	0.8496(3)	0.3963(3)	16.2(7)	8.2(3)	8.1(3)	0.5(4)	6.8(4)	-0.4(3)
C(4)	0.0198(5)	0.9196(3)	0.3418(3)	15.8(7)	8.4(3)	6.6(3)	2.4(4)	5.7(4)	0.1(3)
C(5)	0.1774(5)	0.9869(3)	0.4126(3)	18.8(8)	8.0(3)	8.6(4)	1.4(4)	8.9(5)	0.5(3)
C(6)	0.2853(5)	0.9861(3)	0.5375(3)	17.2(7)	7.5(3)	8.0(3)	-0.3(4)	7.8(4)	-0.1(3)
C(7)	0.7147(8)	1.0349(5)	0.8955(5)	36(1)	12.9(5)	11.6(5)	-7.9(7)	12.9(8)	-1.5(4)
C(8)	0.4023(7)	0.7910(5)	0.9248(5)	29(1)	14.0(5)	13.2(5)	0.1(6)	14.5(7)	3.0(4)
H(1)	-0.133	0.803	0.349	4.5					
H(2)	0.391	1.033	0.586	4.5					

[a] The positional parameters for all atoms are represented in fractional unit cell coordinates.

[b] The β_{ij} are defined by: $T = \exp(-(h^2\beta_{11} + k^2\beta_{22} + \ell^2\beta_{33} + 2hk\beta_{12} + 2h\ell\beta_{13} + 2k\ell\beta_{23}))$. If only the β_{11} column is listed, this corresponds to an isotropic temperature factor. All hydrogen isotropic temperature factors have been set equal to 4.5 . Non-hydrogen thermal parameters are ($\times 10^3$).

[c] In this and succeeding tables estimated standard deviations are given in parentheses for the least significant figures; later tables include the error in the lattice constants. Since the hydrogen parameters were not refined, no standard deviations are given. Positions for the methyl hydrogens are not given as they were approximated.

Table VI. Selected interatomic distances (Å) for ronnel oxon

Bonding Distances		Non-Bonding Distances			
		Interaction	via	Observed Distance	Total van der Waals Distance (from Pauling[39])
C(1)-C(2)	1.388(5)				
C(2)-C(3)	1.382(5)				
C(3)-C(4)	1.382(5)				
C(4)-C(5)	1.395(6)	P···H(1)	Intramolecular	5.487(5)	(3.1)
C(5)-C(6)	1.387(5)	P···H(2)	Intramolecular	3.367(2)	3.1
C(6)-C(1)	1.373(5)	P···Cℓ(1)	Intramolecular	3.770(3)	3.7
		P···C(7)H_3	Intramolecular	2.597(5)	3.9[a]
C(1)-O(1)	1.383(4)	P···C(8)H_3	Intramolecular	2.627(5)	3.9[a]
C(2)-Cℓ(1)	1.726(4)	Cℓ(1)···O(1)	Intramolecular	2.966(3)	3.20
C(3)-H(1)	0.950(4)	C(7)H_3···O(1)	Intramolecular	3.195(6)	3.4[a]
C(4)-Cℓ(2)	1.716(4)	C(8)H_3···Cℓ(1)	Intramolecular	3.772(6)	3.8[a]
C(5)-Cℓ(3)	1.723(4)	C(8)H_3···O(3)	Intramolecular	2.934(6)	3.4[a]
C(6)-H(2)	0.950(4)				
		Cℓ(2)···O(3)	-1cell in x and z	3.048(4)	3.20
P-O(1)	1.599(3)	Cℓ(1)···C(7)H_3	2_1 +1cell in x and z -1in y	3.493(5)	3.8
P=O(2)	1.450(3)	O(2)···C(7)H_3	2_1 +1cell in x and z -1in y	3.669(7)	3.4
P-O(3)	1.552(3)	O(4)···H(2)	2_1 +1cell in x and z -1in y	2.749(3)	3.0
P-O(4)	1.536(3)	O(4)···C(6)	2_1 +1cell in x and z -1in y	3.572(5)	3.1
O(3)-C(7)	1.442(5)	Cℓ(3)···C(8)H_3	2_1 +1cell in x and z -1in y	3.778(6)	3.8
O(4)-C(8)	1.451(6)	O(2)···C(3)	c-glide +1cell in y -1in x and z	3.309(5)	3.1[b]
		O(2)···H(1)	c-glide +1cell in y -1in x and z	2.379(3)	3.6

[a] Assumes linear addition of a "spherical" methyl goup van der Waals radius.
[b] Bondi[46]

Table VII. Bond angles (degrees) for ronnel oxon

Angle	Degrees
C(1)-C(2)-C(3)	120.6(3)
C(2)-C(3)-C(4)	119.4(3)
C(3)-C(4)-C(5)	120.0(3)
C(4)-C(5)-C(6)	120.1(3)
C(5)-C(6)-C(1)	119.8(3)
C(6)-C(1)-C(2)	120.1(3)
O(1)-C(1)-C(2)	120.2(3)
O(1)-C(1)-C(6)	119.6(3)
Cl(1)-C(2)-C(1)	120.1(3)
Cl(1)-C(2)-C(3)	119.3(3)
H(1)-C(3)-C(2)	120.4(4)
H(1)-C(3)-C(4)	120.3(4)
Cl(2)-C(4)-C(3)	118.7(3)
Cl(2)-C(4)-C(5)	121.3(3)
Cl(3)-C(5)-C(4)	121.0(3)
Cl(3)-C(5)-C(6)	118.8(3)
H(2)-C(6)-C(5)	120.1(4)
H(2)-C(6)-C(1)	120.1(4)
C(1)-O(1)-P	123.2(2)
O(1)-P-O(2)	112.9(2)
O(1)-P-O(3)	102.1(2)
O(1)-P-O(4)	106.3(2)
O(2)-P-O(3)	118.4(2)
O(2)-P-O(4)	113.0(2)
O(3)-P-O(4)	102.7(2)
P-O(3)-C(7)	120.3(3)
P-O(4)-C(8)	123.2(3)
P-O(2)...H(1)[a]	128.6(2)
P-O(4)...H(2)[b]	119.7(2)

[a] Through 2_1 + 1 cell in $\underline{x}$ and $\underline{z}$ - 1 in $\underline{y}$.

[b] Through $\underline{c}$-glide + 1 cell in $\underline{y}$ -1 in $\underline{x}$ and $\underline{z}$.

Table VIII. Torsional angles (degrees) and least-squares planes

Torsional Angle	
P-O(1)-C(1)-C(2)	97.98
O(2)-P-O(1)-C(1)	12.51
O(1)-P-O(3)-C(7)	-68.70
O(1)-P-O(4)-C(8)	-55.38
O(2)-P-O(3)-C(7)	55.92
O(2)-P-O(4)-C(8)	-179.80

Plane(I)[a] Defined by C(1), O(1), P and O(2):
(0.56915) X + (0.81552) Y + (0.10483) Z - (7.41029) = 0

Atom	Distance from Plane (Å)
C(1)	-0.033
O(1)	0.059
P	-0.054
O(2)	0.028
C(4)	-0.177
Cℓ(2)	-0.279

Plane(II)[a] Defined by C(8), O(4), P and O(2):
(0.49175) X + (0.06157) Y + (0.86855) Z - (7.11910) = 0

Atom	Distance from Plane (Å)
C(8)	-0.001
O(4)	0.001
P	0.001
O(2)	-0.001

Plane(III)[a] Defined by all twelve phenoxy group members:
(-0.65204) X + (0.75669) Y - (0.04737) Z - (9.69391) = 0

Atom	Distance from Plane Å
C(1)	-0.013
C(2)	-0.028
C(3)	-0.006
C(4)	0.003
C(5)	-0.017
C(6)	-0.010
O(1)	0.083
Cℓ(1)	-0.036
H(1)	0.000
Cℓ(2)	0.062
Cℓ(3)	-0.036
H(2)	-0.003

[a]Planes are defined by $c_1X + c_2Y + c_3Z - d = 0$, where X, Y and Z are Cartesian coordinates which are related to the triclinic cell coordinates (x, y, z) by the transformations:

$$X = xa\sin\gamma + zc[(\cos\beta - \cos\alpha\cos\gamma)/\sin\gamma)] = xa + zc\cos\beta$$
$$Y = xa\cos\gamma + yb + zc\cos\alpha = yb$$
$$Z = zc[1 - \cos^2\alpha - \cos^2\beta - \cos^2\gamma + 2\cos\alpha\cos\beta\cos\gamma)^{1/2}/\sin\gamma] = zc\sin\beta.$$

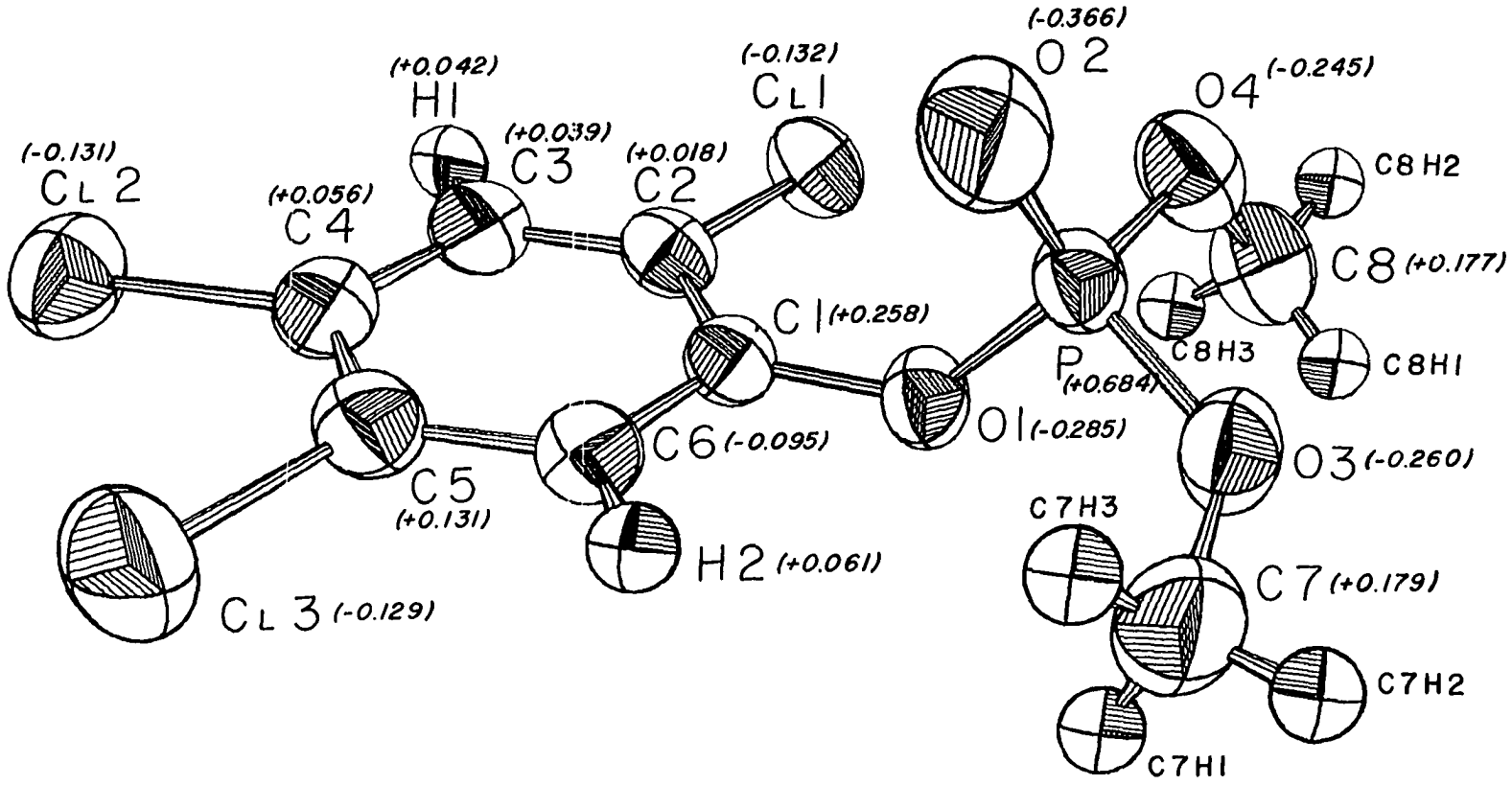

Figure 3. The ronnel oxon molecule showing 50% probability ellipsoids; 30% for hydrogens. The numbers in parentheses refer to partial charge densities from a CNDO II calculation.

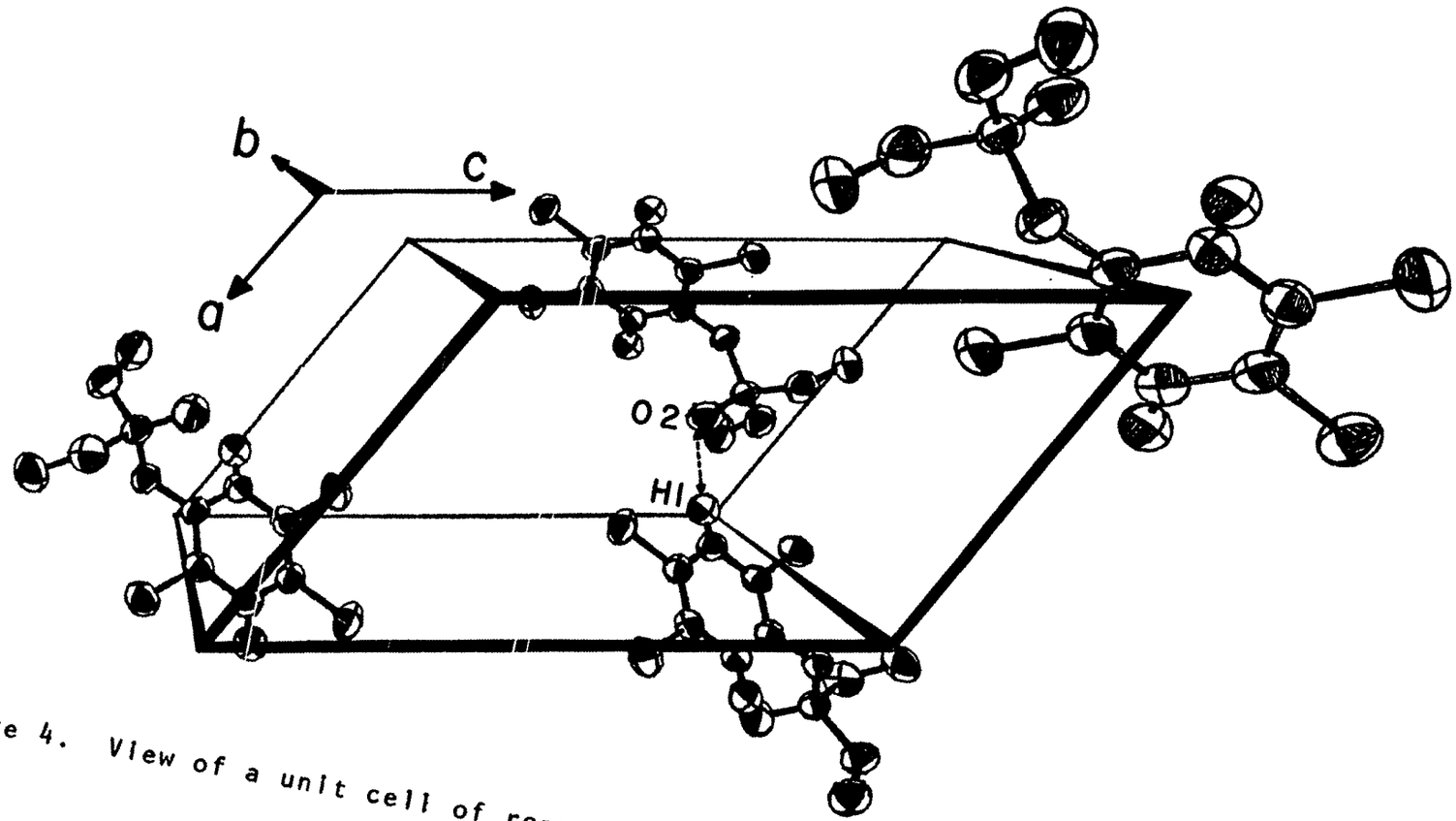

Figure 4. View of a unit cell of ronnel oxon.

p_z orbital on the oxygen with the ring system which simultaneously weakens the O-P bond. The latter effect should enhance phosphorylation[48]. Such variations in bond lengths have been noted earlier as the bond lengths corresponding to P-O(1) and C(1)-O(1) in ronnel oxon, ronnel and Coroxon[42] are all within 3σ of being identical. The angles of the type S=P-O or O=P-O in these compounds are all greater than the tetrahedral angle of 109.47°. In ronnel oxon the angle between the normal to the ring and the P=O vector is 34.4° which is nearly identical to the angle of 34.8° between the normals to the O(1)-O(3)-O(4) plane and the ring. Comparable angles of 23.7, 38.5, 23.9 and 23.5° have been observed in ronnel, Coroxon, azinphosmethyl[49] and amidithion[50], respectively. The latter case is the most surprising as amidithion has many more rotational degrees of freedom and consequently is not as rigid as the other compounds.

As a result of Cℓ(2) and Cℓ(3) being less than the sum of their van der Waals radii apart, the following angles are significantly (>3σ) dissimilar: Cℓ(2)-C(4)-C(5)>Cℓ(2)-C(4)-C(3) and Cℓ(3)-C(5)-C(4)>Cℓ(3)-C(5)-C(6) (*cf.* Figure 3 and Tables VI and VII). The C(1)-O(1)-P angle is considerably greater than the tetrahedral angle (*cf.* Table VII) yet is identical with the corresponding angle in ronnel. Therefore the <u>difference</u> in van der Waals radii of the respective doubly bonded atoms (oxygen *vs.* sulfur) does not seem to be the major source of this discrepancy. The "p_z-ring" bonding noted earlier

likely serves to modify the hybridization on O(2), though van der Waals interactions with the ring are not completely negligible.

In contrast to ronnel the O-Me vectors in ronnel oxon are approximately pointed in the opposite direction as the P-O(2) vector. The actual direction may be a function of crystal packing as intermolecular interactions involving methyl groups exist in both compounds. Yet the sets of methyl groups in both compounds basically tend to align in a pairwise, unidirectional fashion, probably due to the lone pair repulsions of the methoxy oxygens and the doubly-bonded moiety.

As with ronnel, the phosphorus in ronnel oxon is opposite the Cl(1) side of a plane which is perpendicular to the ring and contains the C(1)-O(1) bond. The position of the phosphorus appears to be dictated by the van der Waals interactions of the phosphorus with H(2) and/or Cl(1) (*cf.* Table VI), thus restricting rotation about the C(1)-O(1) bond to quite a small range of angles. Furthermore, the phosphorus is nearly symmetrically placed with respect to the ring, being 3.52 and 3.41 Å away from C(2) and C(6), respectively, and having a C(2)-C(1)-O(1)-P torsional angle of $\sim 98^{\circ}$ (*cf.* Table VIII).

On the basis of a restricted phosphorus position, comparison of some intramolecular distances with literature site-separation distances for AChE should give some insight into the toxicity/activity of ronnel oxon. This should be a reasonable approximation to the true OP site-separation distance even

though the OP's and ACh do not utilize the same site on AChE[12]. But, since the OP's presently being investigated are comparable in size to ACh, comparisons of the distances in the OP's could be utilized to help deduce the OP active site. In addition to being "distance compatible", the two atoms involved must also be "charge compatible" to at least be in agreement with the AChE model of Krupka[17]. Only two atoms are being considered here in accordance with the presence of two residues in Krupka's active site of AChE. Analysis of the steric interactions of the remaining parts of both molecules, without knowing more about the structure(s) of the isozymes of AChE, would be futile.

Using a CNDO II calculation (after Pople and Beveridge[47]) approximate values for the charge density distribution in ronnel oxon can be computed; results are shown in parentheses in Figure 3. Examination of this figure shows than P···H(1) (5.49 Å), P···C(3) (4.78 Å), P···C(4) (5.25 Å) and P···C(5) (4.68 Å) are interesting pairs in this regard. These distances fall outside of or just border the mammalian AChE site-separation range or 4.3-4.7 Å[51,52], and yet are close to or within the range for insect AChE given by Hollingworth *et al.*[51] of 5.0-5.5 Å and O'Brien[52] of 4.5-5.9 Å. It is even conceivable that "C(5)-C(4)-C(3)-H(1)" might correspond to a region of δ(+) charge having P···δ(+) distances of from 4.68 to 5.49 Å. Considering charge, distance, steric factors and overall reactivity, P···H(1) <u>may</u> be slightly favored as a reactive species towards insect AChE in ronnel oxon. The P···C(5) pair, due to

its shorter distance, may play a more important role in mammalian toxicity, unless significant conformational alterations in AChE or ronnel oxon accompany any *in vivo* free energy changes.

It should be noted that even rotations about the C(1)-O(1) bond of $\pm 40^{\circ}$, which may possibly be achieved *in vivo*, would correspond to a maximum change in the P···H(1) distance, for example, of only ± 0.03 Å which is not likely to be critical with respect to the distances in AChE and to the I_{50} of the insecticide as pertains to the conformation which AChE or ronnel oxon might have to distort to in order to achieve a distance "match". However, such a rotation would cause the phosphorus to be in a slightly different position relative to the other ring substituents. This may be partially responsible, then, for changes in I_{50} and/or LD_{50} values as a result ot subtle influences of the insecticide with AChE. In this regard it would be quite interesting to compare the toxicities of the pure d and ℓ forms of ronnel oxon; a 1:1 racemic mixture is present in a centrosymmetric space group. But, in order to make better comparisons and predictions, many heretofore unreported insect and mammalian I_{50} and LD_{50} values will need to be investigated and tabulated, especially for the different isozymes of AChE. In addition, CNDO calculations will need to be performed to obtain a better idea of the charge distribution and potential energy barriers which may be necessary to overcome in adduct formation.

THE CRYSTAL AND MOLECULAR STRUCTURE OF BROMOPHOS

Introduction

The crystal and molecular structure of bromophos (O-(4-bromo-2,5-dichlorophenyl) O,O-dimethyl phosphorothioate), $(H_3CO)_2P(S)OC_6H_2Cl_2Br$, was undertaken to explore any differences and/or similarities with the previous structures resulting from the replacement of a para chlorine atom in ronnel with a bromine. This replacement could explain, in part, the high LD_{50} of 3750-6100 $mg \cdot kg^{-1}$ which bromophos has for rats[28].

Experimental

Crystal Data.-- A sample of 99+% pure bromophos was supplied by the Quality Assurance Section, Pesticides and Toxic Substances Laboratory, U. S. Environmental Protection Agency. From this, a rectangular prismatic crystal with approximate dimensions 0.15 x 0.12 x 0.07 mm was selected and mounted on the end of a glass fiber using Elmer's Glue-All. Preliminary oscillation photographs indicated a single crystal with *mmm* (orthorhombic) symmetry. The crystal was then mounted on a four-circle diffractometer and three ω-oscillation photographs were taken at various χ and ϕ settings.

From these photographs seventeen independent reflections were selected and their coordinates were input into an automatic indexing program[29]. The reduced cell and reduced cell

scalars which resulted from this program indicated orthorhombic symmetry, which was confirmed by inspection of ω-oscillation photographs taken about each of the three axes in turn. All axes showed mirror symmetry. Observed layer-line spacings agreed, within experimental error, with those predicted for this cell by the indexing program.

The lattice constants were obtained from a least-squares refinement using the Nelson-Riley extrapolation function[30] based on the precise ±2θ ($|2\theta| > 20^{\circ}$) measurements of fifteen strong independent reflections. At 27°C using Mo Kα radiation (λ = 0.70954 Å) they are a = 7.308(6), b = 27.17(2) and c = 6.446(8) Å. The observed density of 1.90 ± 0.02 $g \cdot cm^{-3}$ determined by the flotation method is in good agreement with the calculated value of 1.889 $g \cdot cm^{-3}$ for four molecules having a molecular weight of 366.00 $g \cdot mol^{-1}$ per unit cell with a volume of 1279.56 $Å^3$.

Collection and Reduction of X-ray Intensity Data.-- The data were collected at 27°C with graphite monochromated Mo Kα radiation on an automated four-circle diffractometer designed and built in the Ames Laboratory and previously described by Rohrbaugh and Jacobson[31]. All data within a 2θ sphere of 45° ($(\sin\theta)/\lambda$ = 0.539 $Å^{-1}$) in the hkℓ and hk$\bar{\ell}$ octants were measured, using an ω-stepscan technique.

As a general check on electronic and crystal stability, the intensities of three standard reflections were remeasured every seventy-five reflections. These standard reflections

were not observed to vary significantly throughout the entire period of data collection ($\sim$ 2 days). Hence, a decomposition correction was unnecessary. A total of 2533 reflections were recorded in this manner. Examination of the data revealed the following systematic absences: h00 when h = 2n + 1, 0k0 when k = 2n + 1 and 00ℓ when ℓ = 2n + 1. These absences uniquely determine the space group as $P2_12_12_1$.

The intensity data were corrected for Lorentz and polarization effects and, since μ = 40.25 cm^{-1}, absorption corrections were also made; maximum and minimum transmission factors were 0.755 and 0.547, respectively. The estimated error in each intensity was calculated by

$$\sigma_I^2 = \{C_T + 2C_B + (0.03\ C_T)^2 + (0.03\ C_B)^2 + (0.03\ C_N)^2\}/A^2,$$

where C_T, C_B and C_N represent the total, background and net counts, respectively, A is the transmission factor and the factor 0.03 represents an estimate of non-statistical errors. The estimated standard deviations in the structure factors were calculated by the finite difference method[32]. Equivalent data were averaged and 1225 reflections with $|F_o| > 2.5\sigma(F_o)$ were retained for use in subsequent calculations. During later work it was discovered that eight large reflections suffered from secondary extinction effects; these were eliminated from the final stages of refinement. These data are to be found on file with J. Agric. Food Chem. in the 1976 supplementary material and may be obtained by observing the information given on any current masthead page of that journal.

Solution and Refinement

The position of the bromine was obtained from an analysis of a standard three-dimensional Patterson function. The remaining atoms were found by successive structure factor[35] and electron density map calculations[34]. These atomic positions were subsequently refined by a full-matrix least-squares procedure[35] minimizing the function $\Sigma\omega(|F_o|-|F_c|)^2$, where $\omega = 1/\sigma_F^2$, to a conventional discrepancy factor of $R = \Sigma||F_o|-|F_c||/|F_o| = 0.058$. At this stage all sixteen non-hydrogen atoms had been refined with anisotropic thermal parameters. The scattering factors used were those of Hanson, *et al.*[36], modified for the real and imaginary parts of anomalous dispersion[37].

Ring hydrogen atom positions were fixed at 0.95 Å from the corresponding carbons. Analysis of an electron density difference map[34] did not reveal the individual methyl hydrogen positions. Consequently, approximate tetrahedral positions were inferred from the precise corresponding methoxy oxygen and carbon positions. The methyl C-H distances were set equal to 1.0 Å; all isotropic hydrogen temperature factors were set equal to 4.5 Å^2.

Subsequent least-squares refinement without varying the hydrogen parameters converged to R = 0.048. Since this procedure yielded slightly different carbon and oxygen positions, all of the hydrogen positions were recalculated. Further refinement cycles did not significantly alter any atomic param-

eters and the discrepancy factor did not change.

The final positional and thermal parameters are listed in Table IX. Standard deviations were calculated from the inverse matrix of the final least-squares cycle. Bond lengths and angles are listed in Table X and Table XI, respectively[38]. Dihedral angles and least-square planes are listed in Table XII.

Description of Structure and Discussion

The phenoxy group in bromophos shown in Figures 5 and 6[40] is, as expected, essentially planar (*cf.* Table XII, Plane II). The phosphorus is, as with ronnel and ronnel oxon, tilted toward the H(1) side of a plane perpendicular to the ring and coincident with the C(1)-O(1) bond while the sulfur is twisted away from the C(1)-O(1)-P plane towards the Cl(2) side of the ring (*cf.* Table XII and Figures 5 and 7). However, unlike ronnel or ronnel oxon, in bromophos the distance between H(1) and O(3) (2.61 Å) is indicative of a possible hydrogen bond between the aromatic C(2) atom and the O(3) atom (*cf.* Table X and Figure 7). Both the P-O(3)-H(1) angle of 100.5° and the C(8)-O(3)-H(1) angle of 130° would direct H(1) approximately towards a lone pair lobe on O(3), assuming sp^3 hybridization, thus strengthening a hydrogen bond argument (*cf.* Table XI). The P, O(3), H(1) and C(1) atoms form a near planar grouping (*cf.* Table XII, Plane III).

For the most part, packing in the bromophos crystal can be regarded as either weakly coulombic or van der Waals in nature.

Table IX. Final atomic positional[a] and thermal[b] parameters for bromophos

	Fractional Coordinates			Atomic Temperature Factors					
Atom	x	y	z	β_{11}	β_{22}	β_{33}	β_{12}	β_{13}	β_{23}
Br	0.2355(1)[c]	0.18887(2)	0.0773(1)	17.2(1)	0.90(1)	28.3(2)	-0.40(3)	-3.1(2)	-0.46(4)
Cl 1	0.4044(3)	0.22662(8)	0.5173(4)	23.6(5)	1.13(3)	26.0(6)	-0.1(1)	-5.8(5)	1.1(1)
Cl 2	0.1954(3)	0.38363(8)	-0.1393(4)	25.1(5)	1.16(3)	28.8(7)	-0.4(1)	-10.0(5)	0.9(1)
S	0.6609(3)	0.43542(9)	0.0094(4)	21.7(5)	1.37(3)	19.1(6)	-0.3(1)	3.4(5)	-0.0(1)
P	0.5392(2)	0.43276(7)	0.2688(3)	13.9(4)	0.80(2)	17.4(5)	-0.03(9)	-1.0(4)	-0.0(1)
O 1	0.3493(7)	0.4032(1)	0.2780(9)	14(1)	0.92(7)	24(1)	0.0(2)	0(1)	-1.3(3)
O 2	0.4753(8)	0.4838(2)	0.3467(9)	20(1)	0.92(7)	20(1)	0.0(2)	0(1)	-0.3(2)
O 3	0.6439(9)	0.4064(2)	0.451(1)	17(1)	1.35(9)	23(1)	-0.7(2)	-4(1)	1.6(3)
C 1	0.332(1)	0.3536(2)	0.227(1)	12(1)	0.87(9)	23(2)	-0.7(3)	2(1)	0.0(4)
C 2	0.383(1)	0.3189(2)	0.373(1)	12(1)	1.0(1)	22(2)	-0.4(3)	0(1)	-0.4(4)
C 3	0.350(1)	0.2693(2)	0.329(1)	13(1)	1.0(1)	20(2)	0.0(3)	-3(1)	-0.2(4)
C 4	0.279(1)	0.2554(2)	0.143(1)	12(1)	0.9(1)	20(2)	-0.3(3)	0(1)	-0.5(4)
C 5	0.231(1)	0.2911(3)	-0.004(1)	14(1)	1.0(1)	19(1)	0.4(3)	-1(1)	-0.4(4)
C 6	0.258(1)	0.3393(2)	0.040(1)	13(1)	0.9(1)	21(2)	0.0(3)	-3(1)	0.2(4)
C 7	0.324(1)	0.4901(3)	0.546(1)	30(2)	1.0(1)	28(3)	0.3(5)	5(2)	-1.3(5)
C 8	0.837(1)	0.4125(4)	0.478(1)	15(1)	1.8(1)	34(3)	-0.4(4)	-7(2)	-0.4(7)
H 1	0.4380	0.3236	0.5009	45					
H 2	0.1809	0.2816	-0.1338	45					
C7H1	0.2672	0.5084	0.5259	45					
C7H2	0.4609	0.5093	0.6414	45					
C7H3	0.3589	0.4572	0.6084	45					
C8H1	0.8623	0.4449	0.5473	45					
C8H2	0.8859	0.3853	0.5079	45					
C8H3	0.8997	0.4116	0.3406	45					

[a] The positional parameters for all atoms are represented in fractional unit cell coordinates.

[b] The β_{ij} are defined by: $T = \exp(-(h^2\beta_{11} + k^2\beta_{22} + l^2\beta_{33} + 2hk\beta_{12} + 2hl\beta_{13} + 2kl\beta_{23}))$. If only the β_{ij} column is listed, this corresponds to an isotropic temperature factor. All hydrogen isotropic B's have been set equal to 4.5 . Non-hydrogen thermal parameters are ($\times 10^3$). All hydrogen thermal parameters are (x10).

[c] In this and succeeding tables estimated standard deviations are given in parentheses for the least significant figures and include the error in the lattice constants. Since the hydrogens were not refined, no standard deviations are given.

Table X. Selected interatomic distances (Å) for bromophos

Bonding Distances

C(1)-C(2)	1.38(1)
C(2)-C(3)	1.40(1)
C(3)-C(4)	1.36(1)
C(4)-C(5)	1.40(1)
C(5)-C(6)	1.37(1)
C(6)-C(1)	1.38(1)
C(1)-O(1)	1.391(9)
C(2)-H(1)	0.950(9)
C(3)-Cl(1)	1.724(9)
C(4)-Br	1.887(8)
C(5)-H(2)	0.950(9)
C(6)-Cl(2)	1.724(9)
P-O(1)	1.607(6)
P=S	1.892(4)
P-O(2)	1.547(6)
P-O(3)	1.571(7)
O(2)-C(7)	1.46(1)
O(3)-C(8)	1.44(1)

Non-Bonding Distances

Interaction	via	Observed Distance	Total van der Waals Distance (from Pauling[39])
Cl(1)···H(2)	1 cell in z	3.155(4)	3.0
Cl(2)···H(1)	1 cell in z	3.280(4)	3.0
Cl(2)···$C(7)H_3$	1 cell in z	3.79(1)	3.8[a]
S···$C(7)H_3$	1 cell in z	3.90(1)	3.85[a]
S···$C(8)H_3$	1 cell in z	3.71(1)	3.85[a]
Cl(2)···$C(8)H_3$	1 cell in z and x	3.68(1)	3.8[a]
Br···S	2_1(-x direction)	3.467(4)	3.80
Br···H(2)	2_1(-x dirsction)	3.371(3)	3.15
Cl(1)···H(2)	2_1(-x direction)	3.200(4)	3.0
$C(7)H_3$···Cl(2)	2_1(z direction)	3.68(1)	3.80
C(7)···O(1)	2_1(z direction)	3.68(1)	3.40
$C7H_3$···O(2)	2_1(z direction)	3.34(1)	3.40
$C(7)H_3$···$C(7)H_3$	2_1(z direction)	3.82(1)	4.00
S···Cl(2)	Intramolecular	3.798(5)	3.65
S···$C(8)H_3$	Intramolecular	3.35(1)	3.85[a]
O(3)···H(1)	Intramolecular	2.613(6)	2.6
P···Cl(2)	Intramolecular	3.875(4)	3.7
S···O(1)	Intramolecular	2.989(6)	3.25
S···O(2)	Intramolecular	2.877(7)	3.25
S...O(3)	Intramolecular	2.957(8)	3.25
Br···Cl(1)	Intramolecular	3.259(4)	3.75
O(1)···O(2)	Intramolecular	2.416(8)	2.80
O(2)···O(3)	Intramolecular	2.524(9)	2.80
O(3)···O(1)	Intramolecular	2.424(9)	2.80
O(1)···$C(7)H_3$	Intramolecular	2.94(1)	3.4[a]
O(3)···$C(7)H_3$	Intramolecular	3.02(1)	3.4[a]
O(1)···$C(8)H_3$	Intramolecular	3.81(1)	3.4[a]
O(2)···$C(8)H_3$	Intramolecular	3.39(1)	3.4[a]
$C(7)H_3$···$C(8)H_3$	Intramolecular	3.95(2)	4.0[a]
P···H(1)	Intramolecular	3.285(3)	(3.1)
P···H(2)	Intramolecular	5.520(4)	(3.1)

[a] Assumes linear addition of methyl van der Waals radius.

Table XI. Bond angles (degrees) for bromophos

Angle		Degrees
C(1)-C(2)-C(3)		118.3(8)
C(2)-C(3)-C(4)		120.8(8)
C(3)-C(4)-C(5)		120.2(8)
C(4)-C(5)-C(6)		119.2(8)
C(5)-C(6)-C(1)		120.3(8)
C(6)-C(1)-C(2)		121.1(7)
O(1)-C(1)-C(2)		118.7(8)
O(1)-C(1)-C(6)		120.1(8)
H(1)-C(2)-C(1)		120.9(8)
H(1)-C(2)-C(3)		120.8(9)
Cℓ(1)-C(3)-C(2)		117.8(7)
Cℓ(1)-C(3)-C(4)		121.4(6)
Br-C(4)-C(3)		122.1(7)
Br-C(4)-C(5)		117.7(7)
H(2)-C(5)-C(4)		120.4(8)
H(2)-C(5)-C(6)		120.4(9)
Cℓ(2)-C(6)-C(5)		119.1(7)
Cℓ(2)-C(6)-C(1)		120.5(6)
C(1)-O(1)-P		123.2(5)
S-P-O(1)		117.1(3)
S-P-O(2)		113.2(3)
S-P-O(3)		117.0(3)
O(1)-P-O(2)		100.0(3)
O(2)-P-O(3)		108.1(4)
O(1)-P-O(3)		99.4(3)
P-O(2)-C(7)		122.0(5)
P-O(3)-C(8)		121.1(7)
P-O(3)-H(1)		100.5(3)
C(8)-O(3)···H(1)	Intramolecular	130.0(6)
C(4)-Br···H(2)	Intermolecular	65.3(2)
C(3)-Cℓ(1)···H(2)	Intermolecular	93.8(3)
C(6)-Cℓ(2)···H(1)	Intermolecular	90.9(3)

Table XII. Dihedral angles (degrees) and least-squares planes

Planes defined by:	Dihedral Angle[a]	
C(1)-C(2)-C(6); C(1)-O(1)-P	78.4(6)	(Towards H(1))
C(1)-C(2)-C(6); O(1)-P-S	113.4(7)	(Away from ring and towards Cℓ(2))
C(1)-O(1)-P; O(1)-P-S	59.4(7)	(Towards Cℓ(2))
C(1)-C(3)-C(5); O(1)-O(2)-O(3)	39.6(4)	(O(3) fragment above ϕ plane)

Plane (I)[b] defined by carbons (1-6):
(0.91687) X + (-0.05745) Y + (-0.39503) Z - (1.10472) = 0

Atom	Distance from plane (Å)
C(1)	-0.0059
C(2)	0.0129
C(3)	-0.0119
C(4)	0.0036
C(5)	0.0038
C(6)	-0.0025

Plane (II)[b] defined by all 12 phenoxy group members:
(0.91791) X + (-0.05270) Y + (-0.39327) Z - (1.13354) = 0

Atom	Distance from plane (Å)	Atom	Distance from plane (Å)
C(1)	0.0161	H(1)	0.0645
C(2)	0.0324	Cℓ(1)	-0.0564
C(3)	0.0005	Br	-0.0199
C(4)	0.0116	H(2)	0.0161
C(5)	0.0143	Cℓ(2)	-0.0183
C(6)	0.0150	O(2)	0.4834
O(1)	-0.0757	O(3)	1.4541

Plane (III)[b] defined by C(1), H(1), O(3) and P:
(0.67286) X + (-0.48031) Y + (-0.56264) Z - (-3.87615) = 0

Atom	Distance from plane (Å)
C(1)	0.0722
H(1)	-0.0743
O(3)	0.0968
P	0.0947
C(2)	0.2422

Plane (IV)[b] defined by C(1), O(1), S and P:
(0.68424) X + (-0.50462) Y + (0.52647) Z - (2.55342) = 0

Atom	Distance from plane (Å)
C(1)	0.1424
O(1)	-0.2873
S	-0.0839
P	0.2288
C(5)	-0.2941

[a] Angles correspond to proper orientation shown in Figures 5-7 (and calculated intramolecular distances) so that the phosphorus is tilted toward the H(1) side of the ring and the sulfur is directed away from H(1).

[b] Planes are defined as $c_1X + c_2Y + c_3Z - d = 0$, where X, Y and Z are Cartesian coordinates which are related to the triclinic cell coordinates (x,y,z) by the transformations:

$X = xa \sin\gamma + zc((\cos\beta - \cos\alpha \cos\gamma)/\sin\gamma) = xa$
$Y = xa \cos\gamma + yb + zc \cos\alpha = yb$, and
$Z = zc((1-\cos^2\alpha - \cos^2\beta - \cos^2\gamma + 2 \cos\alpha \cos\beta \cos\gamma)^{1/2}/\sin\gamma) = zc$.

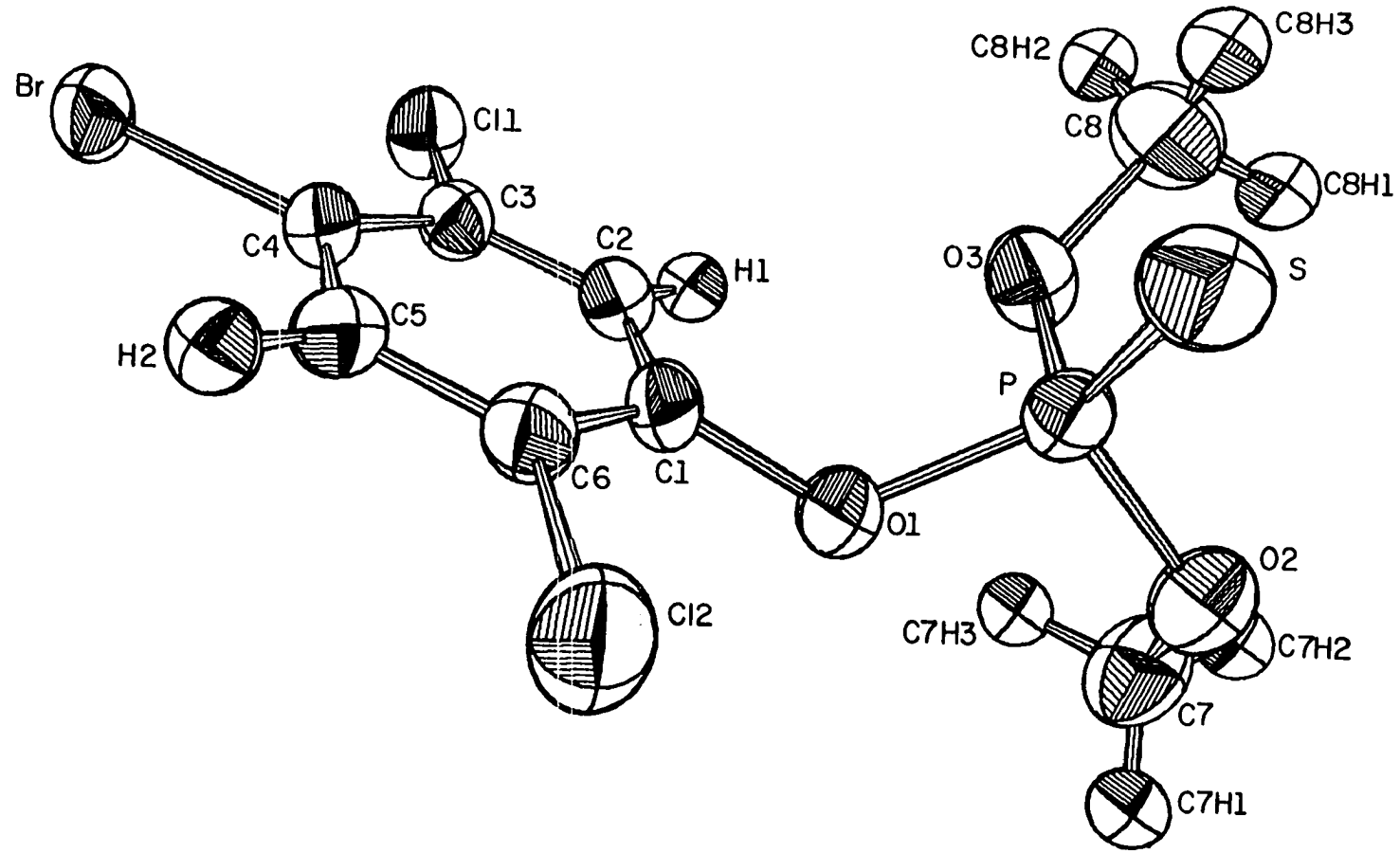

Figure 5. The bromophos molecule showing 50% probability ellipsoids; 30% for hydrogen.

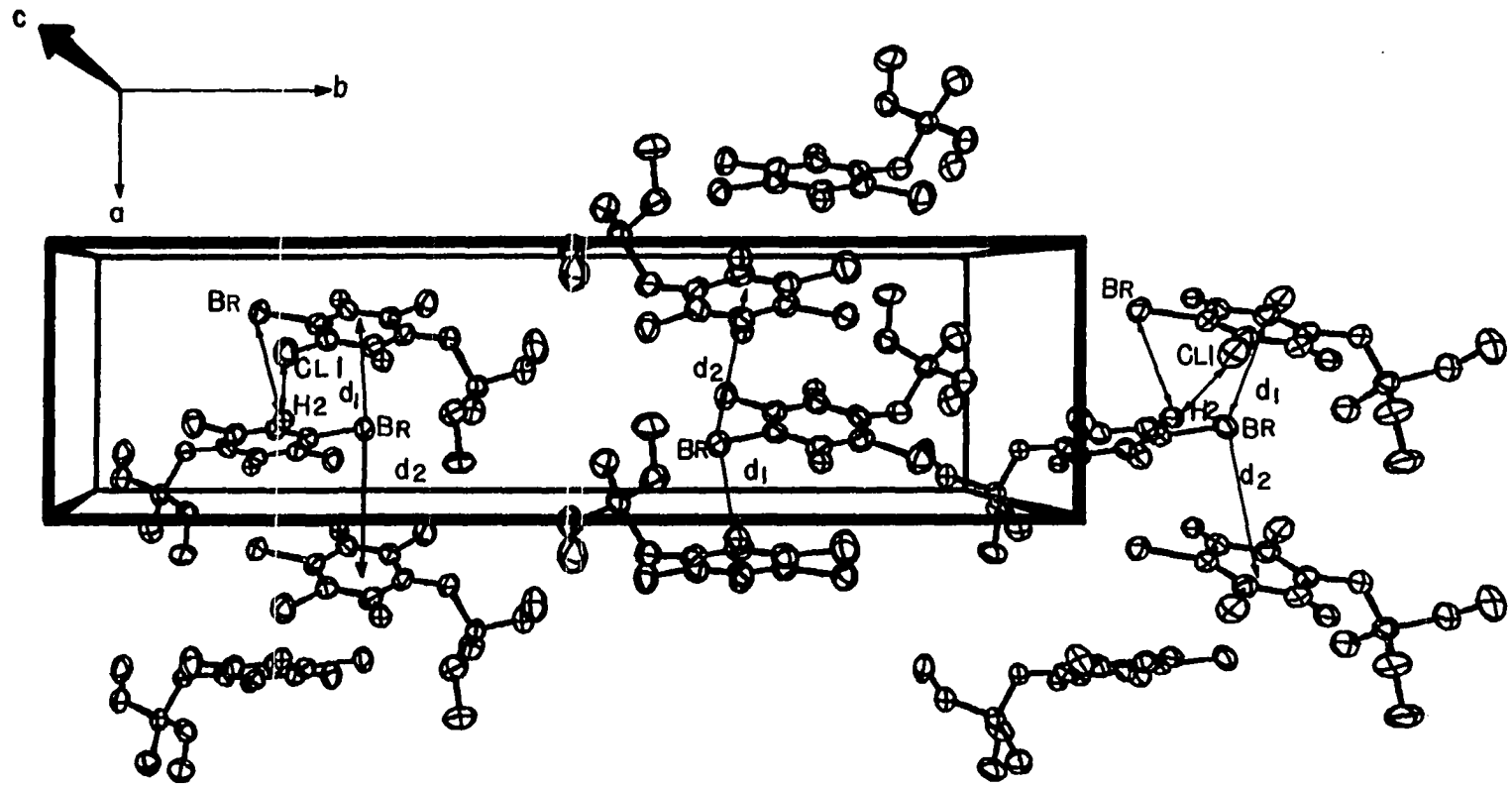

Figure 6. View of three adjacent unit cells illustrating packing in the *a* and *b* directions.

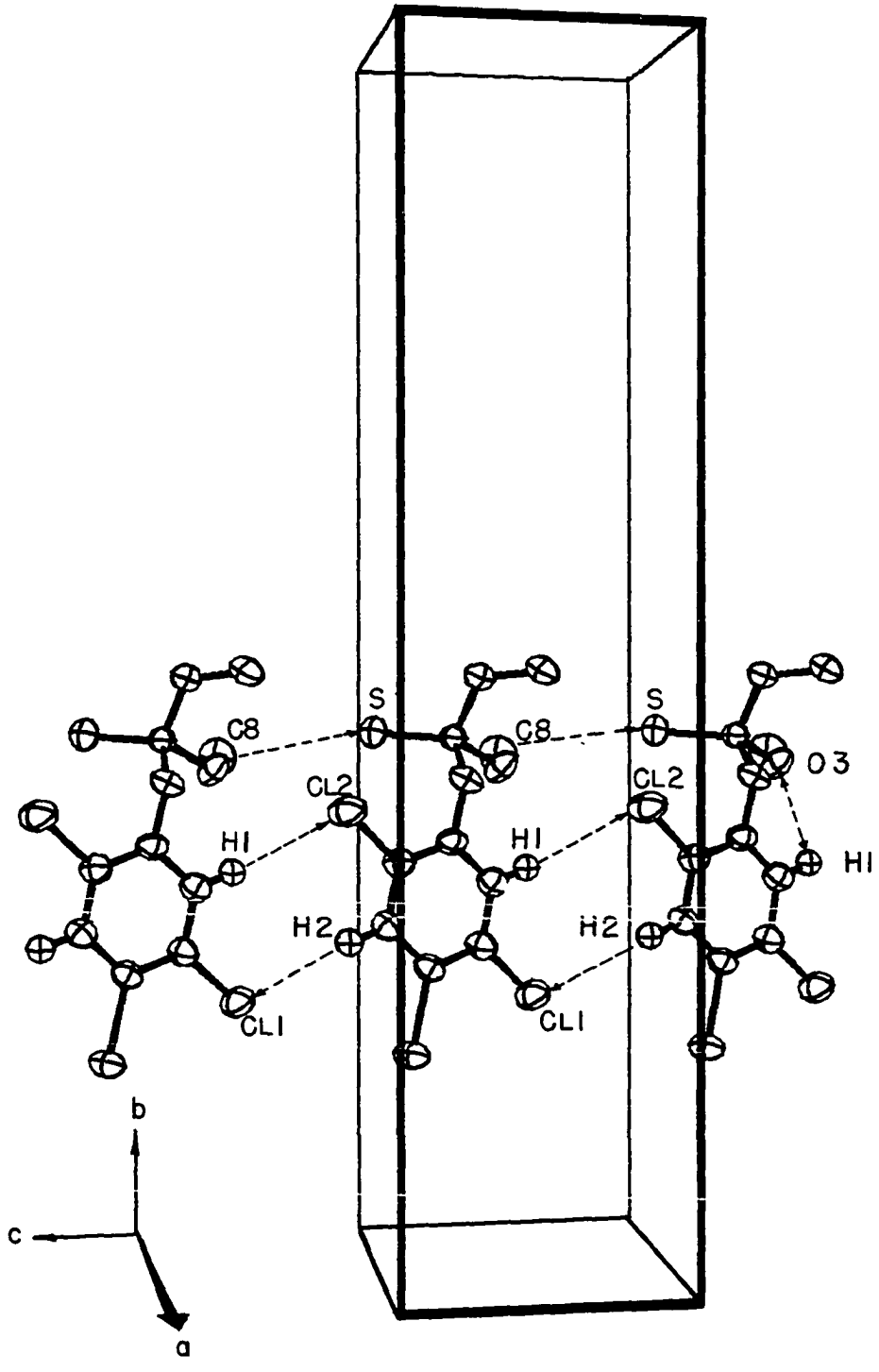

Figure 7. Dovetail packing in the *c* direction.

The former is a manifestation of the charge density distribution within each individual molecule and hence corroborates one's "chemical intuition" of the δ(+) and δ(-) atoms.

Referring to Figure 6 and Table X, interactions such as the following appear to be van der Waals in character: Cℓ(2)···C(8)H_3, Cℓ(2)···C(7)H_3, S···C(8)H_3, C(7)H_3···{Cℓ(2), O(1) and O(2)}, *etc.* The latter interaction causes the C(7) methyl group to be skewed into an orientation unlike that of the C(8) methyl group (*cf.* Figures 5 and 6). Owing to differences in electronegativity, the S···C(8)H_3 interaction is a result of the O(3)···C(2) intramolecular hydrogen bond.

Packing, as shown in Figure 6, is also facilitated by the interactions of the δ(-) bromine with the δ(+) ring centers above and below each bromine: d_1 = 3.57, d_2 = 4.49 Å which may be compared to the van der Waals radii sum of 3.65 Å[39]. This discrepancy in d_1 and d_2 is primarily due to the intrusion of thiophosphate groups. The Br···H(2) distance of 3.37 Å (Table X) and the C(4)-Br···H(2) angle of only 65° (Table XI) indicate that only a very weak intermolecular hydrogen bond is likely.

A very interesting mode of packing takes place in the *c* direction. Due to the fact that each chlorine and ring hydrogen has a para counterpart, the molecules advantageously utilize this arrangement by forming hydrogen bonds in a dovetail fashion (*cf.* Figure 7 and Tables X and XI). Since the rings in the *c* direction are all related by a simple translation, they

are all parallel. However, they are not coplanar, each being 23° from the *b-c* plane (*cf.* Figures 6 and 7).

As with ronnel, ronnel oxon and Coroxon[42], angles of the type S=P-O or O=P-O are all greater than the tetrahedral angle of 109.47°. Non-tetrahedral angles are to be expected due to the different hybridization involved with the doubly-bonded sulfur. The discrepancy also is due to the larger van der Waals radius of the doubly-bonded sulfur *vs.* the singly-bonded oxygens. Presumably similar factors are responsible for the distorted PO_4 sub-units in Coroxon and H_3PO_4[41]. The increase ($\sim 4^{\circ}$) in the S-P-O(3) angle compared to the S-P-O(2) angle in bromophos can be attributed to the increased sulfur···C(8) methyl group interaction (*cf.* Figure 6 and Tables X and XI).

The C(1)-O(1) bond is significantly ($\sim 5\sigma$) shorter than the two methoxy C-O bonds (*cf.* Table IX). This indicates a stronger C(1)-O(1) bond, possibly due to a weak p-"ring" overlap. The P-O(1) bond is the longest of the three P-O bonds being $\geq 5\sigma$ longer than the other two P-O bonds. Hence, the P-O(1) bond lengthening parallels the shortening of the C(1)-O(1) bond (*cf.* Table X), enhancing phosphorylation[48]. The corresponding P-O and C-O bond lengths for bromophos, ronnel, ronnel oxon and Coroxon are all within 3σ of being identical.

Molecular orbital calculations are needed to arrive at quantitative electron distributions and hence a numerical representation of the $\delta(+)$ and $\delta(-)$ regions. Since many of these

types of calculations are useful when used to diagnose trends in similar compounds, an MO calculation on bromophos would be quite useful. However, programs are not typically available with wave functions of heavier atoms.

This information, though, especially with the accurate distances and angles afforded by X-ray crystallography will give an uncustomary microscopic view of the molecule in question.

Alternatively, as noted earlier, the utilization of the $\delta(+)$ and $\delta(-)$ charges in the crystalline packing of bromophos gives one an excellent <u>indirect</u> insight into the probable use of these same $\delta(+)$ and $\delta(-)$ charges in the overall process of AChE inhibition. Charge distribution, as manifested in Hammett σ values, is known to be a major contributor to the inhibition of AChE by OP insecticides[22].

However, one must be concerned not only with <u>amounts</u> of charge but also the relative <u>locations</u> of the charges. The restriction of the rotation about the C(1)-O(1) bond allows bromophos (and conceivably bromophos oxon) less flexibility in reacting with the OP active site(s) on AChE and is manifested in the mammalian LD_{50} value of 3,750-6,100 $mg \cdot kg^{-1}$[53], which is at least 2-3 times greater than for most OP insecticides. Consistent with this, the P···H(2) intramolecular distance of 5.52 Å and the P···H(1) intramolecular distance of 3.29 Å, for example, fall well outside of the mammalian AChE site-separation distance range of 4.3-4.7 Å[51,52], yet the P···H(2) distance of

5.52 Å is well within the 5.0-5.5 Å[51] and 4.5-5.9 Å[52] ranges quoted for insect AChE. As noted before, any distance comparisons to literature values should still be reasonably good even though the characteristics of the actual OP site are not known[12]. The observed disparity in insect *vs.* mammalian LD_{50} values typical of many OP insecticides[54] may be attributable, in part, to an inherently small selective range of favorable intramolecular distances afforded by the OP to provide a "match" with the isozymes of AChE. Restriction of the important distances in bromophos serves to further limit any inhibition reaction. Presumably bromophos oxon, which is present *in vivo*, has a conformation similar to that of bromophos. In addition, the conformation of bromophos (or any other thiophosphate) will be intimately responsible for the oxon's formation.

Accordingly, selective design of an OP (or carbamate) system should be possible. If the OP site would be similar to the ACh site, one could use a modified Krupka-type[17] model. Using this model the design should contain an immobile phosphorus (or carbonyl carbon) and a δ(+) function (-H, $-N(CH_3)_3^+$, *etc.*), enhanced by judiciously selected electron withdrawing substituents, at a distance chosen to fully utilize the disparity in mammalian *vs.* insect AChE sites as well as the disparities in the isozymes of AChE. This latter idea may make it possible to make an insecticide "species specific". If Krupka's model is insufficient as an OP model (and it probably is), the presented distances will be of immense help in deducing the true OP site.

THE CRYSTAL AND MOLECULAR STRUCTURE OF RUELENE

Introduction

The crystal and molecular structure of Ruelene (O-(4-tert-Butyl-2-chlorophenyl)-O-methyl-N-methyl phosphoroamidate), $(H_3CO)(H_3CNH)P(O)OC_6H_3C\ell C(CH_3)_3$, was carried out to investigate any differences and/or similarities to the previous structures resulting from the replacement of meta and para chlorines in ronnel by a hydrogen and t-butyl group, respectively. The former would provide two meta hydrogens, and hence two P···meta hydrogen vectors, and the latter would supply a bulky group having a different Hammett σ value than the halogens studied thus far. The reported LD_{50} for rats is 770 $mg \cdot kg^{-1}$[28].

Experimental

Preparation.-- A sample of 99% pure Ruelene supplied by P. A. Dahm and J. G. Laveglia was recrystallized from reagent grade carbon tetrachloride. It was necessary to evaporate the solution to dryness to obtain the colorless species.

Crystal Data.-- A rectangular prismatic crystal with approximate dimensions 0.03 x 0.40 x 0.50 mm was selected and mounted on the end of a glass fiber using Elmer's Glue-All. The crystal was then mounted on a four-circle diffractometer; three ω-oscillation photographs taken at various χ and φ settings indicated that the crystal was indeed single.

From these photographs sixteen independent reflections were selected and their coordinates were input into an automatic indexing program[29]. The reduced cell and reduced cell scalars which resulted indicated triclinic symmetry, which was confirmed by inspection of ω-oscillation photographs taken about each of the three axes in turn. No axis showed mirror symmetry. Observed layer-line spacings agreed, within experimental error, with those predicted for this cell by the indexing program.

The lattice constants were obtained from a least-squares refinement based on the precise ±2θ ($|2\theta| > 30^{\circ}$) measurements of twenty-two strong independent reflections. At 27°C using Mo Kα radiation (λ = 0.70954 Å) they are a = 9.506(2), b = 11.826(3), c = 7.277(1) Å, α = 106.90(2), β = 91.86(3), γ = 105.11(3)°. The observed density of 1.30 ± 0.03 g·cm^{-3} determined by the flotation method is in good agreement with the calculated value of 1.292 g·cm^{-3} for two molecules with a molecular weight of 292.1 g·mol^{-1} in a unit cell having a volume of 750.49 Å^3.

Collection and Reduction of X-ray Intensity Data.-- The data were collected at 27°C with graphite monochromated Mo Kα radiation on an automated four-circle diffractometer designed and built in the Ames Laboratory and previously described by Rohrbaugh and Jacobson[31]. All data within a 2θ sphere of 45° ($(\sin\theta)/\lambda$ = 0.539 Å^{-1}) in the hkℓ, $\bar{h}$kℓ, h$\bar{k}$ℓ and $\bar{h}\bar{k}$ℓ octants were measured using an ω-stepscan technique.

As a general check on electronic and crystal stability, the intensities of three standard reflections were remeasured every seventy-five reflections. These standard reflections were not observed to vary significantly throughout the entire period of data collection ($\sim$ 2 days). Hence a decomposition correction was unnecessary. A total of 2993 reflections were recorded in this manner. Examination of the data did not reveal any systematic extinctions. As a Howells, Phillips and Rogers[55] plot indicated a centrosymmetric space group, the space group was assigned as $P\bar{1}$.

The intensity data were corrected for Lorentz and polarization effects and, since $\mu = 3.64$ cm^{-1}, absorption corrections were not made; maximum and minimum transmission factors were 0.897 and 0.834, respectively. The estimated variance in each intensity was calculated by

$$\sigma_i^2 = C_T + 2C_B + (0.03\ C_T)^2 + (0.03\ C_B)^2,$$

where C_T and C_B represent the total and background counts, respectively, and the factor 0.03 represents an estimate of non-statistical errors. The estimated deviations in the structure factors were calculated by the finite difference method[32]. Equivalent data were averaged and 1632 reflections with $|F_o| > 2.5\sigma(F_o)$ were retained for use in subsequent calculations. The data will be found in the 1978 supplementary material section of J. Agric. Food Chem. See any current masthead page for ordering the information.

Solution and Refinement

The position of the chlorine atom was obtained from an analysis of a standard three-dimensional Patterson function. The remaining atoms were found by successive structure factor[35] and electron density map calculations[34]. These atomic positions were subsequently refined by a full-matrix least-squares procedure[35] minimizing the function $\Sigma\omega(|F_o|-|F_c|)^2$, where $\omega = 1/\sigma_F^2$. This refinement yielded a conventional discrepancy factor of $R = \Sigma||F_o|-|F_c||/\Sigma|F_o| = 0.178$. At this stage of the refinement all eighteen non-hydrogen atoms had been refined using isotropic thermal parameters. The scattering factors used were those of Hanson, *et al.*[36] modified for the real and imaginary parts of anomalous dispersion[37] . The scattering factor tables for hydrogen were those of Stewart, *et al.*[45]

Ring hydrogen atom positions were fixed at 0.95 Å from the corresponding carbons. Analysis of an electron density difference map[34] did not reveal either the individual methyl or amide hydrogen positions. The methyl hydrogens were inserted in approximately tetrahedral positions using the precise positions of the corresponding methyl carbon and the non-hydrogen atom bonded immediately to the methyl carbon. The methyl C-H distances were set equal to 1.0 Å; all isotropic hydrogen temperature factors were set equal to 4.5 Å^2. As the amide hydrogen did not appear in the electron density map, conformational disordering is likely. The amide hydrogen was not included in least-squares refinements and is not shown in any of the fig-

ures.

In the final stages of refinement, analysis of the weights, ω, was performed *via* the requirement that $\omega\nabla^2(\nabla\Xi||F_o|-|F_c||)$ should be a constant function of $|F_o|$ and $(\sin\theta)/\lambda$[56]. As reflections at very low and very high $(\sin\theta)/\lambda$ were somewhat overweighted, all ω's were subsequently adjusted.

Subsequent anisotropic least-squares refinement without varying the hydrogen parameters converged to R = 0.074. Since this procedure yielded slightly different non-hydrogen atom positions, all of the hydrogen positions were recalculated. Further refinement cycles did not significantly alter any atomic parameters and the discrepancy factor did not change.

The final positional and thermal parameters are listed in Table XIII. Standard deviations were calculated from the inverse matrix of the final least-squares cycle. Bond lengths and angles are listed in Table XIV and Table XV, respectively[38]. Dihedral angles and least-square planes are listed in Table XVI.

Description of Structure and Discussion

The phenoxy group in Ruelene shown in Figures 8 and 9[40] is, as expected, essentially planar (*cf.* Table XVI, Plane II). In addition, the t-butyl group is nearly symmetrically disposed about C(4) as shown in Table XVI, Plane III and Figure 8.

Referring to Table XV it is noted that angles of the type O(2)=P-O or N are all greater than the tetrahedral angle of

Table XIII. Final atomic positional[a] and thermal[b] parameters for Ruelene

	Fractional Coordinates			Atomic Temperature Factors					
Atom	x	y	z	β_{11}	β_{22}	β_{33}	β_{12}	β_{13}	β_{23}
Cl	0.0870(2)[c]	0.0159(1)	0.2456(2)	26.8(3)	9.3(1)	42.7(5)	1.2(1)	-14.4(3)	2.2(1)
P	0.0547(1)	0.3630(1)	0.2406(1)	14.6(1)	9.6(1)	23.7(3)	2.6(1)	0.2(1)	5.6(1)
O(1)	0.1487(3)	0.2653(3)	0.2162(4)	18.1(5)	10.9(3)	22.5(7)	4.9(3)	-0.1(4)	4.7(3)
O(2)	0.1423(4)	0.4909(3)	0.3252(5)	19.2(5)	10.5(3)	33.6(9)	3.7(3)	2.4(5)	6.9(4)
O(3)	-0.0146(3)	0.3246(3)	0.0256(4)	16.9(4)	14.9(4)	26.8(8)	4.1(3)	-0.1(5)	8.6(4)
C(1)	0.2327(5)	0.2582(4)	0.3706(6)	14.8(6)	10.2(4)	19.9(9)	3.4(4)	0.4(6)	4.4(5)
C(2)	0.2132(5)	0.1449(4)	0.3990(6)	16.2(6)	8.2(4)	26(1)	2.3(4)	-2.8(7)	2.4(5)
C(3)	0.2975(5)	0.1335(4)	0.5470(7)	17.0(7)	8.4(4)	27(1)	3.1(4)	-2.0(7)	5.0(5)
C(4)	0.4049(4)	0.2342(4)	0.6712(6)	12.9(5)	9.6(4)	21.9(9)	2.9(4)	1.5(6)	4.5(5)
C(5)	0.4222(5)	0.3460(4)	0.6364(7)	16.4(7)	10.1(4)	27(1)	-0.1(4)	-1.9(7)	4.8(6)
C(6)	0.3365(5)	0.3583(4)	0.4903(7)	17.3(7)	9.7(4)	28(1)	1.2(4)	-3.2(7)	7.8(6)
C(7)	0.4997(5)	0.2209(4)	0.8336(6)	13.4(6)	11.2(4)	25(1)	3.3(4)	1.1(6)	5.7(5)
C(8)	0.4152(9)	0.1246(9)	0.914(1)	27(1)	29(1)	61(3)	-4(1)	-13(1)	31(1)
C(9)	0.544(1)	0.3357(7)	0.998(1)	63(3)	17(1)	46(2)	4(1)	-33(2)	7(1)
C(10)	0.630(1)	0.189(1)	0.755(1)	36(1)	66(3)	38(2)	38(2)	4(1)	15(2)
C(11)	-0.1815(6)	0.2013(5)	0.3061(9)	19.3(9)	13.8(6)	35(1)	-0.2(6)	2.7(9)	7.6(8)
C(12)	0.0727(7)	0.3438(6)	-0.1242(8)	22.6(9)	18.0(7)	25(1)	6.7(7)	2.4(9)	9.5(8)
N	-0.0793(5)	0.3242(3)	0.3604(6)	17.9(6)	10.8(4)	32(1)	1.1(4)	3.6(6)	5.9(5)
H(1)	0.2823	0.0552	0.5645	45					
H(2)	0.4952	0.4164	0.7156	45					
H(3)	0.3496	0.4367	0.4733	45					
C8H(1)	0.3244	0.0741	0.8251	45					
C8H(2)	0.3883	0.1643	1.043[illegible]	45					
C8H(3)	0.4769	0.0703	0.9284	45					
C9H(1)	0.4781	0.3879	0.9918	45					
C9H(2)	0.5369	0.3152	1.1226	45					
C9H(3)	0.6474	0.3819	0.9947	45					
C10H(1)	0.6622	0.2332	0.6593	45					
C10H(2)	0.7111	0.2154	0.8632	45					
C10H(3)	0.6063	0.0989	0.6919	45					
C11H(1)	-0.2831	0.2076	0.3237	45					
C11H(2)	-0.1543	0.1550	0.3901	45					
C11H(3)	-0.1768	0.1568	0.1683	45					
C12H(1)	0.0879	0.4300	-0.1268	45					
C12H(2)	0.1695	0.3298	-0.0995	45					
C12H(3)	0.0214	0.2851	-0.2513	45					

[a] The positional parameters for all atoms are represented in fractional unit cell coordinates.

[b] The β_{ij} are defined by: $T = \exp\{-(h^2\beta_{11} + k^2\beta_{22} + \ell^2\beta_{33} + 2hk\beta_{12} + 2h\ell\beta_{13} + 2k\ell\beta_{23})\}$. If only the β_{11} column is listed, this corresponds to an isotropic temperature factor. All hydrogen isotropic B's have been set equal to 4.5 . Non-hydrogen thermal parameters are (x10^3); hydrogen, (x10).

[c] In this and succeeding tables estimated standard deviations are given in parentheses for the least significant figures and include the error in the lattice constants. Since the hydrogens were not refined, no standard deviations are given.

Table XIV. Selected interatomic distances (Å) for Ruelene

Bonding Distances	
C(1)-C(2)	1.381(7)
C(2)-C(3)	1.380(7)
C(3)-C(4)	1.400(7)
C(4)-C(5)	1.387(7)
C(5)-C(6)	1.383(7)
C(6)-C(1)	1.367(7)
C(1)-O(1)	1.392(6)
C(2)-Cℓ	1.727(5)
C(3)-H(1)	0.947(5)
C(4)-C(7)	1.531(6)
C(5)-H(2)	0.948(5)
C(6)-H(3)	0.948(5)
P-O(1)	1.611(3)
P=O(2)	1.459(4)
P-O(3)	1.566(4)
P-N	1.611(5)
O(3)-C(12)	1.426(7)
N-C(11)	1.456(7)
C(7)-C(8)	1.493(9)
C(7)-C(9)	1.480(10)
C(7)-C(10)	1.473(10)

Non-Bonding Distances			
Interaction	via	Observed Distance	Total van der Waals Distance(Pauling[39])
Cℓ···O(1)	Intramolecular	2.925(4)	3.20
$C(11)H_3$···P	Intramolecular	2.700(6)	3.9
$C(11)H_3$···O(1)	Intramolecular	3.169(7)	3.4
$C(11)H_3$···O(3)	Intramolecular	3.090(7)	3.4
$C(12)H_3$···P	Intramolecular	2.613(6)	3.9
$C(12)H_3$···O(1)	Intramolecular	3.015(6)	3.4
$C(12)H_3$···O(2)	Intramolecular	3.180(7)	3.4
$C(8)H_3$···H(1)	Intramolecular	2.605(8)	3.2
$C(10)H_3$···H(1)	Intramolecular	3.330(12)	3.2
$C(9)H_3$···H(2)	Intramolecular	2.587(8)	3.2
$C(10)H_3$···H(2)	Intramolecular	3.341(12)	3.2
H(3)···O(2)	Intramolecular	2.525(4);2.46[a]	2.6
P···H(1)	Intramolecular	5.680(2)	(3.1)
P···H(2)	Intramolecular	5.127(2)	(3.1)
P···H(3)	Intramolecular	3.006(2)	(3.1)
C(6)···O(2)	Intramolecular	3.126(7)	3.2 [b]
Cℓ···$C(12)H_3$	center of inversion	3.943(7)	3.80
Cℓ···Cℓ	center of inversion	3.764(3)	3.60
$C(10)H_3$···$C(11)H_3$	1 cell in x	3.800(12)	4.0
$C(10)H_3$···O(3)	1 cell in x and z	3.568(12)	3.4
$C(12)H_3$···O(2)	center + 1 cell in y	3.700(7)	3.4

[a] Using a C(6)-proton distance of 1.08 Å (Sutton[57])

[b] Bondi[46]

Table XV. Bond angles (degrees) for Ruelene

Angle	Degrees
C(1)-C(2)-C(3)	120.2(4)
C(2)-C(3)-C(4)	121.9(4)
C(3)-C(4)-C(5)	116.1(4)
C(4)-C(5)-C(6)	122.2(4)
C(5)-C(6)-C(1)	120.4(4)
C(6)-C(1)-C(2)	119.2(4)
O(1)-C(1)-C(2)	118.5(4)
O(1)-C(1)-C(6)	122.3(4)
Cℓ-C(2)-C(1)	120.2(4)
Cℓ-C(2)-C(3)	119.5(4)
H(1)-C(3)-C(2)	118.9(5)
H(1)-C(3)-C(4)	119.1(4)
C(7)-C(4)-C(3)	121.8(4)
C(7)-C(4)-C(5)	122.0(4)
H(2)-C(5)-C(4)	118.9(5)
H(2)-C(5)-C(6)	118.9(5)
H(3)-C(6)-C(5)	119.8(5)
H(3)-C(6)-C(1)	119.8(5)
C(4)-C(7)-C(8)	110.9(4)
C(4)-C(7)-C(9)	111.5(5)
C(4)-C(7)-C(10)	108.5(5)
C(8)-C(7)-C(9)	105.3(7)
C(8)-C(7)-C(10)	110.8(9)
C(9)-C(7)-C(10)	109.8(9)
C(1)-O(1)-P	122.8(3)
O(1)-P-O(2)	113.7(2)
O(2)-P-O(3)	116.4(2)
O(2)-P-N	113.0(2)
O(1)-P-O(3)	98.8(2)
O(1)-P-N	108.1(2)
O(3)-P-N	105.7(2)
P-O(3)-C(12)	121.6(4)
P-N-C(11)	123.4(4)
P-O(2)···H(3)	94.2(2); 119.2[a]
P-O(2)···C(12)[b]	101.9(2)
C(2)-Cℓ···C(12)[c]	143.9(2)
P-O(3)···C(10)[d]	138.0(3)
C(6)-H(3)···O(2)[a]	118.8

[a] Using a C(6)-proton distance of 1.08 Å (Sutton[57])

[b] Through center + one cell in y.

[c] Through center.

[d] One cell in x and z.

Table XVI. Dihedral angles (degrees) and least-squares planes

Planes Defined by:		Dihedral Angles of Planes[a]
C(1)-C(3)-C(5);	O(1)-O(3)-N	89.1(2)
P-O(1)-C(1);	C(1)-C(3)-C(5)	53.1(3)
P-O(1)-O(2);	O(1)-C(1)-P	57.1(4)
O(1)-C(1)-P;	O(1)-O(3)-N	141.4(3)
C(1)-C(3)-C(5);	O(1)-P-N	102.6(2) (away from H(3))

Plane(II)[b] defined by all twelve phenoxy group members:
(0.76106) X + (-0.20334) Y + (-0.61599) Z - (-0.51205) = 0

Atom	Distance from Plane (Å)	Atom	Distance from Plane (Å)
C(1)	-0.0161	C(7)	0.0130
C(2)	-0.0160	H(2)	0.0343
C(3)	-0.0159	H(3)	-0.0274
C(4)	-0.0060	C(8)	-0.7431
C(5)	0.0096	C(9)	-0.6626
C(6)	-0.0127	P	-1.0238
O(1)	0.0244	O(2)	-1.0537
C4	0.0319	O(3)	-0.4948
H(1)	-0.0192		

Plane(IV)[b] defined by P, O(1), O(3) and C(1):
(0.81180) X + (0.55454) Y + (-0.18295) Z - (1.97098) = 0

Atom	Distance from plane (Å)
P	0.0025
O(1)	0.0085
O(3)	-0.0047
C(1)	-0.0063

Plane (VI)[b] defined by N, P, O(3), and C(12):
(-0.17249) X + (0.97126) Y + (0.16401) Z -(3.77236) = 0

Atom	Distance from Plane (Å)
N	-0.0032
P	0.0022
O(3)	0.0052
C(12)	-0.0041

Plane (I)[b] defined by carbons (1-6):
(0.75594) X + (-0.020612) Y + (-0.62135) Z - (-0.55649) = 0

Atom	Distance from Plane (Å)
C(1)	0.0004
C(2)	0.0043
C(3)	-0.0026
C(4)	-0.0037
C(5)	0.0085
C(6)	-0.0068

Plane (III)[b] defined by O(1), C(1), C(4), C(7), C(10) and N:
(0.46838) X + (0.84994) Y + (0.24128) Z - (2.90656) = 0

Atom	Distance from Plane (Å)
O(1)	-0.0155
C(1)	0.0181
C(4)	0.0003
C(7)	-0.0083
C(10)	0.0036
N	0.0018

Plane(V)[b] defined by P, C(2), C(6) and C(1):
(-0.61217) X + (-0.07460) Y + (0.78720) Z - (0.51254) = 0

Atom	Distance from Plane (Å)
P	0.0398
O(1)	-0.5352
O(2)	-0.0334
C(1)	-0.0425
C(6)	0.0360
H(3)	-0.2090

Plane (VII)[b] defined by C(11), N, P and C(2):
(-0.53184) X + (0.63700) Y + (-0.55802) Z - (1.23345) = 0

Atom	Distance from Plane (Å)
C(11)	-0.0036
N	0.0042
P	0.0026
O(2)	-0.0032

[a]Angles correspond to proper orientation shown in Figures 8 and 9, so that the phosphorus and O(2) are both directed towards the H(3) side of the ring.

[b]Planes are defined as $c_1X + c_2Y + c_3Z - d = 0$, where X, Y and Z are Cartesian coordinates which are related to the triclinic cell coordinates (x, y, z) by the transformations:

$X = xa \sin\gamma + zc((\cos\beta - \cos\alpha\cos\gamma)/\sin\gamma)$

$Y = xa \cos\gamma + yb + zc \cos\alpha$

$Z = zc((1-\cos^2\alpha-\cos^2\beta-\cos^2\gamma+2\cos\alpha\cos\beta\cos\gamma)^{1/2}/\sin\gamma)$.

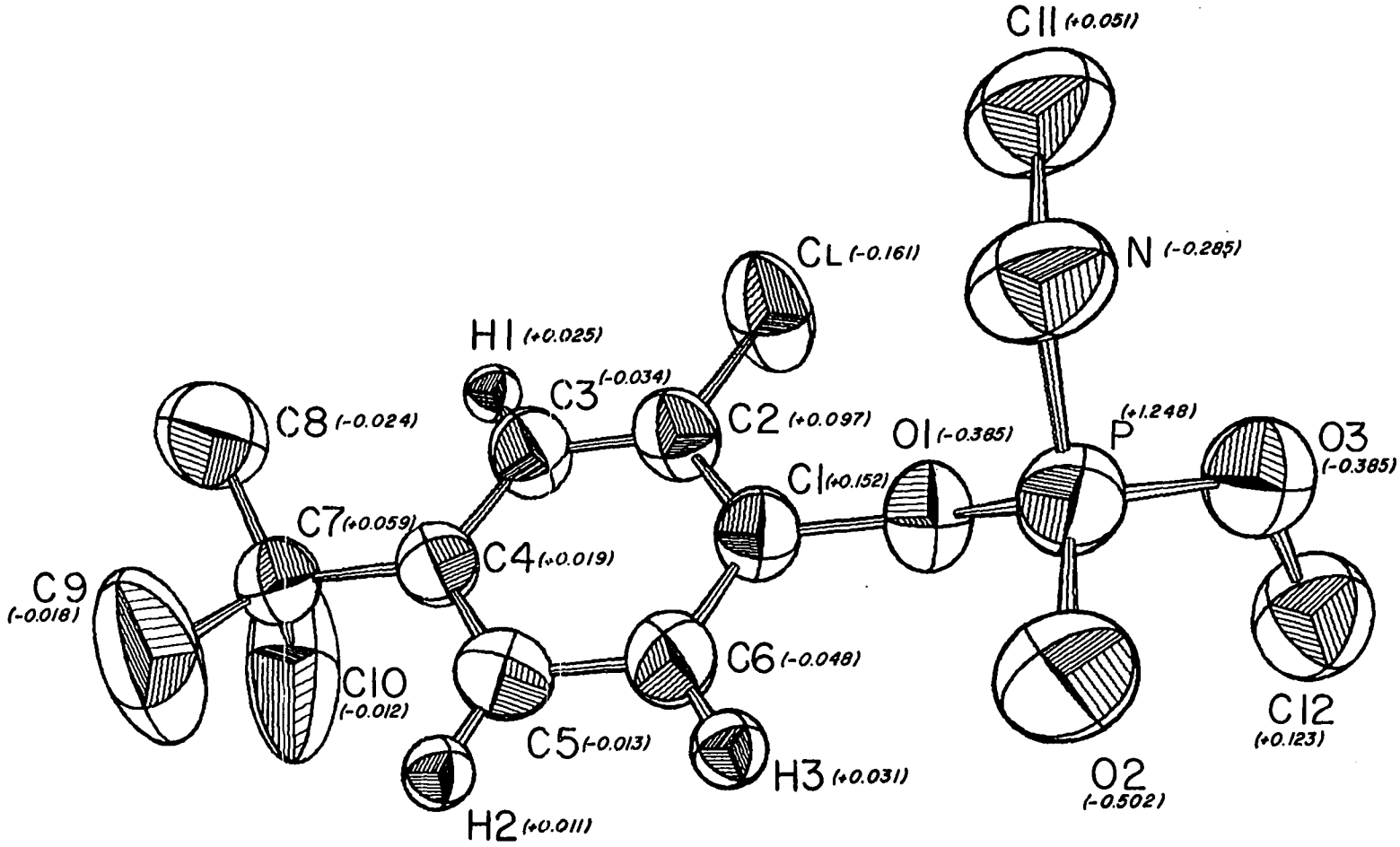

Figure 8. The Ruelene molecule showing 50% probability ellipsoids; 30% for hydrogens. For clarity, the methyl hydrogens are not shown. The numbers in parentheses refer to partial charge densities from a CNDO II calculation.

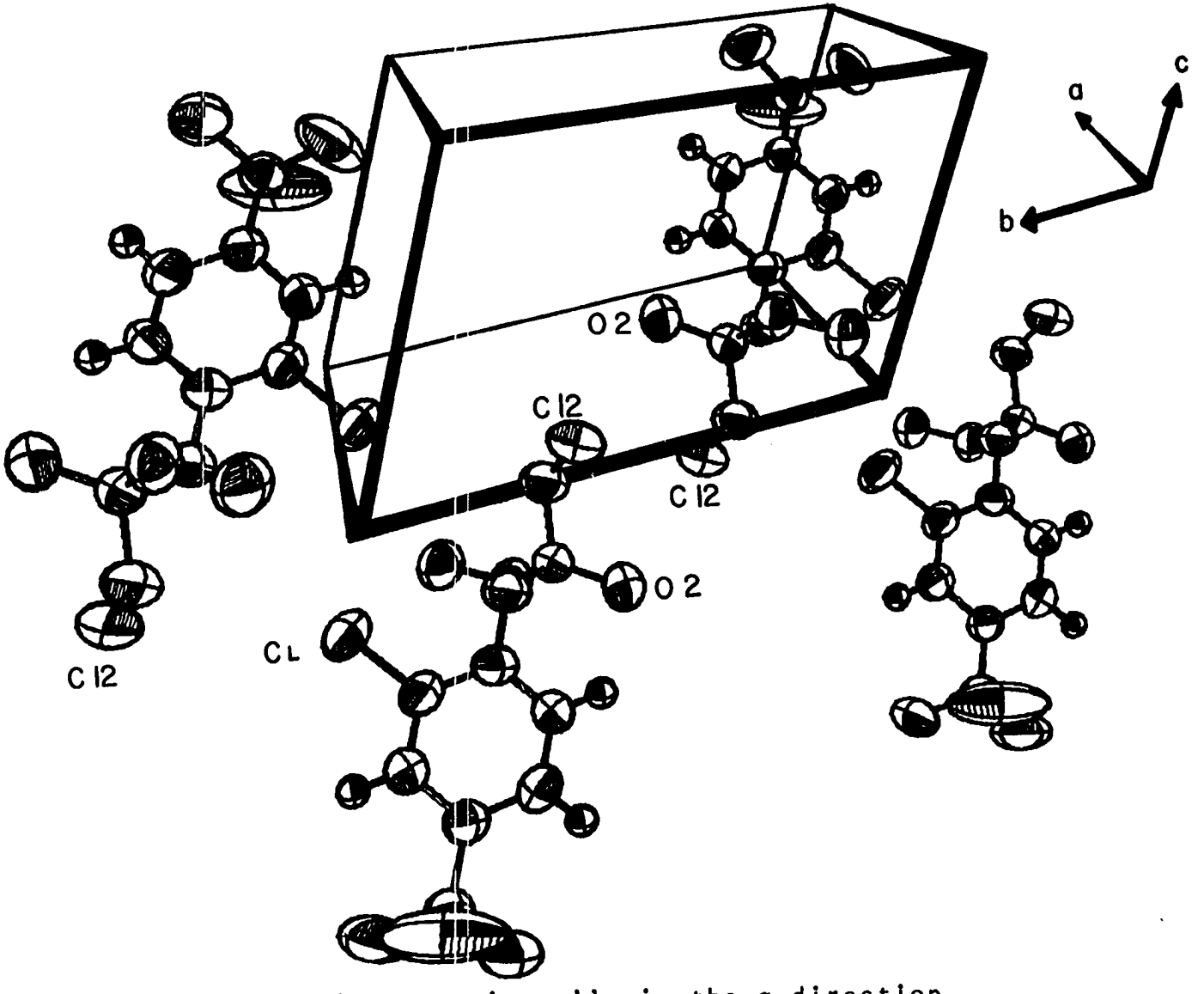

Figure 9. View of two adjacent unit cells in the *a* direction.

109.47°. Those angles about the phosphorus not involving O(2) are all less than 109.47°. This was also noted with ronnel, ronnel oxon, bromophos and Coroxon[42].

With the exception of the very weak Coulombic interactions Cℓ···C(12)H_3, C(10)H_3···O(3) and C(12)H_3···O(2), packing in the Ruelene crystal can be regarded as primarily van der Waals in nature; only a few short intermolecular contacts are observed (*cf.* Tables XIV and XV and Figure 8).

The C(1)-O(1) bond in Ruelene is significantly ($\sim 5\sigma$) shorter than the single methoxy C-O bond (*cf.* Table XIV), while the P-O(1) bond is $\gtrsim 5\sigma$ longer than the P-O(3) bond. These observations, which when coupled with a CNDO II molecular orbital calculation of the Pople and Beveridge[47] type, are consistent with a bonding formulation in which there is a weak overlap of the p_z orbital on the oxygen with the ring system which simultaneously weakens the O(1)-P bond. The latter effect should enhance phosphorylation[48]. The corresponding P-O and C-O bond lengths in Ruelene, ronnel oxon and Coroxon (another phosphate) are within 3σ of being identical, while only slight differences are noted in comparison with the thiophosphate ronnel.

As with ronnel, ronnel oxon and bromophos, the phosphorus in Ruelene is on the H(3) side of a plane which is perpendicular to the ring and contains the C(1)-O(1) bond. However, the doubly-bonded moiety in Ruelene (O(2)) is not skewed towards the ortho chlorine as are the sulfur atoms in ronnel and bromo-

phos. The H(3)···O(2) and C(6)···O(2) distances of 2.46 and 3.13 Å, respectively, and the P-O(2)···H(3) and C(6)-H(3) O(2) angles of 119.2 and 118.8°, respectively , suggest the existence of a weak intramolecular hydrogen bond, assuming sp^2 hybridization on O(2). The O(2)-P-O(1) angle is $\sim 3\sigma$ smaller than both the O(2)-P-O(3) and the previously reported S-P-O(1) angles possibly as a result of the hydrogen bond tending to draw O(2) towards H(3). Consequently, the phosphorus would tend to be restricted to a limited range of possible positions. The formation of a six-membered ring in a distorted "boat" conformation can be envisioned with the P, O(2) H(3) and C(1) atoms making up a nearly planar grouping (*cf.* Figure 8 and Table XVI, Plane V).

The possibility of additional intramolecular hydrogen or van der Waals bonds, occurring simultaneously with the H(3)··· O(2) bond, involving the amide hydrogen and any of the neighboring lone pairs, though, is ruled out since either of the probable hydrogen positions would be directed away from the lone pairs, assuming sp^3 hybridization for the singly-bonded oxygens and sp^2 for O(2) (*cf.* Figure 8 and Planes VI and VII of Table XVI). This is consistent with the observation that the amide hydrogen does not appear in the difference map; it is not restricted to any one configuration.

To further substantiate the possibility of a reasonably immobilized backbone in this molecule, CNDO II molecular orbi-

tal calculations[47] were carried out for Ruelene in order to obtain information on the change in the potential energy surface as a function of incremental rotations about the C(1)-O(1) or O(1)-P bonds. To accomplish the calculations with the program used, though, it was necessary to "replace" the t-butyl group with a methyl function. In the case of rotation about the O(1)-P bond, the C(6)-C(1)-O(1)-P angle was kept at 53.1° (*i.e.* the angle in the solid state). Results of this calculation are shown in Figure 10.

Since these results were obtained using CNDO methods, the absolute values of the energies and charges, as well as the differences in energies, are not as exact as with *ab initio* calculations. The latter methods are extremely cost-prohibitive and are usually unavailable for this size of a problem. Although admittedly approximate, the energies and charges obtained in this CNDO ii calculation certainly give better than "order of magnitude" information, especially since d-orbital contributions are included for the phosphorus and chlorine atoms.

The minimum in Figure 10 coincides with a C(1)-O(1)-P-O(2) angle which is only ∿9° greater than the observed angle of 57.1°. This discrepancy is not too surprising since Figure 10 represents an uncoupled degree of freedom and because of the approximate nature of the calculations. Unfortunately, as a consequence of the approximations used in the CNDO method, the corresponding calculated potential energy curve for the rota-

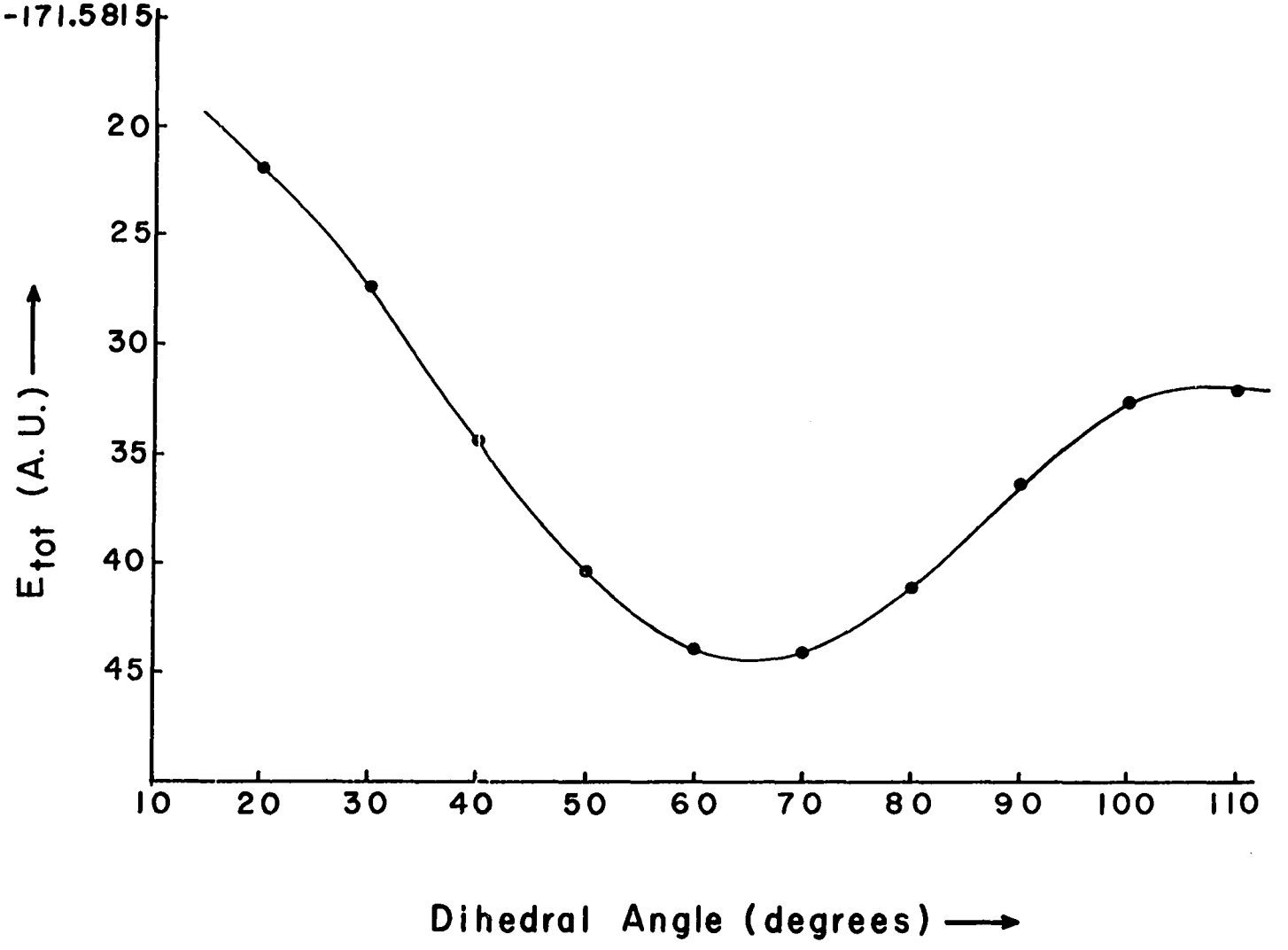

Figure 10. Total energy *vs.* C(1)-O(1)-P-O(2) dihedral angle from CNDO calculations.

tion about the C(1)-O(1) bond is inconclusive. However, the atomic van der Waals radii of Cℓ and H(3) do provide a limit to rotation about the C(1)-O(1) bond. Looking at this rotation is most conveniently accomplished by using a three-dimensional model so that concurrent rotations about other bonds may also be performed. It turns out that the solid state structure corresponds almost exactly to the P/H(3) van der Waals limit while the P···Cℓ interaction is ∿1 Å greater than the sum of their van der Waals radii. So, the calculations and van der Waals restrictions seem to make the solid state structure a plausible *in vivo* model.

As discussed previously, both charge density and placement are critical to inhibition. Using the CNDO II method, approximate values for the charge density distribution in Ruelene can be computed, the results of which are shown in Figure 8. Examination of this figure and Table XIV shows that the P···H(1) (5.68 Å), P···H(2) (5.13 Å), P···C(3) (4.91 Å), P···C(4) (5.29 Å) and P···C(5) (4.53 Å) pairs are quite interesting in this regard. Again, these distances are presented as examples of distances which, because of the OP's similarity in size to ACh, should still be useful to compare to literature values. Rotation primarily about the C(1)-O(1) bond to the van der Waals limit on the Cℓ side of the molecule would yield the following P···δ(+) distances: P···H(1), 5.5 Å; P···H(2), 5.3 Å; P···C(3), 4.8 Å; P···C(4), 5.2 Å; P···C(5), 4.6 Å. That is, even if rotations occur the P···δ(+) distances do not vary by more than

±0.2 Å from the solid state distance, which should be preferred on a "time-averaged" basis.

These distances could be important since the range of ACh active site-separation distances for insect AChE is 5.0-5.5 Å[51] or 4.5-5.9 Å[52]. Therefore nearly all of the pairs presented may enter into the inhibition process as reactive species. The similarities in partial charge of all of the partner atoms to phosphorus do not help to rule out any pair entirely. In addition, the distances of all but one of the five pairs fall outside of the mammalian AChE distance range of 4.3-4.7 Å[51,52]. On the other hand, these site-separation ranges alone essentially rule out P···C(7) (6.79 Å) and P···H(3) (3.01 Å) as primary inhibition factors for either form of AChE. On the basis of steric factors the P···meta hydrogen pair(s) would have been the most plausible of the reactive moieties (assuming Krupka's[17] model). This all seems, though, to be in accord with the somewhat elevated mammalian (rat) LD_{50} of 770-1000 $mg \cdot kg^{-1}$[53] thus making Ruelene more of a "specific" OP insecticide than, say, the non-specific OP azinphos-methyl[49].

The observed disparity in insect *vs.* mammalian LD_{50} values typical of many OP insecticides[54] appears to be attributable, in part, to the inherently small selective range of favorable intramolecular distances afforded by the OP to provide a "match" with the isozymes of AChE. Restrictions of both the important distances and the possible steric conformations in Ruelene serve to further specify any inhibition reaction route, as well

to possibly narrow the predicted active site-separation distance ranges, thus giving a better idea of the topography and possible distortions of the OP active site on AChE. If the Ruelene molecule were not "semi-rigid", rotational freedom about the C(1)-O(1) bond would cause the P···H(1) distance, for exapmle, to vary by ∿±0.7 Å; P···H(2), by ∿±0.9 Å. Parallel to this the possible conformations would have different overall steric properties.

It is noteworthy that since, as a phosphate, Ruelene will not undergo *in vivo* oxidation, as the thiophosphate compounds can, it is likely therefore that Ruelene, with the presented structure, is the predominant AChE inhibitor.

THE CRYSTAL AND MOLECULAR STRUCTURE OF FOSPIRATE

Introduction

Thus far the studies have centered on homonuclear ring systems. However a number of commercially useful OP's have heteronuclear rings. Therefore, it now is quite appropriate to investigate some of these insecticides. The first such structure is that of fospirate (O,O-dimethyl O-3,5,6-trichloro-2-pyridyl phosphate), $(H_3CO)_2P(O)OC_5NHCl_3$. Fospirate has an LD_{50} of 225 and 263 $mg \cdot kg^{-1}$ for male and female CD-1 mice, respectively[58].

Experimental

Crystal Data.-- From a 99+% pure sample of the title compound, supplied by D. W. Osborne, a rectangular prismatic crystal with approximate dimensions 0.20 x 0.23 x 0.30 mm was selected and mounted on the end of a glass fiber using Elmer's Glue-All. The crystal was then mounted on a four-circle diffractometer and three ω-oscillation photographs were taken at various χ and ϕ settings, and verified that the crystal was indeed single.

From these photographs fifteen independent reflections were selected and their coordinates were input into an automatic indexing program[29]. The reduced cell scalars which resulted indicated monoclinic symmetry, which was confirmed by

inspection of ω-oscillation photographs taken about each of the three axes in turn. Only the *b* axis showed a mirror plane. Observed layer-line spacings agreed, within experimental error, with those predicted for this cell by the indexing program.

The lattice constants were obtained from a least-squares refinement based on the precise ± 2θ ($|2\theta| > 30^{\circ}$) measurements of twenty-five strong independent reflections. At 27°C using Mo Kα (λ = 0.70954 Å) they are a = 12.267(5), b = 8.685(1), c = 14.102(6) Å and β = 126.62(3)°. The observed density of 1.67(2) $g \cdot cm^{-3}$ determined by the flotation method is in good agreement with the calculated value of 1.688 $g \cdot cm^{-3}$ for four molecules with a molecular weight of 306.46 $g \cdot mol^{-1}$ in a unit cell having a volume of 1205.83 $Å^3$.

Collection and Reduction of X-ray Intensity Data.-- The data were collected at 27°C with graphite-monochromated Mo Kα radiation on an automated four-circle diffractometer designed and built in the Ames Laboratory and previously described by Rohrbaugh and Jacobson[31]. All data within a 2θ sphere of 45° ($(\sin\theta)/\lambda$ = 0.539 $Å^{-1}$) in the hkℓ and $\bar{h}$kℓ octants were measured using an ω-stepscan technique.

As a general check on electronic and crystal stability, the intensities of three standard reflections were remeasured every seventy-five reflections. These standard reflections were not observed to vary significantly throughout the entire period of data collection (∿2 days). Hence, a decomposition correction was unnecessary. A total of 2424 reflections were

recorded in this manner. Examination of the data revealed the following systematic absences: h0ℓ when ℓ = 2n + 1 and 0k0 k = 2n + 1. These absences uniquely determine the space group as $P2_1/c$.

Ths Intensity data were corrected for Lorentz and polarization effects and, since $\mu = 8.84\ cm^{-1}$, absorption corrections were not made; maximum and minimum transmission factors were 0.838 and 0.767, respectively. The estimated variance in each intensity was calculated by:

$$\sigma_I^2 = C_T + 2C_B + (0.03C_T)^2 + (0.03C_B)^2,$$

where C_T and C_B represent the total and background counts, respectively, and the factor 0.03 represents an estimate of non-statistical errors. The estimated deviations in the structure factors were calculated by the finite difference method[32]. Equivalent data were averaged and 1114 reflections with $|F_o| > 2.5\sigma(F_o)$ were retained for use in subsequent calculations. During later work it was discovered that ten large reflections suffered from secondary extinction effects. These data were eliminated from the final stages of refinement. The data will be found in the 1977 supplementary material section of J. Agric. Food Chem. See any current masthead page for ordering the information.

Solution and Refinement

The position of a chlorine was obtained from an analysis of a standard three-dimensional Patterson function. The re-

maining atoms were found by successive structure factor[35] and electron density map calculations[34]. These atomic positions were subsequently refined by a full-matrix least-squares procedure[35] minimizing the function $\Sigma\omega(|F_o|-|F_c|)^2$, where $\omega=1/\sigma_F^2$. This refinement yielded a conventional discrepancy factor of $R = \Sigma||F_o|-|F_c||/\Sigma|F_o| = 0.125$. At this stage of the refinement all sixteen non-hydrogen atoms had been refined using isotropic thermal parameters. The scattering factors used were those of Hanson, *et al.*[36], modified for the real and imaginary parts of anomalous dispersion[37]. The scattering factors for hydrogen were those of Stewart, *et al.*[45]

Analysis of an electron density difference map did not reveal either the ring or the methyl hydrogens. Consequently, the ring hydrogen atom position was fixed at 0.95 Å from the corresponding carbon (C(3)). The methyl hydrogens were inserted in approximately tetrahedral positions using the precise positions of the corresponding methyl carbon and the methoxy oxygen. The methyl C-H distances were set equal to 1.0 Å; all isotropic hydrogen temperature factors were set equal to 4.5 Å^2.

Subsequent anisotropic least-squares refinement without varying the hydrogen parameters converged to R = 0.062. Since this procedure yielded slightly different non-hydrogen atom positions, all of the hydrogen positions were recalculated. Further refinement cycles did not significantly alter any atomic parameters and the discrepancy factor did not change.

The final positional and thermal parameters are listed in Table XVII. Standard deviations were calculated from the inverse matrix of the final least-squares cycle. Bond lengths and angles are listed in Table XVIII and Table XIX, respectively. Dihedral angles and least-square planes are listed in Table XX.

Description of Structure and Discussion

The pyridoxyl group in fospirate, shown in Figures 11 and 12[40], is essentially planar (*cf.* Table XX, Plane II). For the most part, packing in the fospirate crystal can be regarded as either weakly Coulombic or van der Waals in nature. The former is a manifestation of the charge density distribution within each individual molecule and hence corroborates one's "chemical intuition" of atoms with $\delta(+)$ and $\delta(-)$ charges. The H(1)···O(2) interaction related *via* the two-fold screw operation serves as such an example (Figure 12 and Tables XVIII and XIX), while on the other hand, the N···C(7)H_3 and C(6)H_3···O(4) interactions appear to be van der Waals in character (Figure 12 and Table XVIII).

The C(1)-O(1) bond in fospirate is significantly ($\sim 7\sigma$) shorter than the two methoxy C-O bonds (*cf.* Table XVIII), while the P-O(1) bond is the longest of the three P-O bonds, being at least 6σ longer than the other two. These observations, which when coupled with a CNDO II molecular orbital calculation

Table XVII. Final positional[a] and thermal[b] parameters for fospirate

	Fractional Coordinates			Atomic Temperature Factors					
Atom	x	y	z	β_{11}	β_{22}	β_{33}	β_{12}	β_{13}	β_{23}
Cℓ(1)	0.0378(3)[c]	0.2057(3)	0.1357(2)	21.8(4)	14.5(4)	13.5(3)	0.1(3)	11.2(3)	-0.3(2)
Cℓ(2)	-0.3799(2)	0.5855(4)	-0.0065(2)	11.4(3)	32.4(6)	15.4(3)	-0.6(3)	8.0(2)	0.2(3)
Cℓ(3)	-0.1786(2)	0.8647(3)	0.0668(2)	17.2(3)	18.3(4)	14.1(3)	3.5(3)	9.7(3)	2.9(2)
P	0.3017(2)	0.6126(2)	0.2664(2)	10.4(3)	18.3(4)	9.0(2)	0.5(3)	6.3(2)	0.4(2)
O(1)	0.1800(5)	0.4959(6)	0.1782(4)	11.7(7)	17.0(9)	12.0(5)	-1.3(6)	7.6(5)	-1.8(6)
O(2)	0.3051(6)	0.6550(6)	0.3684(5)	14.4(7)	22(1)	9.1(5)	1.9(7)	6.9(5)	0.6(6)
O(3)	0.4225(5)	0.5200(7)	0.2878(5)	12.7(7)	24(1)	14.3(6)	2.3(7)	9.3(6)	0.5(7)
O(4)	0.2924(6)	0.7460(6)	0.1888(5)	18.8(9)	19(1)	13.6(6)	-1.3(8)	11.8(6)	0.1(7)
N	0.0046(6)	0.6569(7)	0.1253(5)	10.8(9)	13(1)	10.0(6)	-0.4(7)	6.2(6)	-0.1(6)
C(1)	0.0491(7)	0.5162(9)	0.1392(6)	10.9(9)	18(1)	6.7(6)	-1.6(9)	5.6(6)	-0.1(7)
C(2)	-0.0281(8)	0.3863(8)	0.1149(7)	16(1)	13(1)	8.7(7)	-2(1)	7.5(8)	-1.1(7)
C(3)	-0.1634(8)	0.407(1)	0.0696(7)	14(1)	19(2)	9.2(8)	-4(1)	7.6(8)	-2.2(8)
C(4)	-0.2126(8)	0.556(1)	0.0519(6)	12(1)	20(1)	9.0(7)	-3(1)	6.6(7)	-0.9(8)
C(5)	-0.1247(9)	0.6770(9)	0.0813(7)	14(1)	15(1)	8.0(7)	2(1)	6.8(7)	2.9(7)
C(6)	0.457(1)	0.371(1)	0.3415(9)	17(1)	32(2)	16(1)	10(1)	9(1)	7(1)
C(7)	0.254(1)	0.900(1)	0.1966(8)	22(2)	15(1)	15(1)	-1(1)	11(1)	1(1)
H(1)	-0.2210[c]	0.3216	0.0509	4.5					
C6H(1)	0.3744	0.3034	0.2975	4.5					
C6H(2)	0.4898	0.3808	0.4255	4.5					
C6H(3)	0.5296	0.3244	0.3392	4.5					
C7H(1)	0.3326	0.9711	0.2282	4.5					
C7H(2)	0.2265	0.9002	0.2507	4.5					
C7H(3)	0.1758	0.9352	0.1162	4.5					

[a] The positional parameters for all atoms are represented in fractional unit cell coordinates.

[b] The β_{ij} are defined by: $T = \exp\{-(h^2\beta_{11} + k^2\beta_{22} + \ell^2\beta_{33} + 2hk\beta_{12} + 2h\ell\beta_{13} + 2k\ell\beta_{23})\}$. If only the β_{11} column is listed, this corresponds to an isotropic temperature factor. All hydrogen isotropic temperature factors have been set equal to 4.5 . Non-hydrogen thermal parameters are ($\times 10^4$).

[c] In this and succeeding tables estimated standard deviations are given in parentheses for the least significant figures and include the error in the lattice constants. Since the hydrogens were not refined, no standard deviations are given.

Table XVIII. Selected interatomic distances (Å) for fospirate

Bonding Distances					
C(1)-C(2)	1.38(1)	Interaction	via	Observed Distance	Total van der Waals Distance (from Pauling[39])
C(2)-C(3)	1.39(1)	Cℓ(1)···O(1)	Intramolecular	2.917(5)	3.20
C(3)-C(4)	1.39(1)	Cℓ(2)···Cℓ(3)	Intramolecular	3.161(4)	3.60
C(4)-C(5)	1.38(1)	$C(6)H_3$···O(2)	Intramolecular	3.24(1)	3.4
C(5)-N	1.33(1)	$C(7)H_3$···O(2)	Intramolecular	3.00(1)	3.4
N-C(1)	1.30(1)				
		N···O(2)	Intramolecular	3.204(8)	2.9
C(1)-O(1)	1.364(9)	N···O(4)	Intramolecular	3.177(8)	2.9
C(2)-Cℓ(1)	1.709(8)	N···$C(7)H_3$	Intramolecular	3.34(1)	3.5
C(3)-H(1)	0.950(8)				
C(4)-Cℓ(2)	1.714(8)	H(1)···O(2)	2_1	2.419(5); 2.32[a]	2.6
C(5)-Cℓ(3)	1.725(8)	Cℓ(2)···Cℓ(2)	(center of inversion + 1 cell in x and y)	3.400(5)	3.60
		$C(6)H_3$···O(4)	2_1 + one cell in x	3.52(1)	3.4
P-O(1)	1.609(5)				
P=O(2)	1.461(6)				
P-O(3)	1.549(6)				
P-O(4)	1.551(6)				
O(3)-C(6)	1.43(1)				
O(4)-C(7)	1.44(1)				

[a] Using a C(6)-proton distance of 1.08 Å (Sutton[57])

Table XIX. Bond angles (degrees) for fospirate

Angle	Degrees
C(1)-C(2)-C(3)	117.5(7)
C(2)-C(3)-C(4)	118.6(7)
C(3)-C(4)-C(5)	118.5(7)
C(4)-C(5)-N	123.0(7)
C(5)-N-C(1)	118.0(6)
N-C(1)-C(2)	124.5(7)
O(1)-C(1)-N	117.9(6)
O(1)-C(1)-C(2)	117.6(7)
Cℓ(1)-C(2)-C(1)	121.6(6)
Cℓ(1)-C(2)-C(3)	120.9(6)
H(1)-C(3)-C(2)	120.7(9)
H(1)-C(3)-C(4)	120.7(8)
Cℓ(2)-C(4)-C(3)	119.5(6)
Cℓ(2)-C(4)-C(5)	122.0(7)
Cℓ(3)-C(5)-C(4)	120.5(7)
Cℓ(3)-C(5)-N	116.5(6)
C(1)-O(1)-P	123.8(5)
O(1)-P-O(2)	112.8(3)
O(1)-P-O(3)	99.3(3)
O(1)-P-O(4)	106.3(3)
O(2)-P-O(3)	118.5(3)
O(2)-P-O(4)	117.0(3)
O(3)-P-O(4)	100.6(3)
P-O(3)-C(6)	121.1(6)
P-O(4)-C(7)	121.9(5)
P-O(2)···H(1)[a]	149.5
P-O(4)···C(6)[b]	127.9(4)
C(7)-O(4)···C(6)[b]	94.2(5)
O(2)···H(1)-C(3)[a]	140.7

[a] Through 2_1, using a C(3)-proton distance of 1.08 Å (Sutton[57])

[b] Through 2_1 and one cell in x.

Table XX. Dihedral angles (degrees) and least-squares planes

Planes Defined By:	Dihedral Angle of Planes[a]
O(1)-O(3)-O(4); N-C(2)-C(4)	18.1(3)
O(1)-O(3)-O(4); C(1)-C(3)-C(5)	18.5(3)
O(1)-O(3)-O(4); O(1)-P-C(1)	47.3(5)
O(1)-P-C(1); C(1)-C(3)-C(5)	11.6(5)
O(1)-P-C(1); C(2)-C(4)-N	11.5(5)
O(1)-P-C(1); P-O(2)-O(1)	47.5(6)

Plane (II)[b] defined by all eleven pyridoxyl members:
(-0.36624) X + (-0.00126) Y + (0.93052) Z - (1.66461) = 0

Atom	Distance from plane (Å)	Atom	Distance from plane (Å)
C(1)	0.0048	O(1)	-0.0530
C(2)	0.0222	C*(1)	0.0110
C(3)	0.0120	H(1)	0.0182
C(4)	-0.0082	C*(2)	-0.0525
C(5)	-0.0046	C*(3)	0.0371
N	0.0132	O(3)	0.3494
		O(4)	-0.4161

Plane (IV)[b] defined by P, O(2), O(4) and C(7);
(0.78723) X + (0.19757) Y + (0.58415) Z - (4.03107) = 0

Atom	Distance from plane (Å)
P	-0.0688
O(2)	0.0349
O(4)	0.0710
C(7)	-0.0371

Plane (I)[b] defined by carbons (1-5) and N:
(-0.37180) X + (0.00525) Y + (0.92830) Z - (1.70879) = 0

Atom	Distance from plane (Å)
C(1)	-0.0106
C(2)	0.0042
C(3)	0.0035
C(4)	-0.0054
C(5)	-0.0003
N	0.0085

Plane (III)[b] defined by P, O(2), O(3) and C(6):
(0.61564) X + (0.54225) Y + (0.57179) Z - (5.75549) = 0

Atom	Distance from plane (Å)
P	-0.2470
O(2)	0.1093
O(3)	0.2563
C(6)	-0.1186

Plane (V)[b] defined by P, O(1), O(2) and C(1):
(0.03263) X + (0.86730) Y + (-0.49671) Z - (2.97294) = 0

Atom	Distance from plane (Å)
P	0.1914
O(1)	-0.2162
O(2)	-0.0895
C(1)	0.1143

[a] Angles correspond to the orientation shown in Figures 11 and 12 so that the phosphorus is directed towards the N side of the ring.

[b] Planes are defined by $c_1X + c_2Y + c_3Z - d = 0$, where X, Y and Z are Cartesian coordinates which are related to the triclinic cell coordinates (x,y,z) by the transformations:

$X = xa \sin\gamma + zc\{(\cos\beta - \cos\alpha \cos\gamma)/\sin\gamma\} = xa + zc \cos\beta$
$Y = xa \cos\gamma + yb + zc \cos\alpha = yb$
$Z = zc\{1 - \cos^2\alpha - \cos^2\beta - \cos^2\gamma + 2\cos\alpha \cos\beta \cos\gamma)^{\frac{1}{2}}/\sin\gamma\} = zc \sin\beta$.

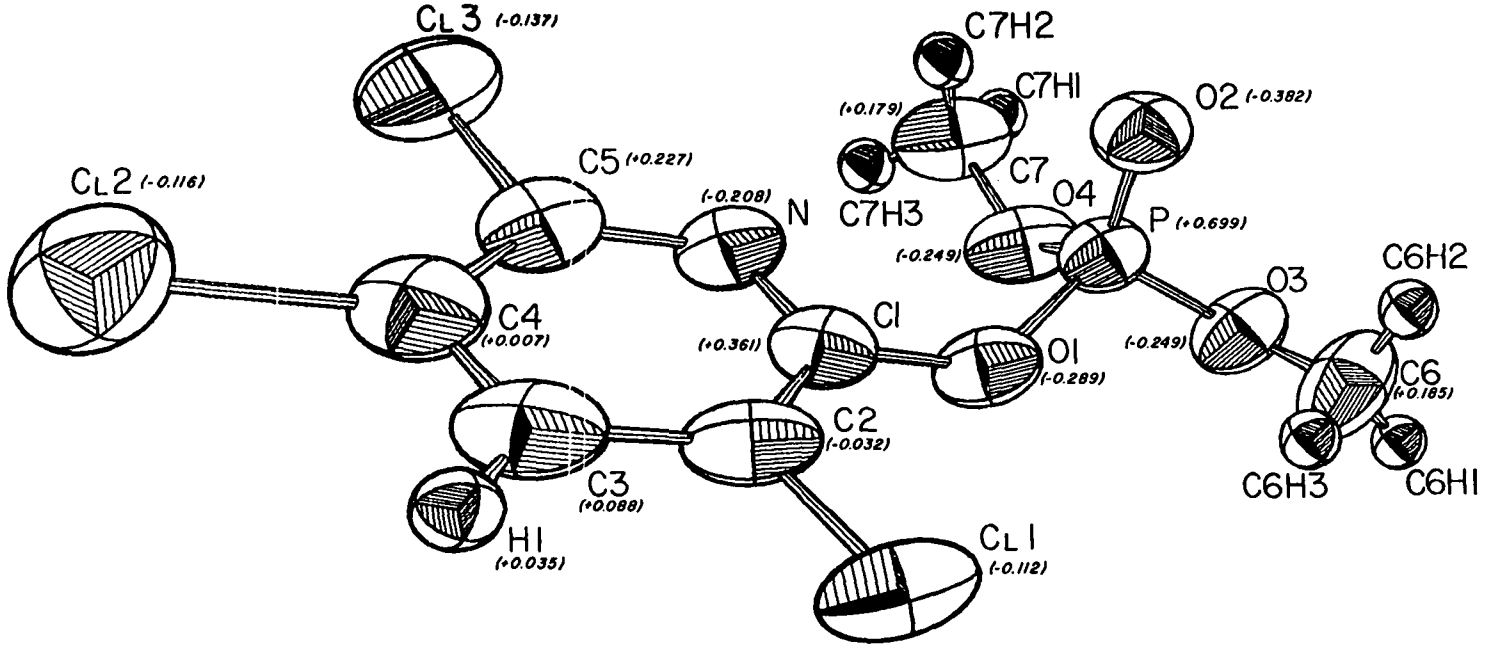

Figure 11. The fospirate molecule showing 50% probability ellipsoids; 30% for hydrogens. The numbers in parentheses refer to partial charge densities from a CNDO II calculation.

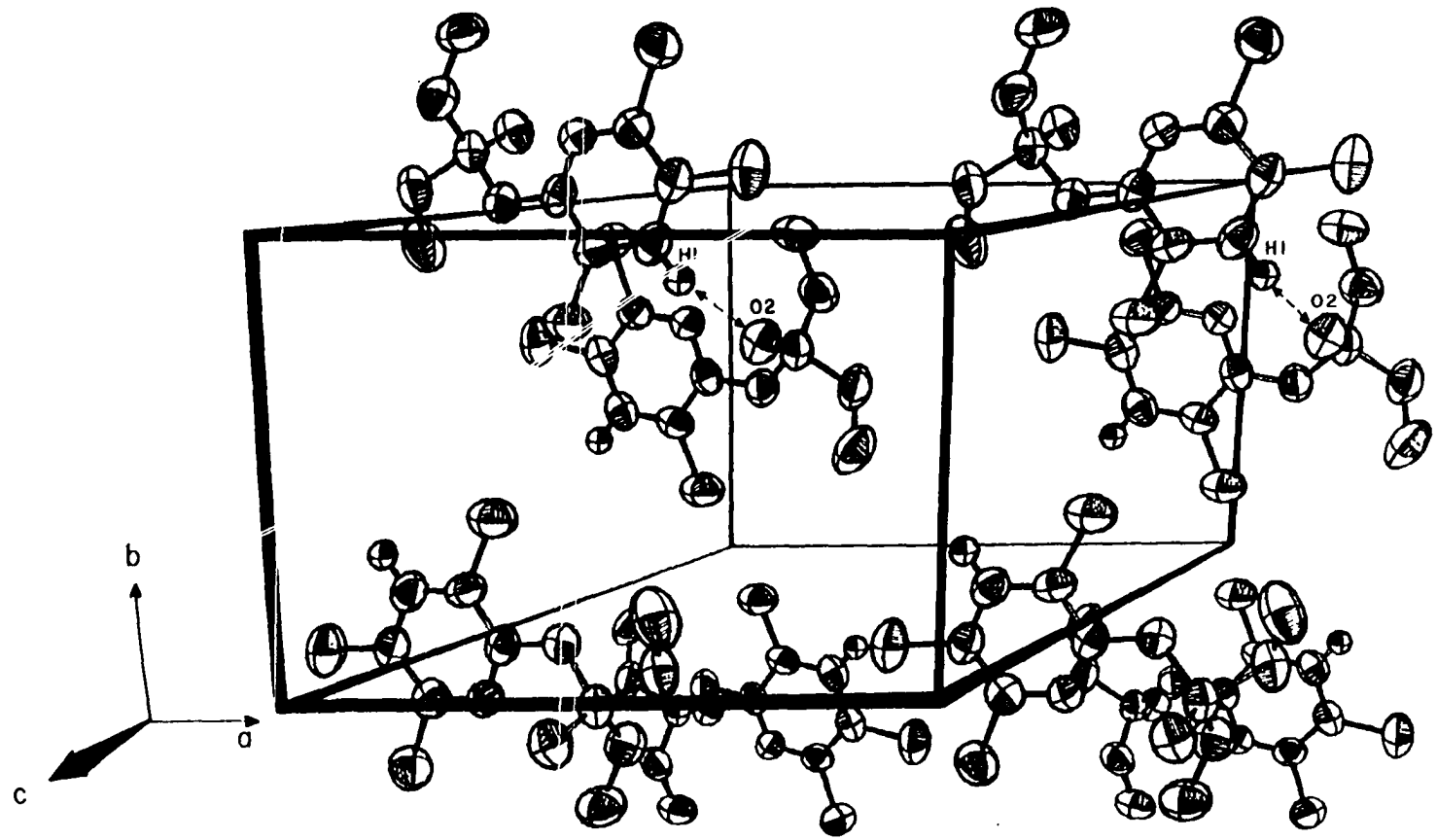

Figure 12. View of two adjacent unit cells illustrating packing in the *a* and *b* directions.

of the Pople and Beveridge[47] type, are consistent with a bonding formulation in which there is a weak π overlap of the p_z orbital on the oxygen with the ring system which simultaneously weakens the O-P bond. The latter effect should enhance phosphorylation[48]. Such variations in bond lengths have been noted earlier as the bond lengths corresponding to P-O(1) and C(1)-O(1) in fospirate, ronnel, ronnel oxon, bromophos, Ruelene, Coroxon[42], methyl parathion[6] and a new OP whose structure was done by Grand and Robert[59] are all within 3σ of being identical. The angles of the type S=P-O or O=P-O in these compounds are all greater than the tetrahedral angle of 109.47°. In fospirate the angle between the normal to the ring and the P-O(2) vector is 19.9° which is only ∿1.5° greater than the angle between the normals to the O(1)-O(3)-O(4) plane and the ring (*cf.* Table XX).

As with all of the OP's presented here, the phosphorus in fospirate is opposite the Cℓ(1) side of a plane which is perpendicular to the ring and contains the C(1)-O(1) bond. The position of the phosphorus appears to be dictated by the interactions of O(2), $C(7)H_3$ and O(4) with N as well as the phosphate group with Cℓ(1). Both the O(2) and O(4) atoms are essentially equidistant (∿3.2 Å) from the nitrogen (*cf.* Table XVIII). This is only 0.3 Å longer than the sum of the van der Waals radii. As a result, the N-C(1)-O(1)-P torsional angle is only 11.5° and O(2) is skewed away from the C(1)-O(1)-P plane towards the Cℓ(1) side of the ring (*cf.* Figure 11 and Table XX).

The fact that the oxygens are symmetrically disposed seems to imply that the two-fold screw related H(1)···O(2) interaction, which is the only significant intermolecular interaction involving either O(2) or O(4), is of little or no consequence in determining the position of the phosphorus, as the H(1)···O(2) distance of 2.3 Å would only indicate a weak hydrogen bond at best (*cf.* Tables XVIII and XIX and Figure 12). The molecular configuration especially in the neighborhood of the phosphorus atom may therefore be somewhat immobilized primarily as a result of van der Waals restrictions to rotation about the C(1)-O(1) and O(1)-P bonds; the forces involved would not be expected to be as strong as those due to the intramolecular hydrogen bonds in bromophos or Ruelene.

To further substantiate such a view, a CNDO II molecular orbital calculation (after Pople and Beveridge[47]) was carried out for fospirate in order to obtain information on the change in the potential energy surface as a function of incremental rotations about the C(1)-O(1) or O(1)-P bonds. In the case of rotation about the C(1)-O(1) bond, the C(1)-O(1)-P-O(2) torsional angle was maintained at 47.5° (*i.e.* the angle in the solid state) throughout the calculations. Similarly, the C(2)-C(1)-O(1)-P angle was kept at 11.6° during the set of calculations involving the rotation about the O(1)-P bond. Results of these calculations are shown in Figures 13 and 14, respectively. Since they represent plots of uncoupled degrees of freedom and because of the approximate nature of the calcu-

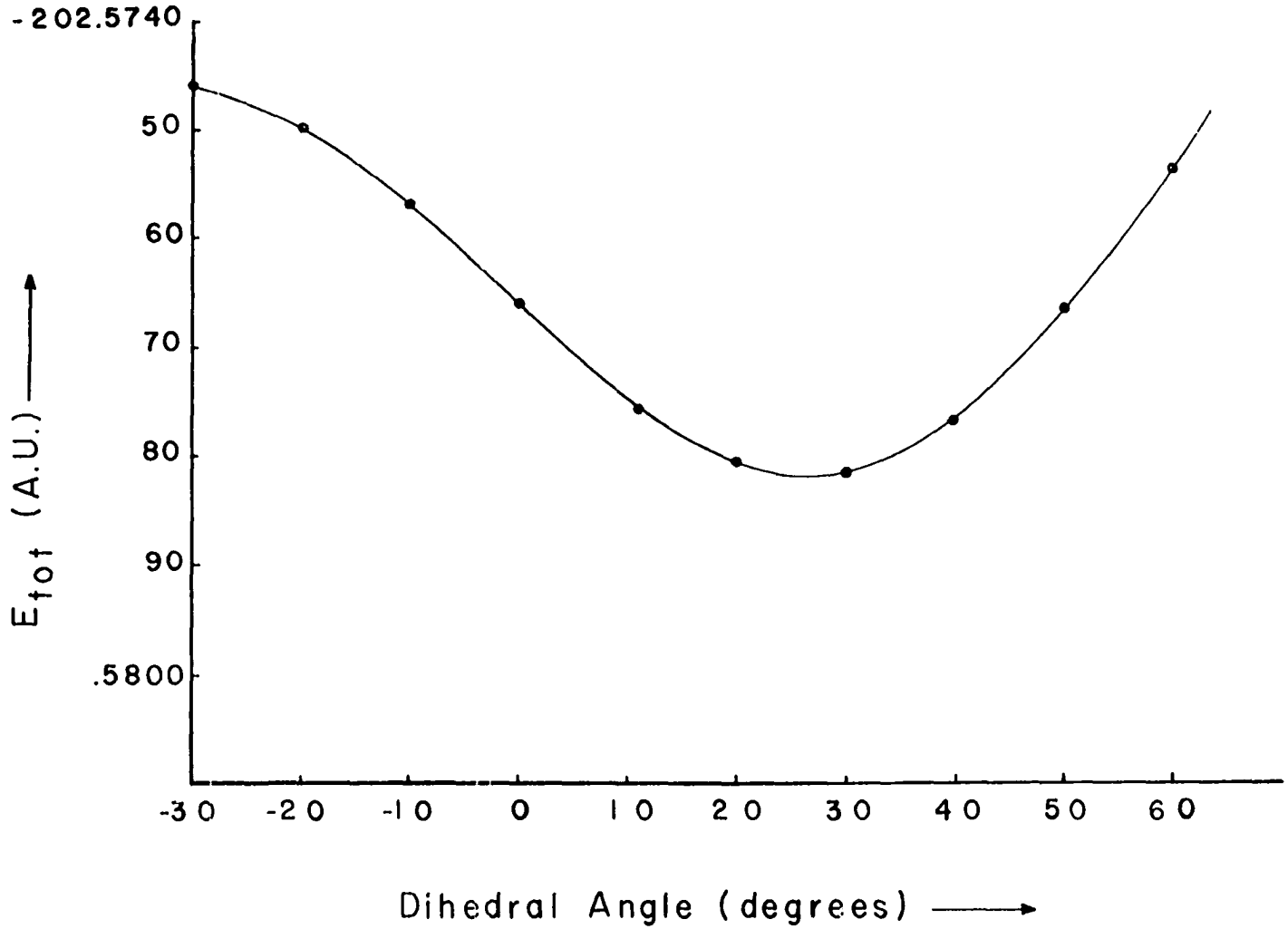

Figure 13. Total energy *vs.* C(2)-C(1)-O(1)-P dihedral angle from CNDO calculations.

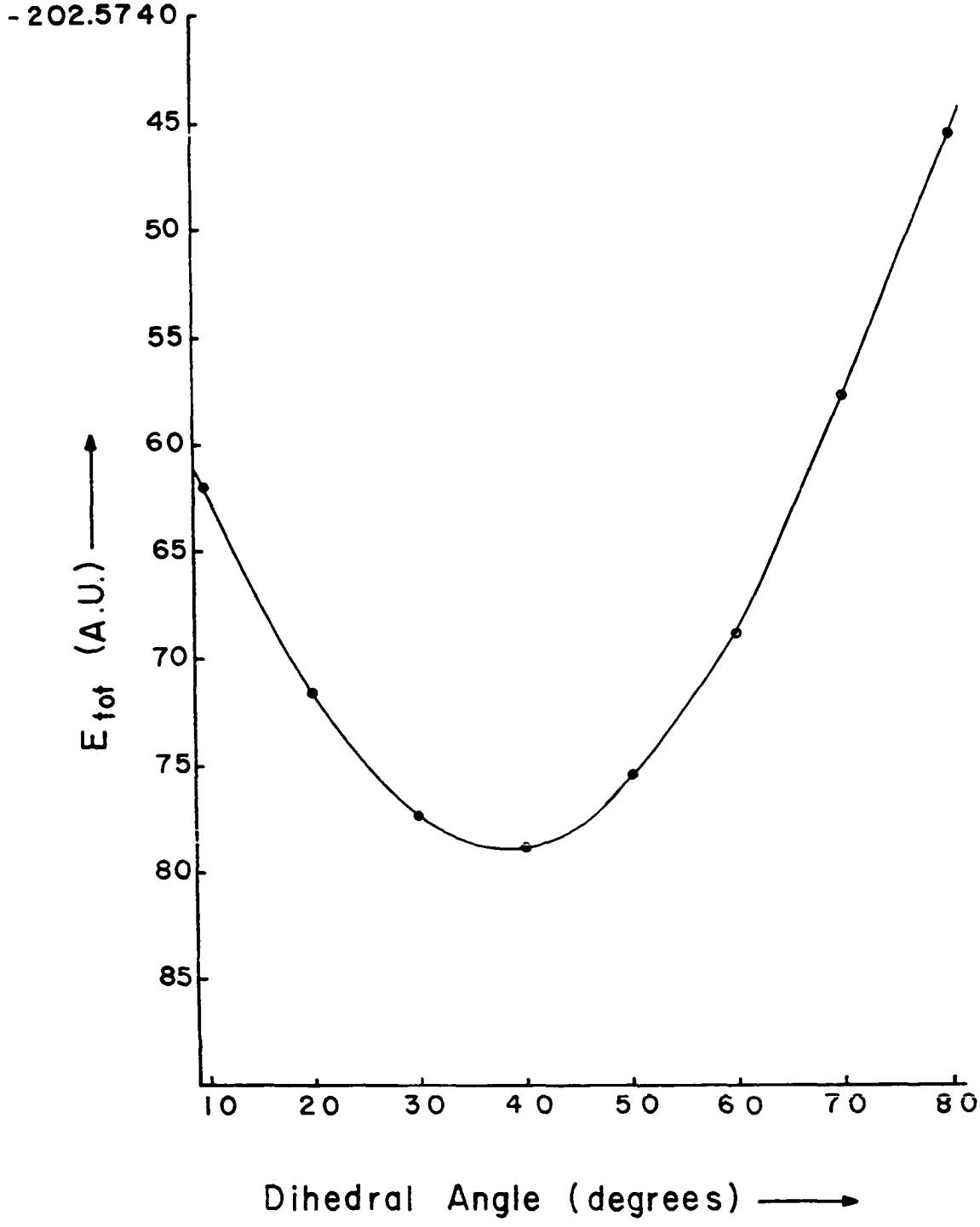

Figure 14. Total energy *vs.* C(1)-O(1)-P-O(2) dihedral angle from CNDO calculations.

lations, it is not too surprising that the minima of each plot correspond to slightly different dihedral angles than are actually observed in the solid state. A similar result was obtained with Ruelene. The minimum in Figure 13 coincides with a C(2)-C(1)-O(1)-P angle only $\sim 12^{\circ}$ greater than the observed angle of 11.6°. Figure 14 indicates a C(1)-O(1)-P-O(2) angle just $\sim 8^{\circ}$ less than 47.5°. It is also interesting to note that the depths of both potential wells are ~ 2.5 kcal·mol^{-1} (1 A.U.= 627.4 kcal·mol^{-1}) and the energy minima on both plots occur at $\sim$ -202.5780 A.U., as expected.

As these results were obtained using CNDO methods, the absolute values of the energies and charges, as well as the differences in energies, are not as exact as with *ab initio* calculations. The latter methods are usually unavailable for this size of a problem and are extremely cost-prohibitive. Although admittedly approximate, the energies and charges obtained in this CNDO II calculation certainly give better than "order of magnitude" information especially since d-orbital contributions are included for the phosphorus and chlorine atoms.

On the basis of a restricted phosphorus position, comparison of some intramolecular distances with literature site-separation distances for AChE should give some insight into the "toxicity/activity of fospirate. Again, these distances are presented as examples of distances which, because of the OP's similarity in size to ACh, should still be useful to compare to

literature values. In addition to being "distance compatible", the atoms involved must also be "charge compatible". For example, if one were to use the (possibly incorrect) model of Krupka[17], the two atoms of the OP likely involved would both need to be δ(+). Only two atoms would be considered in accordance with the presence of two residues in the ACh active site of AChE. Analysis of the steric interactions of the remaining parts of both molecules, without knowing more about the structure(s) of AChE, would be somewhat futile.

Using the CNDO II method, approximate values for the charge density distribution in fospirate can be computed; results are shown in Figure 11. Examination of this figure (and Table XVIII) shows that P···H(1) (5.79 Å), P···C(3) (4.95 Å), P···C(4) (5.14 Å) and P···C(5) (4.27 Å) are quite interesting pairs in this regard. The small charge on C(4) of +0.007e would appear to rule out the P···C(4) pair as an important contributor to inhibition. The P···H(1) and P···C(3) distances fall outside of the mammalian AChE site-separation range of 4.3-4.7 Å[51,52], and yet are close to or within the range for insect AChE given by Hollingworth *et al.*[51] of 5.0-5.5 Å and O'Brien[52] of 4.5-5.9 Å. It is even conceivable with Krupka's[17] model that since both H(1) and C(3) are δ(+) and are both "distance compatible" with insect AChE, the C(3)-H(1) pair might correspond to a region of δ(+) charge having P···δ(+) distances of from 4.95 to 5.79 Å. Considering charge, distance, steric factors and overall reactivity, P···H(1) could be slightly favored as the reac-

tive species towards insect AChE in fospirate. The P···C(5) pair, due to its shorter distance, may play a more important role in mammalian toxicity, unless significant conformational alterations in AChE or fospirate accompany any *in vivo* free energy changes.

It should be noted that even rotations about the C(1)-O(1) bond of, say, ±40°, which, according to Figure 13, may possibly be achieved *in vivo*, would correspond to a maximum change in the P···H(1) distance, for example, of only ±0.03 Å. This is not likely to be critical with respect to the distances in AChE and to the I_{50} of the insecticide as pertains to the conformation which AChE or fospirate might have to distort to in order to react. However, such a rotation would cause the phosphorus to be in a slightly different position relative to the ring substituents. This may be partially responsible, then, for changes in i_{50} and/or LD_{50} values as a result of subtle steric influences of the insecticide with AChE. But, in order to make better comparisons and predictions, many heretofore unreported insect and mammalian I_{50} and LD_{50} values will need to be investigated and tabulated, especially for the different isozymes of AChE. In addition, further similar CNDO calculations will need to be performed to obtain a better idea of the potential energy barriers which may be necessary to overcome in adduct formation.

THE CRYSTAL AND MOLECULAR STRUCTURE OF CHLORPYRIFOS

Introduction

The crystal and molecular structure of chlorpyrifos (O,O-diethyl O-3,5,6-trichloro-2-pyridyl thiophosphate), $(H_5C_2O)_2P(S)OC_5NHCl_3$, was undertaken to further investigate the effects of a heteronuclear ring system. As the di-ethoxy thiophosphate analog of fospirate, chlorpyrifos now affords the opportunity to study structural vagaries due both to homologous series and the replacement of an oxygen atom with a sulfur.

Experimental

Crystal Data.-- From a 99+% pure sample of the title compound, supplied by D. W. Osborne, a rectangular prismatic crystal with approximate dimensions 0.20 x 0.20 x 0.10 mm was selected and mounted on the end of a glass fiber using Elmer's Glue-All. The crystal was then mounted on a four-circle diffractometer and three ω-oscillation photographs were taken at various χ and ϕ settings, and verified that the crystal was indeed single.

From these photographs fifteen independent reflections were selected and their coordinates were input into an automatic indexing program[29]. The reduced cell scalars which resulted indicated monoclinic (2/m) symmetry, which was confirmed by inspection of ω-oscillation photographs taken about each of

the three axes in turn. Only the *b* axis showed a mirror plane. Observed layer-line spacings agreed, within experimental error, with those predicted for this cell by the indexing program.

The lattice constants were obtained from a least-squares refinement based on the precise ±2θ (20 ($20^\circ < |2\theta| < 30^\circ$) measurements of twenty strong independent reflections. At 27°C using Mo Kα (λ = 0.70954 Å) they are a = 22.06(1), b = 9.485(2) c = 15.990(6) Å and $\beta = 114.63(4)^\circ$. The observed density of 1.49(2) $g \cdot cm^{-3}$ determined by the flotation method is in good agreement with the calculated value of 1.532 $g \cdot cm^{-3}$ for eight molecules with a molecular weight of 350.52 $g \cdot mol^{-1}$ in a unit cell having a volume of 3041.33 $Å^3$.

Collection and Reduction of X-ray Intensity Data.-- The data were collected at 27° with graphite-monochromated Mo Kα radiation on an automated four-circle diffractometer designed and built in the Ames Laboratory and previously described by Rohrbaugh and Jacobson[31]. All data within a 2θ sphere of 50° ($(\sin\theta)/\lambda$ = 0.596 $Å^{-1}$) in the hkℓ, $\bar{h}k\ell$, $hk\bar{\ell}$ and $\bar{h}k\bar{\ell}$ octants were measured using an ω-stepscan technique.

As a general check on electronic and crystal stability, the intensities of three standard reflections were remeasured every seventy-five reflections. These standard reflections were not observed to vary significantly throughout the entire period of data collection (∿ 4 days). Hence a decomposition correction was unnecessary. A total of 5687 reflections were recorded in this manner. Examination of the data revealed the

following systematic absences: hkℓ when h+k = 2n+1 and h0ℓ when ℓ = 2n+1 (h=2n+1) and 0k0 when k = 2n+1. These absences, coupled with a statistical indication[55] of a center of symmetry, implied C2/c as the space group.

The intensity data were corrected for Lorentz and polarization effects and, since $\mu = 8.39$ cm^{-1}, absorption corrections were not made; maximum and minimum transmission factors were 0.92 and 0.85, respectively. The estimated variance in each intensity was calculated by:

$$\sigma_I^2 = C_T + 2C_B + (0.03\ C_T)^2 + (0.03\ C_B)^2,$$

where C_T and C_B represent the total and background counts, respectively, and the factor 0.03 represents an estimate of non-statistical errors. The estimated deviations in the structure factors were calculated by the finite difference method[32]. Equivalent data were averaged and the 1426 reflections with $|F_o| > 2.5\sigma(F_o)$ were retained for use in subsequent calculations. During later work it was discovered that five large reflections suffered from secondary extinction effects; these were eliminated from the final stages of refinement.

Solution and Refinement

The position of a chlorine was obtained from an analysis of a standard three-dimensional Patterson function. The remaining atoms were found by successive structure factor[35] and electron density map calculations[34]. These atomic positions were subsequently refined by a full-matrix least-squares

procedure[35] minimizing the function $\Sigma\omega(|F_o|-|F_c|)^2$, where $\omega = 1/\sigma_F^2$. This refinement yielded a conventional discrepancy factor of $R = \Sigma||F_o|-|F_c||/\Sigma|F_o| = 0.125$. At this stage of the refinement all eighteen non-hydrogen atoms had been refined using isotropic thermal parameters. The scattering factors used were those of Hanson, *et al.*[36], modified for the real and imaginary parts of anomalous dispersion[37]. The scattering factors for hydrogen were those of Stewart, *et al.*[45]

Analysis of an electron density difference map did not reveal either the ring or the methyl hydrogens. Consequently the ring hydrogen atom position was fixed at 0.95 Å from the corresponding carbon (C(3)). Methyl hydrogens were inserted in approximately tetrahedral positions using the precise positions of the corresponding methyl carbon and the methoxy oxygen. Each set of methyl hydrogens was rotated by 60° about the corresponding O-Me bond; all twelve methyl hydrogens were assigned half-occupancy. As a result, a "doughnut" of hydrogens was approximated. The methyl C-H distances were set equal to 1.0 Å; all isotropic hydrogen temperature factors were set equal to 4.5 Å^2.

Subsequent anisotropic least-squares refinement without varying the hydrogen parameters converged to R = 0.066. Since this procedure yielded slightly different non-hydrogen atom positions, all of the hydrogen positions were recalculated. Further refinement cycles did not significantly alter any

atomic parameters and the discrepancy factor did not change.

The final positional and thermal parameters are listed in Table XXI. Standard deviations were calculated from the inverse matrix of the final least-squares cycle. Bond lengths and angles are listed in Table XXII and Table XXIII, respectively[38]. Dihedral angles and least-square planes are listed in Table XXIV.

Description of Structure and Discussion

The pyridoxyl group in chlorpyrifos, shown in Figures 15 and 16[40], is essentially planar (*cf.* Table XXIV, Plane IV). For the most part, packing in the chlorpyrifos crystal can be regarded as primarily van der Waals in nature as all close intermolecular interactions are greater than or comparable to the sum of the van der Waals radii (*cf.* Table XXII).

The unusually elongated C(6) and C(7) thermal ellipsoids (*cf.* Figure 15) suggest some disordering of these atoms. Therefore an attempt was made to account for such disorder *via* a least-squares refinement replacing each carbon with two carbons having an assigned occupancy of one-half and being displaced initially by $\sim$0.8 Å along the major axis of each ellipsoid. This procedure reduced R by only 0.006 but did account for the distance and angle discrepancies involving O(3), C(6) and C(7) (*cf.* Tables XXII and XXIII). That is, instead of short O(3)-C(6) and C(6)-C(7) bonds connecting the centers of the ellipsoids, the "left" half of C(6) is actually bonded to

Table XXI. Final positional[a] and thermal[b] parameters for chlorpyrifos

	Fractional Coordinates			Atomic Temperature Factors					
Atom	x	y	z	β_{11}	β_{22}	β_{33}	β_{12}	β_{13}	β_{23}
Cl(1)	0.4939(1)[c]	-0.1379(2)	0.6295(2)	5.9(1)	24.7(4)	10.7(2)	0.1(1)	3.6(1)	2.6(2)
Cl(2)	0.3266(1)	0.2230(3)	0.3841(1)	4.1(1)	38.9(5)	9.0(1)	1.1(2)	0.1(1)	0.7(2)
Cl(3)	0.4195(1)	0.4722(2)	0.5010(2)	4.6(1)	27.2(4)	10.8(2)	2.0(1)	1.8(1)	4.3(2)
S	0.6679(1)	0.2277(2)	0.6677(1)	4.2(1)	25.6(4)	7.8(1)	-1.2(1)	2.5(1)	0.1(2)
P	0.6304(1)	0.2115(2)	0.7546(1)	3.3(1)	19.3(3)	6.3(1)	0.2(1)	1.3(1)	1.3(1)
O(1)	0.5620(2)	0.1222(5)	0.7177(3)	3.1(1)	26.6(9)	7.9(3)	-1.1(3)	0.9(2)	3.6(4)
O(2)	0.6697(2)	0.1269(5)	0.8449(3)	4.1(1)	21.1(8)	6.4(3)	1.5(3)	1.1(2)	2.3(4)
O(3)	0.6160(3)	0.3471(6)	0.7958(3)	6.7(2)	20.1(8)	8.9(3)	2.4(4)	3.1(2)	0.8(5)
N	0.4924(3)	0.2773(7)	0.6095(4)	3.3(2)	24(1)	7.3(4)	0.3(4)	1.7(2)	2.6(5)
C(1)	0.5080(3)	0.147(1)	0.6370(5)	2.9(2)	27(1)	6.3(4)	-0.5(5)	1.8(2)	1.1(7)
C(2)	0.4711(4)	0.0316(8)	0.5908(5)	4.0(2)	21(1)	7.5(4)	0.2(4)	2.7(3)	1.6(6)
C(3)	0.4147(4)	0.055(1)	0.5116(5)	3.9(2)	26(2)	7.5(5)	-1.5(5)	2.5(3)	-1.7(7)
C(4)	0.3971(3)	0.193(1)	0.4829(5)	2.9(2)	30(2)	6.5(4)	0.8(5)	1.3(2)	0.5(7)
C(5)	0.4377(4)	0.3000(9)	0.5338(5)	3.7(2)	26(1)	7.2(4)	1.7(5)	1.9(3)	2.5(7)
C(6)	0.620(1)	0.483(2)	0.766(1)	23(2)	23(3)	22(2)	9(2)	15(1)	3(2)
C(7)	0.621(1)	0.585(2)	0.797(1)	25(2)	35(3)	23(2)	6(2)	17(1)	10(2)
C(8)	0.6971(5)	-0.009(1)	0.8437(6)	6.7(4)	24(2)	10.4(6)	3.4(6)	2.3(4)	3.0(8)
C(9)	0.7284(5)	-0.065(1)	0.9355(7)	7.0(4)	37(2)	13.8(8)	7.0(7)	5.4(5)	10(1)
H(1)	0.388	-0.022	0.477	4.5					
C6H(1)	0.573	0.492	0.715	4.5					
C6H(2)	0.654	0.480	0.738	4.5					
C8H(1)	0.732	-0.004	0.813	4.5					
C8H(2)	0.660	-0.076	0.811	4.5					

[a]The positional parameters for all atoms are represented in fractional unit cell coordinates.

[b]The β_{ij} are defined by: $T = \exp(-(h^2\beta_{11} + k^2\beta_{22} + \ell^2\beta_{33} + 2hk\beta_{12} + 2h\ell\beta_{13} + 2k\ell\beta_{23})$. If only the β_{11} column is listed, this corresponds to an isotropic temperature factor. All hydrogen isotropic temperatures factors have been set equal to 4.5 . Non-hydrogen thermal parameters are ($X\ 10^3$).

[c]In this and succeeding tables estimated standard deviations are given in parentheses for the least significant figures; later tables include the error in the lattice constants. Since the hydrogen positions were not refined, no standard deviations are given. Positions for the methyl hydrogens are not given as they were approximated.

Table XXII. Selected interatomic distances (Å) for chlorpyrifos

Bonding Distances		Interaction	via	Observed Distance	Total van der Waals Distance (Pauling[39])
C(1)-C(2)	1.38(1)				
C(2)-C(3)	1.37(1)				
C(3)-C(4)	1.39(1)	P···H(1)	Intramolecular	5.78(2)	(3.1)
C(4)-C(5)	1.37(1)	Cℓ(2)···Cℓ(3)	Intramolecular	3.175(6)	3.6
C(5)-N	1.32(1)	P···N	Intramolecular	3.02(1)	3.4
N-C(1)	1.308(9)	P...Cℓ(1)	Intramolecular	4.364(3)	3.7
		P···C(1)	Intramolecular	2.64(1)	3.6[b]
		P···C(3)	Intramolecular	4.953(8)	(3.6)[b]
C(1)-O(1)	1.364(9)	P···C(4)	Intramolecular	5.172(7)	(3.6)[b]
C(2)-Cℓ(1)	1.721(8)	P···C(5)	Intramolecular	4.328(7)	(3.6)[b]
C(3)-H(1)	0.950(8)				
C(4)-Cℓ(2)	1.717(9)				
C(5)-Cℓ(3)	1.711(8)	S···C(9)H_3	2_1+1cell in x and z - 1 in y	3.87(1)	3.85
		Cℓ(2)···O(2)	n-glide +1cell in y - 1 in x	3.548(6)	3.20
P-O(1)	1.611(5)	Cℓ(2)···C8H(1)	n-glide +1cell in y - 1 in x	3.286(4)	3.0
P=S	1.898(4)	Cℓ(2)···C(8)	n-glide +1cell in y - 1 in x	3.79(1)	3.5[b]
P-O(2)	1.562(5)	Cℓ(3)···C(9)H_3	n-glide +1cell in y - 1 in x	3.99(1)	3.8
P-O(3)	1.538(6)[a]	Cℓ(1)···C(7)H_3	2-fold +1cell in x and z - 1 in y	4.15(2)	3.8
O(2)-C(8)	1.426(9)	S···C8H(1)	2_1 +1cell in x and z - 1 in y	3.300(2)	3.05
O(3)-C(6)	1.39(2)[a]	Cℓ(2)···C(7)H_3	Center +1cell in x and z - 1 in y	3.97(2)	3.8
C(6)-C(7)	1.08(2)[a]				
C(8)-C(9)	1.44(1)				
C(6)-C6H(1)	1.00(2)				
C(6)-C6H(2)	1.00(2)				
C(8)-C8H(1)	1.00(1)				
C(8)-C8H(2)	1.00(2)				

[a] Due to disorder. See text.

[b] Bondi[46]

Table XXIII. Bond angles (degrees) for chlorpyrifos

C(1)-C(2)-C(3)	118.0(7)
C(2)-C(3)-C(4)	118.6(7)
C(3)-C(4)-C(5)	118.5(7)
C(4)-C(5)-N	122.9(7)
C(5)-N-C(1)	118.2(7)
N-C(1)-C(2)	123.7(6)
O(1)-C(1)-N	119.0(7)
O(1)-C(1)-C(2)	117.2(8)
Cl(1)-C(2)-C(1)	122.0(6)
Cl(1)-C(2)-C(3)	120.0(7)
H(1)-C(3)-C(2)	120.5(9)
H(1)-C(3)-C(4)	120.9(8)
Cl(2)-C(4)-C(3)	118.9(7)
Cl(2)-C(4)-C(5)	122.6(7)
Cl(3)-C(5)-C(4)	120.8(6)
Cl(3)-C(5)-N	116.4(6)
C(1)-O(1)-P	124.8(5)
O(1)-P-S	113.7(2)
O(1)-P-O(2)	98.2(3)
O(1)-P-O(3)	105.6(3)
S-P-O(2)	118.4(2)
S-P-O(3)	118.5(3)
O(2)-P-O(3)	99.6(3)
P-O(2)-C(8)	121.8(5)
P-O(3)-C(6)	125.1(8)
O(2)-C(8)-C(9)	110.2(8)
O(3)-C(6)-C(7)	132(2)[a]

[a] Due to disordering. See text.

Table XXIV. Dihedral angles (degrees) and least-square planes

Torsional Angle	
P-O(1)-C(1)-C(2)	145.90
C(1)-O(1)-P-S	-52.21
C(1)-O(1)-P-O(2)	-178.23
C(1)-O(1)-P-O(3)	79.32
S-P-O(2)-C(8)	-47.56
S-P-O(3)-C(6)	8.85

Plane(I)[a] defined by C(1), O(1), P and S:
(0.28582) X - (0.95817) Y - (0.01473) Z - 0.65256 = 0

Atom	Distance from Plane (Å)
C(1)	-0.136
O(1)	0.260
P	-0.199
S	0.075

Plane(II)[a] defined by S, P, O(2), C(8), C(9):
(0.58516) X + (0.62456) Y + (0.51721) Z - 12.30 = 0

Atom	Distance from Plane (Å)
S	0.114
P	-0.152
O(2)	0.181
C(8)	-0.273
C(9)	0.131

Plane(III)[a] defined by S, P, O(3), C(6), C(7):
(0.67723) X - (0.01214) Y + (0.73567) Z - 14.10 = 0

Atom	Distance from Plane (Å)
S	0.020
P	-0.002
O(3)	0.023
C(6)	-0.114
C(7)	0.074

Plane(IV)[a] defined by all eleven pyridoxyl members:
(0.84045) X - (0.06324) Y - (0.53818) Z - 0.77239 = 0

Atom	Distance from Plane (Å)
C(1)	0.008
C(2)	0.013
C(3)	0.016
C(4)	-0.008
C(5)	-0.003
N	0.008
O(1)	-0.059
Cℓ(1)	0.018
H(1)	0.018
Cℓ(2)	-0.008
Cℓ(3)	-0.004
O(2)	0.225
O(3)	-0.242
C(6)	0.151
C(9)	0.214

[a]Planes are defined by $c_1X + c_2Y + c_3Z - d = 0$, where X, Y and Z are Cartesian coordinates which are related to the triclinic cell coordinates (x, y, z) by the transformations:

$X = xa\sin\gamma + zc\{(\cos\beta - \cos\alpha\cos\gamma)/\sin\gamma\} = xa + zc\cos\beta$

$Y = xa\cos\gamma + yb + zc\cos\alpha = yb$

$Z = zc\{1 - \cos^2\alpha - \cos^2\beta - \cos^2\gamma + 2\cos\alpha\cos\beta\cos\gamma)^{\frac{1}{2}}/\sin\gamma\} = zc\sin\beta.$

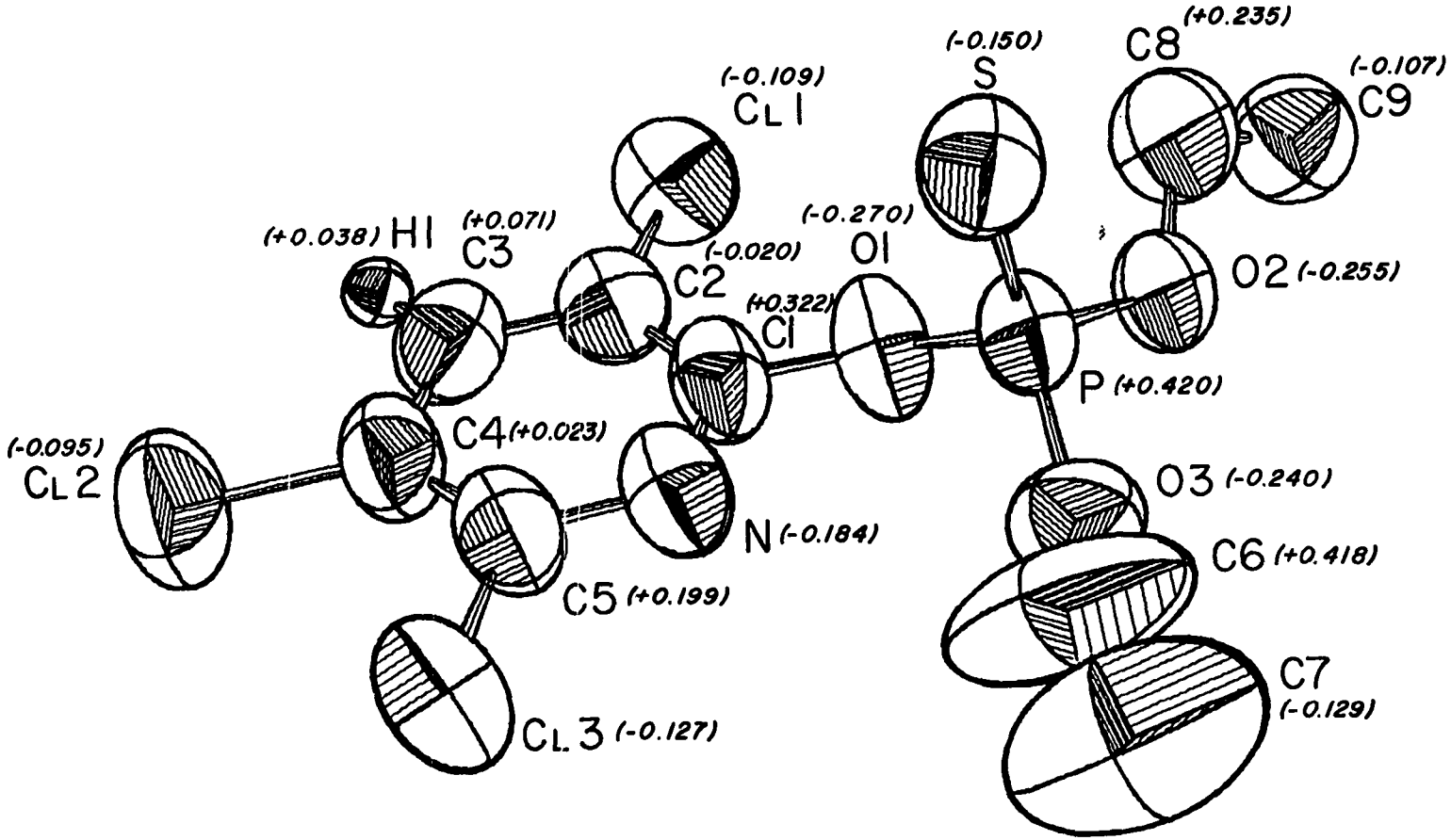

Figure 15. The chlorpyrifos molecule showing 50% probability ellipsoids; 30% for hydrogens. The numbers in parentheses refer to partial charge densities from a CNDO II calculation.

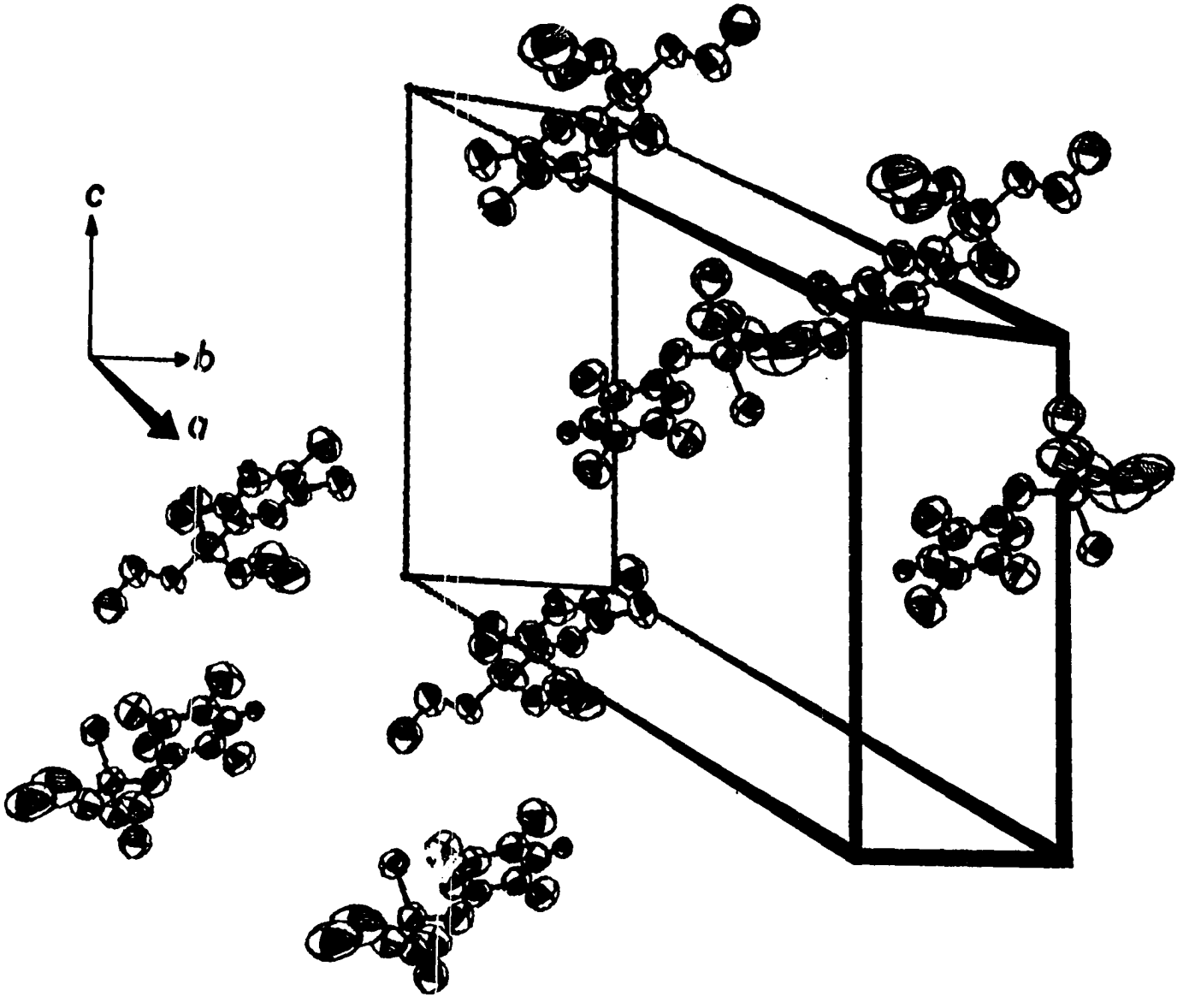

Figure 16. View of a unit cell of chlorpyrifos.

the "right" half of C(7) and *vice versa*, with O(3) remaining essentially fixed and intact; intermediate conformations would also occur. As the distances and angles in the remaining (and chemically significant) portion of the molecule were unchanged throughout either refinement, only the time-averaged model will be reported here.

The C(1)-O(1) bond in chlorpyrifos is significantly (>3σ) shorter than the two methoxy C-O bonds (*cf.* Table XXII), while the P-O(1) bond is the longest of the three P-O bonds, being at least 5σ longer than the other two. These observations, which when coupled with a CNDO II molecular orbital calculation of the Pople and Beveridge[47] type, are consistent with a bonding formulation in which there is a weak π overlap of the p_z orbital on the oxygen with the ring system which simultaneously weakens the O-P bond. The former effect is the likely cause of the C(1)-O(1)-P angle being greater than tetrahedral (*cf.* Table XXIII) while the latter should enhance phosphorylation[48]. Such variations in bond lengths have been noted earlier as the bond lengths corresponding to P-O(1) and C(1)-O(1) in chlorpyrifos, ronnel, ronnel oxon, bromophos, Ruelene, fospirate, Coroxon[42] and the OP reported by Grand and Robert[59] are all essentially identical. So, the pyridoxy OP's (fospirate and chlorpyrifos) do not display a C(1)-O(1) bond length any different than for the phenoxy OP's, even though there has been a replacement of a ring carbon with a more electronegative nitrogen.

Angles of the S=P-O or O=P-O type in these compounds are all greater than the tetrahedral angle of 109.47°, while angles of the O-P-O type are all smaller than tetrahedral. The internal ring angles in chlorpyrifos are identical with their counterparts in fospirate. Those with nitrogen at the vertex are less than 120°, but, when nitrogen is the terminal atom, they are greater than 120°; the two types of angles are significantly ($\sim 5\sigma$) different from each other (*cf.* Table XXIII). In chlorpyrifos the angle between the normal to the ring and the P=S vector is 34.1° which is not too surprising as angles between 20 and 40° have already been observed with most of the OP's studied. This phenomenon is probably just a consequence of the similarities of these somewhat immobilized ring-containing compounds but could prove to be a reaction variable with OP's having rotational degrees of freedom.

As with the other OP's presented, the phosphorus in chlorpyrifos is opposite the Cl(1) side of a plane which is perpendicular to the ring and contains the C(1)-O(1) bond. Since each molecule interacts only weakly with all of the other molecules in the unit cell (*cf.* Table XXII), the configuration of chlorpyrifos in the solid state is primarily dictated by intramolecular forces. Consequently, the position of the phosphorus is a result of the van der Waals barrier to rotation about the C(1)-O(1) bond which is afforded by Cl(1) and N. By not having any substituent on N, the thiophosphate group is allowed to avoid Cl(1). As a result the P-O(1)-C(1)-C(2) torsional angle

is 145.90° which is ∿23° smaller than the corresponding angle in fospirate. Tha lack of a substituent on nitrogen may be the major cause of the disordered C(6)-C(7) ethyl group, though disordering was noted in fospirate (the only other previously studied pyridoxy OP). This also allows the Cℓ(3)-C(5)-C(4) angle to be >5σ larger than the Cℓ(3)-C(5)-N angle. A minor factor which may contribute to the disordered ethyl group is the near total absence of intermolecular interactions involving C(7) which are very much present (though weakly) with C(9) (*cf.* Table XXII). The upshot of this is that the P···N distance turns out to be less than a van der Waals separation apart while P···Cℓ(1) is not (*cf.* Table XXII). The S···N, C(6)···N and O(3)···N separations (3.62, 3.48 and 3.16 Å, respectively) are all just ∿0.2 Å greater than the sum of the respective van der Waals radii, thus reflecting a slight stabilization of the phosphorus position on the N side os the ring.

On the basis of a restricted phosphorus position, comparison of some intramolecular distances with literature site-separation distances for AChE should give some insight into the toxicity/activity of chlorpyrifos. In addition to being "distance compatible", the atoms involved must also be "charge compatible" with AChE. As a first approximation to the OP active site[12] only two atoms will be considered here in accordance with the presence of two residues in Krupka's[17] (assumed[12]) active site model of AChE. Analysis of the steric interactions of the remaining parts of both molecules, without knowing more

about the structure(s) of AChE, would be futile.

Using the CNDO II method of Pople and Beveridge[47], approximate values for the charge density distribution in chlorpyrifos can be computed; results are shown in Figure 15. The use of this method is not as exact as with *ab initio* calculations which are extremely cost-prohibitive and are usually unavailable for this size of a problem. Although admittedly approximate, the charges obtained certainly give much better than "order of magnitude" information especially since d-orbital contributions are included for the phosphorus, sulfur and chlorine atoms. Owing to the similarities of the OP's investigated, relative comparisons of, say, charge densities using the same CNDO II program for each molecule is a valid procedure even if the charge densities are not "absolute". It is for this reason that the CNDO results of ronnel oxon, Ruelene, fospirate and chlorpyrifos may be compared. For example, the mammalian LD_{50}'s of chlorpyrifos and fospirate differ by a factor of 5 (~168 *vs.* 869 $mg \cdot kg^{-1}$[60], respectively) while the charge densities on the phosphorus atoms are +0.420e and 0.699e, respectively. On the basis of these charges alone, the LD_{50} values might have been reversely predicted. This implies that, in addition to the charge on the phosphorus, many other variables (*i.e.* the charges on other atoms, steric interactions, *etc.*) need to be considered. But until the true[12] OP active site is known, few good inferences can be made. However, the OP site separation distances should still be <u>comparable</u> to literature

values for the ACh site-separation since (fortunately) the sizes of many OP's are similar to that of ACh. Therefore, this study now provides preliminary information which will prove to be of immense value in deducing the true OP site.

Examination of Figure 15 and Table XXII shows that, in the case of chlorpyrifos, P···H(1) (5.78 Å), P···C(3) (4.95 Å), P···C(4) (5.17 Å) and P···C(5) (4.33 Å) are interesting reaction pairs to consider. These distances are nearly identical with those in fospirate. The small charge on C(4) of +0.023e may possibly rule out the P···C(4) pair as an important contributor to inhibition. The P···H(1) and P···C(3) distances fall outside of the mammalian AChE site-separation range of 4.3-4.7 Å[51,52] and yet are close to or within the range for insect AChE given by Hollingworth, *et al.*[51] of 5.0-5.5 Å and/or O'Brien[52] of 4.5-5.9 Å. It is even conceivable that since both H(1) and C(3) are δ(+) and may both be "distance compatible" with AChE, the C(3)-H(1) pair might correspond to a region of δ(+) charge having P···δ(+) distances of from 4.95 to 5.78 Å. Considering charge, distance, steric factors and overall reactivity, P···H(1) may be slightly favored as a specific reactive species towards insect AChE in chlorpyrifos. The P···C(5) pair, due to its shorter separation, may play a more important role in mammalian toxicity, unless significant conformational alterations in AChE or chlorpyrifos accompany any *in vivo* free energy changes.

It should be noted that even a rotation of the phosphorus

about the C(1)-O(1) bond to the Cℓ(1) van der Waals limit would only decrease, say, the P···H(1) distance by only ∿0.03 Å. This may possibly happen *in vivo*, even with the comparatively increased moment of inertia caused by the addition of C(7) and C(9), yet is not likely to be critical with respect to the distances in AChE and to the I_{50} of the insecticide as pertains to the conformation which AChE or chlorpyrifos might have to distort to in order to react. However, such a rotation would cause the phosphorus to be in a slightly different position relative to the other ring substituents. This may be partially responsible, then, for changes in I_{50} and/or LD_{50} values as a result of subtle steric influences of the insecticide with AChE. But, in order to make better comparisons and predictions, many heretofore unreported insect and mammalian I_{50} and LD_{50} values will need to be investigated and tabulated, especially for the isozymes of AChE.

Since chlorpyrifos, as well as many of the other OP's investigated to date, crystallize in a centrosymmetric space group, this implies the existence of d and ℓ forms. Therefore, I_{50} and LD_{50} values for both OP configurations, when applicable, would need to be known also. In addition, further similar CNDO calculations will need to be performed to obtain a better idea of the molecular charge distribution and how it pertains to toxicity.

SUMMARY AND CONCLUSIONS

In order to envision why one organophosphorus compound makes a good insecticide while another has relatively poor insecticidal properties, it becomes necessary to look at features which are peculiar to each OP group. From the information in Table XXV it would be tempting to say that in general if an OP compound is to have any useful insecticidal properties there should be at least one long P-X bond. In this study "X" would correspond to O(1). This elongation is observed for all of these P-O(1) bonds with a concurrent shortening of the C(1)-O(1) bond (*cf.* Table XXV). Not only are the P-O(1) bonds longer than the other P-O bonds in each molecule, but they are also generally longer than the P-O bonds reported for, say, H_3PO_4[41] but may be comparable to other OP's. Probably the important idea, though, is that a P-O(1) bond be longer relative to the remaining P-O bonds. In this way phosphorylation is facilitated[48].

The ring systems are the likely cause of the simultaneous lengthening-shortening effect as a result of the O(1) p_x-ring molecular orbital system. Possibly this is why a variation of toxicity with Hammett σ constants has been observed[22]. It would be quite interesting subsequent to this study to look at what makes a poor insecticide so that further gross differences may be noted.

Pertaining to more subtle differences, it is not too

Table XXV. Comparison of a few corresponding distances (Å) and the angle (degrees) between the P=S or O vector and the vector normal to the ring

Insecticide	P-O(1)	C(1)-O(1)	P-O($^{3}_{4}$)	methoxy C-O	Angle
ronnel	1.592(4)	1.400(6)	1.535(5) 1.545(4)	1.347(8)[a] 1.369(4)	23.5
ronnel oxon	1.599(3)	1.383(4)	1.552(3) 1.536(3)	1.442(5) 1.451(6)	34.4
bromophos	1.607(6)	1.391(9)	1.547(6) 1.571(7)	1.46(1) 1.44(1)	39.6
Ruelene	1.611(3)	1.392(6)	1.566(4) -	1.47(1) -	26.1 (P-N)
fospirate	1.609(5)	1.364(9)	1.549(6) 1.551(6)	1.43(1) 1.44(1)	19.9
chlorpyrifos	1.611(5)	1.364(9)	1.562(5) 1.538(6)[a]	- -	34.1
Coroxon[42]	1.593(3)	1.394(5)	1.551(4) 1.554(4)	1.455(7) 1.427(7)	38.5
azinphos-methyl[49]	-	-	-	-	23.9
methyl parathion[6]	1.60	1.43	1.58 1.56	1.33 1.46	33.3
"Grand's"[59]	1.594(7)	1.410(11)	1.567(9)[b] 1.584(8)	-	12.3[b]

[a] Disordered.
[b] Both oxygens are in a heterocyclic ring.

surprising that the corresponding bond distances of these and other OP insecticides are quite similar (*cf.* Table XXV). Consequently, bond lengths should have little to do explicitly with explaining why one "good" OP is, say, ten times more effective than another "good" OP.

A variety of intramolecular non-bonding distances may play a key role in the inhibition process. For example, if a distance does not match with, say, the serine hydroxyl to anionic site distance in the model of Krupka[17], inhibition may not occur. As shown in Table XXVI, intramolecular distances involving phosphorus show only a little variation, though the LD_{50} values vary by as much as ∿300-fold. Therefore, <u>these</u> distances may only play a small part in inhibition. However, with non-"rigid" molecules in which a wider range of distances may occur, the phosphorus-containing distances may actually be quite important. It is possible also that one or more of the <u>many</u> other distance combinations may be a key factor(s).

As noted earlier, charge density may play an equally important part in the activity of an OP insecticide. A few charge densities are compared in Table XXVII. If these charges are either sitting at improper distances or are sterically "misplaced" difficulty will be encountered in reacting with AChE. Unfortunately, many more such calculations need to be done as little correlation can currently be made between charge alone and toxicity.

Table XXVI. Selected intramolecular distances (Å) involving phosphorus

Insecticide	P···meta H	P···Carbon adjacent to meta H	P···C(4)	LD_{50} (mg/kg)[a]
ronnel	5.51	4.84	5.25	1740[28]
ronnel oxon	5.49	4.78	5.25	-
bromophos	5.52	4.79	5.25	3750-6100[53]
Ruelene	5.68 5.13	4.91 4.53	5.29	770-1000[53]
fospirate	5.79	4.95	5.14	168[60]
chlorpyrifos	5.78	4.95	5.17	869[60]
Coroxon[42]	5.76	5.00	5.30	-
azinphos-methyl[49]	-	-	4.83 ($^{not\ a}_{para}$ C)	16[28]

[a] LD_{50} values are not as reliable an index of comparison as I_{50} values since LD_{50}'s include *in vivo* metabolism, absorption, *etc.* but I_{50}'s are not as readily available.

Table XXVII. Selected partial charge densities[a] from CNDO II calculations[47]

Insecticide	P	O(1)	C(1)	Doubly bonded S or O	meta H	Carbon adjacent to meta H	C(4)
ronnel oxon	+0.684	-0.285	+0.258	-0.366	+0.042	+0.039	+0.056
Ruelene[b]	+1.248	-0.385	+0.152	-0.502	+0.025 +0.011	-0.034 -0.013	+0.019
fospirate	+0.699	-0.289	+0.361	-0.382	+0.035	+0.088	+0.007
chlorpyrifos	+0.420	-0.270	+0.322	-0.150	+0.038	+0.071	+0.023

[a] See the respective single molecule figures for additional charge densities.

[b] As noted earlier in the text, these calculations were done on a molecule in which the t-butyl group was replaced with a methyl function.

One limited proposition can be made regarding the number, and to some extent type, of substituents on either ring system and the partial charges on O(1) and C(1). Referring to Table XXVII it is noted for ronnel oxon, fospirate and chlorpyrifos that if three chlorines are in a "2,4,5" ("3,5,6" in the pyridyl OP's) the O(1) δ(-) charges are nearly identical. The difference in the phenyl *vs.* pyridyl ring is noted in the C(1) δ(+) charges in these three OP's, apparently a result of having the nitrogen adjacent to C(1). In either ring system the two phosphates (ronnel oxon and fospirate) have nearly identical charges on the respective P and O(2) atoms. When an ortho chlorine and para methyl group are present (similar to Ruelene) both the O(1) and C(1) charges decrease with a dramatic increase and decrease, respectively, in the charges on P and O(2). This occurs in spite of a less electronegative nitrogen bonded to the phosphorus.

All of the angles between the P=S or O vector and the vector normal to the ring are within a $\pm\sim 10^{\circ}$ range (*cf.* Table XXV) but this <u>may</u> be enough to promote steric problems. The fact that these angles are relatively comparable suggests a general preference for this orientation by ring-containing OP's such that the P-O(1)-ring skeleton is quite comparable for all of the OP's studied. These limited angles along with CNDO II potential energy calculations show that the solid state structures are likely to be very good models to use for *in vivo* compari-

sons.

As illustrated by the ronnel/ronnel oxon and fospirate/chlorpyrifos pairs, there are a few structural differences between the thiophosphate and the corresponding oxon (phosphate). For example, the directions of the methyl groups are different. Whereas they are both "up" in ronnel, they are both "down" in ronnel oxon (see Figures 1 and 3). A similar pattern is noted for chlorpyrifos (thiophosphate) and fospirate (phosphate), though they have methyl groups which are "down"/"up", respectively. In addition, a few angles involving ring substituents are different between the phenyl and pyridyl systems.

Structural limitations have been observed in both bromophos and Ruelene as a result of weak intramolecular hydrogen bond formation. Obviously this causes restrictions on any steric interactions between these OP's and AChE so that it may be feasible to take advantage of this in the design of future OP insecticides.

It would presently appear, then, that the major keys to better understanding the inhibition process may rest with steric interactions, charge distribution (viz. Hammett σ's) and intramolecular separations. Although this study has been limited to OP's having a ring system, and thus a reduced number of rotational degrees of freedom, a result is that the total number of reaction variables is narrowed. Once the true OP site structure of AChE is known, along with more tabulated I_{50} and LD_{50} values

for the possible isozymes of AChE, more specific conclusions can be drawn leading to the design of superior insecticides.

BIBLIOGRAPHY

1. M. Schneider and t. Fankuchen, J. Am. Chem. Soc., 68, 2669 (1946).

2. H. Wild and E. Brandenberger, Helv. Chim Acta, 29, 1024 (1946).

3. G. W. van Vloten, C. A. Kruissink, B. Strijk, and J. M. Bijvoet, Nature, 162, 771 (1948).

4. G. W. van Vloten, C. A. Kruissink, B. Strijk, and J. M. Bijvoet, Acta Crystallogr., 3, 139 (1950).

5. F. Lappe, Naturwissenshaften, 53(16), 405 (1966).

6. P. R. Bally, Acta Crystallogr., B26(5), 477 (1970).

7. T. P. DeLacy and C. H. L. Kennard, J. Chem. Soc. Perkin Trans. II, 14, 2141 (1972).

8. T. P. DeLacy and C. H. L. Kennard, J. Chem. Soc. Perkin Trans. II, 14, 2148 (1972).

9. T. P. DeLacy and C. H. L. Kennard, J. Chem. Soc. Perkin Trans. II, 14, 2153 (1972).

10. G. Holan, C. Kowala, and J. A. Wunderlich, J. Chem. Soc. Chem. Comm., 2, 34 (1973).

11. M. E. Gress and R. A. Jacobson, Cryst. Struct. Comm., 3, 485 (1973).

12. R. D. O'Brien, B. Hetnarski, R. K. Tripathi, and G. J. Hart in "Mechanism of Pesticide Action," ACS Symposium Series #2, G. K. Kohn, Ed., American Chemical Society, Washington, D. C., 1974, pp 1-13.

13. R. D. O'Brien, "Toxic Phosphorus Esters," Academic Press, New York, 1960, pp 73-4, 176, 248.

14. N. G. Berim and A. I. Bykhovets, Entomol. Rev., 52(4), 512 (1973).

15. N. H. Proctor and J. E. Casida, Science, 190, 580 (1975).

16. T. R. Fukuto, Bull. Wld. Hlth. Org., 44, 31 (1971).

17. R. M. Krupka, Canad. J. Biochem., 42, 677 (1964).

18. I. B. Wilson, F. Bergmann, and D. Nachmanson, J. Biol. Chem., 186, 781 (1950).

19. F. Bergmann and R. Segal, Biochem. J., 58, 692 (1954).

20. F. Bergmann, Disc. Faraday Soc., 20, 126 (1955).

21. J. L. Zettler and U. E. Brady, Pestic. Biochem. Physiol., 5(5), 471 (1975).

22. T. R. Fukuto and R. L. Metcalf, J. Agric. Food Chem., 4, 930 (1956).

23. C. Hansch and E. W. Deutsch, Biochem. Biophys. Acta, 126, 117 (1966).

24. F. G. Canepa, P. Pauling, and H. Sörum, Nature, 210, 907 (1966).

25. F. Takusagawa and R. A. Jacobson, J. Agric. Food Chem., 25(2), 329 (1977).

26. F. Takusagawa and R. A. Jacobson, J. Agric. Food Chem., 25(2), 333 (1977).

27. F. Takusagawa and R. A. Jacobson, J. Agric. Food Chem., 25(3), 577 (1977).

28. Pesticides and Toxic Substances Effects Laboratory, "Pesticide Reference Standards and Supplemental Data," National Environmental Research Center, Office of Research and Development, U. S. Environmental Protection Agency, Research Triangle Park, NC, 1973.

29. R. A. Jacobson, J. Appl. Crystallogr., 9, 115 (1976).

30. D. E. Williams, "LCR-2, A Fortran Lattice Constant Refinement Program," U. S. Atomic Energy Commission Report IS-1052, Iowa State University and Institute for Atomic Research, Ames, IA, 1964.

31. W. J. Rohrbaugh and R. A. Jacobson, Inorg. Chem., 13(11), 2535 (1974).

32. S. L. Lawton and R. A. Jacobson, Inorg. Chem., 7, 2124 (1968).

33. P. M. Main, M. M. Woolfson, and G. Germain, "MULTAN: A Computer Program for the Automatic Determination of Crystal Structures," Department of Physics, University of York, York, England, 1971.

34. C. A. Hubbard, C. O. Quicksall, and R. A. Jacobson, "The Fast Fourier Algorithm and the Programs ALFF, ALFFDP, ALFFPROJ, ALFFT and FRIEDEL," U. S. Atomic Energy Commission Report IS-2625, Iowa State University and Institute for Atomic Research, Ames, IA, 1971.

35. W. R. Busing, K. O. Martin, and H. A. Levy, "OR FLS, A Fortran Crystallographic Least Squares Program," U.S. Atomic Energy Commission Report ORNL-TM-305, Oak Ridge National Laboratory, Oak Ridge, TN, 1962.

36. H. P. Hanson, F. Herman, J. D. Lea, and S. Skillman, Acta Crystallogr., 17, 1040 (1960).

37. D. H. Templeton in "International Tables for X-ray Crystallography," Vol. III, pp. 215-6, Table 3.3.2c, The Knoch Press, Birmingham, England, 1962.

38. W. R. Busing, K. O. Martin, and H. A. Levy, "OR FEE, A Fortran Crystallographic Function and Error Program," U. S. Atomic Energy Commission Report ORNL-TM-306, Oak Ridge National Laboratory, Oak Ridge, TN, 1964.

39. L. Pauling, "Nature of the Chemical Bond," Cornell University Press, Ithaca, NY, 1960, pp 260-1.

40. C. A. Johnson, "OR TEP-II: A Fortran Thermal-Ellipsoid Plot Program for Crystal Structure Illustrations," U. S. Atomic Energy Commission Report ORNL-3794 (Second Revision with Supplemental Instructions), Oak Ridge National Laboratory, Oak Ridge, TN, 1971.

41. S. Furberg, Acta Chem. Scand., 9, 1557 (1955).

42. M. R. Gifkins and R. A. Jacobson, J. Agric. Food Chem., 24(2), 232 (1976).

43. M. E. Senko and D. H. Templeton, Acta Crystallogr., 13, 281 (1960).

44. F. Jellinek, Acta Crystallogr., 10, 277 (1957).

45. R. F. Stewart, E. R. Davidson, and W. T. Simpson, J. Chem. Phys., 42, 3175 (1965).

46. A. Bondi, J. Phys. Chem., 68(3), 441 (1964).

47. J. A. Pople and D. L. Beveridge, "Approximate Molecular Orbital Theory," McGraw-Hill, New York, 1970.

48. V. M. Clark, D. W. Hutchinson, A. I. Kirby, and S. G. Warren, Angew. Chem., 76, 704 (1964).

49. W. J. Rohrbaugh, E. K. Myers, and R. A. Jacobson, J. Agric. Food Chem., 24(4), 713 (1976).

50. W. J. Rohrbaugh and R. A. Jacobson, J. Agric. Food Chem., 25(3), 588 (1977).

51. R. M. Hollingworth, T. R. Fukuto, and R. L. Metcalf, J. Agric. Food Chem., 15(2), 235 (1967).

52. R. D. O'Brien, J. Agric. Food Chem., 11(2), 163 (1963).

53. M. Eto, "Organophosphorus Pesticides: Organic and Biological Chemistry," CRC Press, Cleveland, OH, 1974.

54. R. White-Stevens, Ed., "Pesticides in the Environment," Vol. 1, part 1, Marcel Dekker, New York, 1971, pp 106-7.

55. E. R. Howells, D. C. Phillips, and D. Rogers, Acta Crystallogr., 3, 210 (1950).

56. D. W. J. Cruickshank and D. E. Pilling in "Computing Methods and the Phase Problem in X-ray Crystal Analysis," R. Pepinsky, J. M. Roberts, and J. C. Speakman, Eds., Pergamon Press, Inc., New York, 1961.

57. L. E. Sutton, Ed., "Tables of Interatomic Distances and Configuration in Molecules and Ions," The Chemical Society, Burlington House, London, W.1, 1958.

58. T. J. Haley, J. H. Farmer, J. R. Harmon, and K. L. Dooley, Arch. Toxicol., 34(2), 103 (1975).

59. P. A. Grand and J. B. Robert, Acta Crystallogr., B31, 2502 (1975).

60. D. W. Osborne, Dow Chemical Co., Midland, MI, private communication, 1976.

ACKNOWLEDGEMENTS

The author would like to thank Dr. R. A. Jacobson for his superb guidance, inspiration and patience and all the members of X-ray Group I for making graduate school challenging, exciting and enjoyable.

For the support through the years, thanks must also be given to the parents, family and friends of the author.

In addition, for the support, understanding and love, the author wishes to extend his deepest thanks to his wife Debby and son Steve.